Faculty of Aerospace Engineering

Accuracy of Conflict Count Models

Analyzing the effect of traffic scenario on conflict count models for unstructured and layered airspaces.

Olafur Thordarson

January 29, 2018

TU Delft Delft University of Technology

Challenge the future

Accuracy of Conflict Count Models

Analyzing the effect of traffic scenario on conflict count models for unstructured and layered airspaces.

Master of Science Thesis

For obtaining the degree of Master of Science in Aerospace Engineering
at Delft University of Technology

Olafur Thordarson

January 29, 2018

Faculty of Aerospace Engineering · Delft University of Technology

Delft University of Technology

Delft University Of Technology
Department Of
Control and Simulation

The undersigned hereby certify that they have read and recommend to the Faculty of Aerospace Engineering for acceptance a thesis entitled **"Accuracy of Conflict Count Models"** by **Olafur Thordarson** in partial fulfillment of the requirements for the degree of **Master of Science**.

Dated: January 29, 2018

Readers:

Prof.dr.ir. J. M. Hoekstra

Dr.ir. J. Ellerbroek

Ir. E. Sunil

Dr. M.A. Mitici

Acronyms

ADS-B	Automatic Dependent Surveillance - Broadcast
ASAS	Airborne Separation Assurance System
ATC	Air Traffic Control
ATCo	Air Traffic Controller
ATM	Air Traffic Management
CD	Conflict Detection
CR	Conflict Resolution
TAS	True Airspeed

List of Symbols

Greek Symbols

α	Heading range for a layer.
ϵ	Ratio of cruising aircraft in the airspace.
$\gamma_{C/D}$	Climbing or descending angle.

Roman Symbols

A_c	The area searched by the conflict detection.
A_{total}	Total area of the airspace.
C_{layer_i}	Conflict count in a single layer.
C_{layer_i}	Conflict count for layered airspace.
C_{total}	Total number of conflict.
$C_{total_{UA,3D}}$	Total number of conflict for unstructured airspace, in 3D.
C_{cruise}	Conflict count for cruising aircraft.
$C_{cruise-C/D}$	Conflict cont for cruising and climbing or descending aircraft.
$C_{C/D}$	Conflict count for climbing or descending aircraft.
C_{Area_i}	Conflict count within a specific area in the airspace.
$C_{Area_{1,2}}$	Conflict count between two areas.
d_{sep_h}	Minimum horizontal separation.
d_{sep_h}	Minimum vertical separation.
H	Altitude range.
h_{ua}	Altitude for specific aircraft in UA.
h_{lay}	Altitude for specific aircraft in layered airspace.
k	The fitting parameter for UA.
k_{cruise}	The fitting parameter for cruising aircraft.

$k_{cruise-CD}$	The fitting parameter for cruising and climbing or descending aircraft.
k_{CD}	The fitting parameter for climbing or descending aircraft.
N_{total}	Total number of aircraft in the airspace.
N_{cruise}	Number of cruising aircraft.
$N_{C/D}$	Number of aircraft that are climbing or descending.
N_{Area_i}	Number of aircraft within a specific area.
p_2	Conflict probability between two aircraft.
p_v	Part of the conflict probability caused by the altitude distribution.
t_l	look a-head time.
v	Average speed of aircraft.
$\bar{v}_{rel_h}$	Expected horizontal relative velocity.
$\bar{v}_{rel_v}$	Expected vertical relative velocity.
V_c	Volume searched by the conflict detection.

List of Figures

List of Tables

Contents

Thesis Outline

This thesis is divided into three parts. The first part is the scientific paper. It describes the overall research in detail. The second part of this report is the appendix of the paper, and it contains extra figures related to the experiments described in the scientific paper. The final part is the preliminary report of the MSc thesis. This preliminary report is already graded, and it is included in this final MSc thesis report for completeness.

Part I

Scientific Paper

Analyzing the effect of traffic scenario on conflict count models for unstructured and layered airspaces

Ólafur Þórðarson
Supervisors: Emmanuel Sunil, Joost Ellerbroek, Jacco Hoekstra

***Abstract*—Decentralized airspace concepts have been proposed to increase the capacity of airspace. Previous research has showed that decentralized airspace concepts show great improvements in capacity, such as the Layers concept, where height rules are implemented, and unstructured airspace, where there are no procedural constraints. One aspect that determines capacity is safety. Measuring the number of instantaneous conflicts can be used as an intrinsic safety metric for new airspace design. Conflict counts can be measured by doing experiments which can be time consuming, or by using mathematical models. However, these models are derived using certain assumptions about the traffic. The ideal traffic settings for the models may not always be realistic in practice. This research attempts to improve the models and validate how accurate the models are with varying traffic scenarios, so that the conflict count models may be used for more realistic traffic scenarios.**

***Index Terms*—Decentralized Airspace, Conflict Count Models, BlueSky**

I. Introduction

Air traffic demand is ever increasing. According to Eurocontrol [1] the number of flights per year is expected to increase by about 2.2% annually for the next 7 years. Between 2014 and 2015 delays in flight increased by 23%, which may indicate that there are issues with airspace capacity. Action is needed to increase the capacity of the airspace, either to improve the current en route system or to implement a completely new system.

A system that has been suggested is decentralized airspace [2]. A *centralized* system is where the traffic flow and separation are maintained by a central controller like Air Traffic Control (ATC), but when an airspace concept is *decentralized*, the separation is maintained by the pilots themselves and routes can be chosen by them as well. Recent studies [3] [4] have proposed Unstructured Airspace (UA) and Layered Airspace concepts, which are types of decentralized airspace concepts. The UA concept is where there are no procedural constraints, which gives the pilots complete flexibility in selecting their routes. The only constraints in the UA concept are physical constraints such as terrain and weather. On the other hand, layered concepts apply altitude constraints, and heading-altitude rules are used to determine the cruising altitude of an aircraft.

To ensure safety, and avoid possible collisions, aircraft have a predefined separation zone which is defined with a horizontal and vertical distance. If two aircraft enter each other's separation zone, it is refereed to as an *intrusion*, when an intrusion is predicted it is referred to as a *conflict*. In a decentralized airspace, pilots make use of Conflict Detection (CD) to detect conflicts, which is a part of an on-board aircraft system called Airborne Separation Assurance System (ASAS).

The number of conflicts that occur in an airspace has been used as a metric for *intrinsic safety* which is the ability of the airspace design to prevent conflicts. The analytical conflict count of an airspace design can be obtained by doing experiments or by using conflict count models. Previous studies have made use of conflict count models [4][3], and the accuracy have been found to be high. However the models are derived using assumptions regarding *traffic scenario* properties [5] [6] [7]. A traffic scenario defines the heading and routes for all aircraft in the airspace. The routes include origin and destination points, cruising altitude and the speed. The assumptions that are made in the derivation of these models are:

- Heading distribution is uniform
- Aircraft speeds are equal
- Altitude distribution is uniform
- Traffic density is uniform for the whole airspace

In practice, a traffic scenario with these exact combination of properties is not likely to occur. The question still remains how discarding the model assumptions will affect the accuracy of the model, i.e., if the models are still applicable when the traffic scenario varies from the ideal conditions, and if the accuracy error can be predicted and compensated. Another consideration is whether any assumption affects the accuracy more than other assumptions.

In this research the models will be tested for traffic scenarios which do not respect the above assumptions. This is done by varying the distributions of aircraft headings, speeds, altitude, spatial organization, and speeds for a number of cases. Five experiments will be performed; one assumption will be disregarded in each experiment while respecting all the other assumptions. The results will be compared with an additional experiment with the ideal model settings as a baseline. Furthermore, a numerical approach is proposed to adjust the predictions of the analytical models. The effectiveness of these numerical adjustments is also investigated using the data collected during the simulation experiments. The adjustments are made form complex integrals, which is why a numerical approximation is used.

This paper is structured as follows. The baseline analytical conflict count models will be discussed in Section II. In Section III, the effect of each assumption is analyzed and a numerical approach is used to suggest model corrections for non-ideal traffic scenarios. The experiments and their setup are explained in Section IV. The results from the experiments are

presented in Section V and discussed in Section VI. Finally a conclusion is made in Section VII.

II. Analytical Conflict Count Models

The theoretical approach to compute the instantaneous conflict count is to use so-called Conflict Count Models. They consider the maximum possible combinations of two aircraft in the airspace, which is the maximum number of possible conflicts. However, not all of those conflict do occur, so the number of combinations is scaled down with the conflict probability, see Eq. 1, where N_{total} is the number of instantaneous aircraft in the airspace and p_2 is the probability of conflict between two aircraft [2]. This section only summarises the 3D models, but to see the full derivations see [6] and [7].

$$C_{total} = \binom{N_{total}}{2} p_2 = \frac{N_{total}}{2}(N_{total}-1)\ p_2 \tag{1}$$

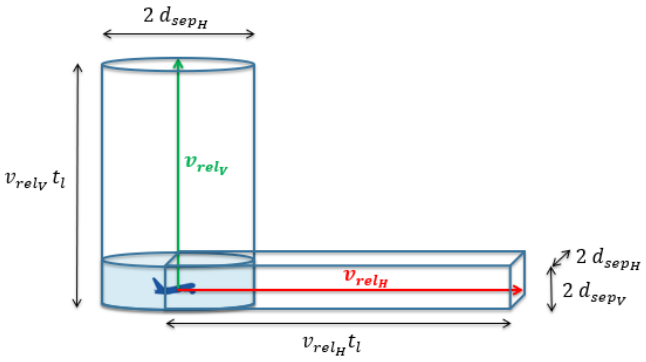

Figure 1. *The volume searched by the CD. [7]*

Conflict probability is the chance of two aircraft trajectories getting too close in the future. The conflict probability is based on the ratio between an area/volume of airspace that an aircraft searches for conflicts during conflict detection (CD) (see Figure 1), and total area/volume of the airspace region . The choice between area and volume depends on the phase of flight, and the specific airspace design under consideration. The models used in this study include climbing and descending aircraft for both UA and Layered airspace. These models are adapted from [6] and [8] in a paper by Sunil et al. [7].

A. Unstructured Airspace

When Unstructured Airspace (UA), there are no procedural constraints regarding the air traffic. The pilots can choose their own direction and altitude. Consequently, the conflict count model for UA does not consider the flight phase of an aircraft.

The model for the UA concept is presented in Eq. 2. The symbols in the equations are described in Table I

Table I
Symbols used for the model.

Horizontal Separation	d_{sep_h}
Vertical Separation	d_{sep_v}
Expected Horizontal Relative Velocity	$\bar{v}_{rel_h}$
Expected Vertical Relative Velocity	$\bar{v}_{rel_v}$
Look-ahead	t_L
Average Speed	v
Climbing/Descending Angle	$\gamma_{C/D}$
Ratio of Cruising Aircraft	ϵ
Heading Range	α

$$C_{total_{UA,3D}} = \frac{N_{total}}{2}(N_{total}-1)\ p_{2_{UA,3D}} \tag{2a}$$

$$p_{2_{UA,3D}} = \frac{4\ d_{sep_h} d_{sep_v} \bar{v}_{rel_h}\ t_L}{V_{total}} + \frac{\pi\ d_{sep_h}^2 \bar{v}_{rel_v}\ t_L}{V_{total}} \tag{2b}$$

$$\bar{v}_{rel_h} = \frac{4v}{\pi} \tag{2c}$$

$$\bar{v}_{rel_v} = v\sin(\gamma_{C/D})(1-\epsilon^2) \tag{2d}$$

$$\epsilon = \frac{N_{cruise}}{N_{total}} \tag{2e}$$

B. Layered Airspace

In layered airspace concepts, the cruising altitude of an aircraft depends on its heading, and this is defined using heading-altitude rules. These heading-altitude rules specify the heading range, α, which is allowed in each altitude band. Furthermore, the spacing between the altitude bands is at least equal to the vertical separation requirement to prevent conflicts between cruising aircraft in different altitude layers. In these two ways, layered airspaces aim to reduce the probability of conflict when compared to UA. Figure 2 gives a visual description of a layered concept.

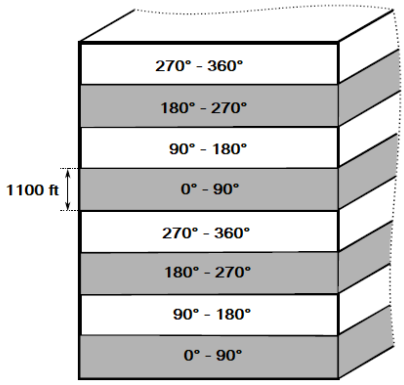

Figure 2. *A visualization of a layered concept, with a heading range of* $\alpha = 90°$. *Adapted from [3].*

The model for Layered airspace is derived in [6] as a 2D model, but then expanded to 3D model in [7] where climbing and descending aircraft are included. The model

for the Layered concept needs to consider the number of aircraft per layer. Because the layered airspace design only applies constraints on cruising aircraft, the conflict count model layered airspaces is composed of three parts; a part that counts the number of conflicts between cruising aircraft, C_{cruise}, a part that considers conflicts between cruising and climbing/descending aircraft,$C_{cruise-C/D}$, and a part for conflicts between climbing/descending aircraft, $C_{C/D}$:

$$C_{SS_{Lay}} = C_{cruise} + C_{cruise-C/D} + C_{C/D} \tag{3}$$

The conflict count model between the cruising aircraft is the same as for the 2D and 3D cases, as there are no climbing or descending aircraft to be considered. In Eq. 4, N_{cruise} is the number of cruising aircraft, L is the number of altitude layers, A_{total} is the total area of the airspace and α is the size of the heading range per altitude band.

$$C_{cruise} = \frac{N_{cruise}}{2}\left(\frac{N_{cruise}}{L} - 1\right)\ p_{2_{cruise}} \tag{4a}$$

$$p_{2_{cruise}} = \frac{2\ d_{sep_h}\bar{v}_{rel_h}\ t_L}{A_{total}} \tag{4b}$$

$$\bar{v}_{rel_h} = \frac{8v}{\alpha}\left(1 - \frac{2}{\alpha}\sin\frac{\alpha}{2}\right) \tag{4c}$$

The $C_{cruise-C/D}$ part of Eq. 3 is the conflict count for conflicts between a cruising aircraft and climbing or descending aircraft. The number of possible combinations of aircraft is a bit different here than for the other case and the conflict probability is based on the volume.

$$C_{cruise-C/D} = N_{cruise}\ N_{C/D}\ p_{2_{cruise-C/D}} \tag{5a}$$

$$p_{2_{cruise-C/D}} = \frac{4\ d_{sep_h} d_{sep_v}\bar{v}_{rel_h}\ t_L}{V_{total}} + \frac{\pi\ d_{sep_h}^2\bar{v}_{rel_v}\ t_L}{V_{total}} \tag{5b}$$

$$\bar{v}_{rel_h} = \frac{4v}{\pi} \tag{5c}$$

$$\bar{v}_{rel_v} = 2v\sin(\gamma_{C/D})(\epsilon - \epsilon^2) \tag{5d}$$

$$\epsilon = \frac{N_{cruse}}{N_{total}} \tag{5e}$$

The final part of the Conflict Count model for layered airspace considers aircraft that are climbing or descending. Here the conflict probability is based on the volume as well, thus it has to include the expected vertical relative velocity, $\bar{v}_{rel_v}$.

$$C_{C/D} = \frac{N_{C/D}}{2}\left(N_{C/D} - 1\right)\ p_{2_{C/D}} \tag{6a}$$

$$p_{2_{C/D}} = \frac{4\ d_{sep_h} d_{sep_v}\bar{v}_{rel_h}\ t_L}{V_{total}} + \frac{\pi\ d_{sep_h}^2\bar{v}_{rel_v}\ t_L}{V_{total}} \tag{6b}$$

$$\bar{v}_{rel_h} = \frac{4v}{\pi} \tag{6c}$$

$$\bar{v}_{rel_v} = v\sin(\gamma_{C/D})(1-\epsilon)^2 \tag{6d}$$

Now Eqs. 4, 5 and 6 are substituted in Eq. 3, to get the final Conflict Count model for the Layered Airspace concepts.

III. Adjusted Conflict Count Models

As mentioned before, several assumptions concerning the heading, speed, altitude and spatial distribution of traffic are made during the derivation of the analytical conflict count models. These assumptions are expected to lead to inaccurate conflict count predictions, if they are not respected. It is hypothesized that the errors can be predicted and compensated for by making adjustments to the model. By analysing the assumptions and where they affect the equations, the adjustments can be derived and included in the model to make them more adaptable to the traffic scenario.

The changes to the model are to be validated by fitting the experiment results with the adjusted models to investigate the accuracies. As the experiments are designed so the traffic follows a specific heading, speed, altitude and spatial distributions. The same distributions that are used in the experiments are used in the derivations of the adjustments.

A. Heading Distribution Adjustment

When deriving the expected horizontal relative velocity ($\bar{v}_{rel_h}$), in Section II it is assumed that the heading distribution is uniform. There are two parts in finding $\bar{v}_{rel_h}$, the probability density function for the absolute heading difference ($P(|\Delta hdg|)$), and the relative velocity ($v_{rel_h}(|\Delta hdg|)$), see equation 7. $|\Delta hdg|$ is the distribution of the absolute heading difference, in Figure 3 the probability density function of the absolute heading difference for uniform heading distribution can be seen.

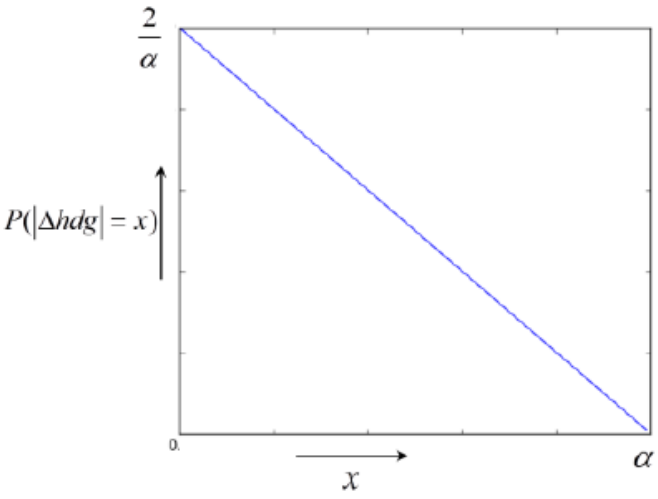

Figure 3. *The distribution of the absolute heading difference for uniformly distributed heading.*

$$\bar{v}_{rel_h} = \int_0^{\alpha} P(x = |\Delta hdg|)\ v_{rel_h}(x = |\Delta hdg|)dx \tag{7a}$$

$$v_{rel_h}(x) = 2v\sin\left(\frac{x}{2}\right) \tag{7b}$$

$$P(x) = \frac{2}{\alpha}\left(1 - \frac{x}{\alpha}\right) \tag{7c}$$

When the heading distribution is uniform, the expected horizontal relative velocity is as described in Eqs. 2c, 4c, 5c, 6c and Figure 3. But when using different heading distributions these equations are not valid. For these cases, new probability density functions need to be defined instead of Eq. 7c.

Three different heading distributions were chosen to be tested in this research. Normal distribution was chosen to simulate traffic that is mostly heading relatively in the same direction, ranged-uniform distribution was chosen to be similar to the normal distribution, but to be more spread out. These two distributions can be an example of traffic moving towards oceanic airspace in the morning for example where there is no head-on traffic. A bimodal distribution was chosen to simulate head-on traffic, for example like when aircraft are in a narrow sector and meet head on traffic. These distributions are shown in Figure 4. For the numerical adjustment for these distributions, the corresponding probability density functions of absolute heading difference need to be used:

$$P(x)_{normal} = \frac{\sqrt{2}}{\sigma\sqrt{\pi}} e^{-\frac{x^2}{2\sigma^2}} \tag{8}$$

$$P(x)_{bimodal} = \frac{1}{2\sqrt{2\pi\sigma^2}} e^{\frac{(x-\pi)^2}{2\sigma^2}} + \frac{1}{\sqrt{2\pi\sigma^2}} e^{-\frac{x^2}{2\sigma^2}} \tag{9}$$

$$P(x)_{ranged-uniform} = \frac{4}{\alpha^2}(\alpha - 2x) \tag{10}$$

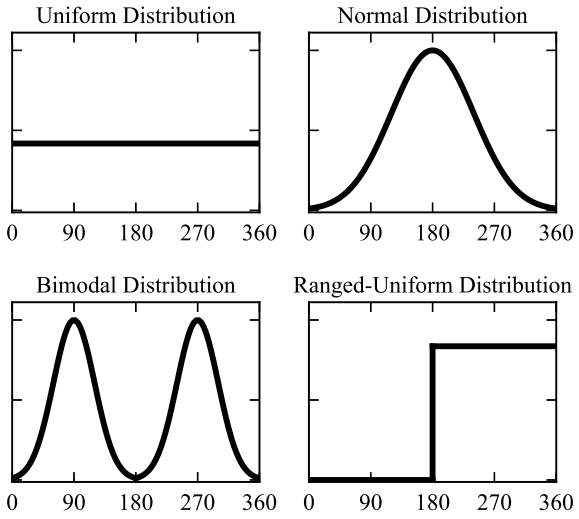

Figure 4. *The probability density functions for the four heading distributions used in the heading experiments.*

Inserting these equations into Eq. 7 instead of Eq. 7c, results in the expected horizontal relative velocity for different heading distribution. Using numerical evaluation, the values for $\bar{v}_{rel_h}$ were obtained and are listed in Table II. The evaluations are only done for airspace concepts that have an $\alpha = 360°$ heading range. For layered concepts with smaller heading range, the altitude distribution would not remain uniform if the heading is not uniform as well.Since the goal of the simulation experiments is to only vary one traffic scenario assumption at a time, only UA and a layered concept with $\alpha = 360^o$ are, therefore, considered for testing the heading distribution adjustment.

Table II
NUMERICALLY COMPUTED VALUES FOR $\bar{v}_{rel_h}$ FOR DIFFERENT HEADING DISTRIBUTION.

Distribution	$\bar{v}_{rel_h}$	Accuacy
Uniform	509 kts	100%
Bimodal	485 kts	95.3%
Normal	395 kts	77.6%
Ranged-Uniform	370 kts	72.7%

The accuracies in Table II are the predicted accuracies and are derived from the error from the $\bar{v}_{rel_h}$ of the uniform distribution. These accuracies are expected to mirror the accuracy of the conflict count model when assuming uniform heading distribution regardless of the actual distribution of aircraft headings. By using the correct $\bar{v}_{rel_h}$ value for the right heading distributions it should be possible to improve the accuracy of the model so it can be valid.

B. Speed Distribution Adjustment

The other part of the derivation of the expected horizontal relative velocity ($\bar{v}_{rel_h}$) is that the speed is assumed to be equal for all aircraft. However, for real life operations, the speeds of aircraft can vary, because of different aircraft types and airline procedures. The relative velocity equation (v_{rel}) in Eq. 7b, is derived from Fig. 5. When the aircraft all have the same speed this equation can be used, but when this is not the case the probability density function of the speed needs to be taken into account. Instead of using Eq. 7b, Eq. 11b is used when aircraft speeds are not equal:

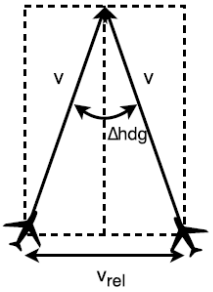

Figure 5. *Representation of relative velocity.[3]*

$$\bar{v}_{rel_h} = \int_{v_1}\int_{v_2}\int_{0}^{\alpha} v_{rel}(x, v_1, v_2) P(v_1) P(v_2) P(x) dx dv_2 dv_1 \tag{11a}$$

$$v_{rel}(x, v_1, v_2) = (v_1^2 + v_2^2 - 2v_1 v_2 \cos(x))^{\frac{1}{2}} \tag{11b}$$

Here v_1 and v_2 is the speeds for two arbitrary aircraft, x is a stand-in for the absolute heading difference ($|\Delta hdg|$) and where of course the P stands for the corresponding probability density function of speed and heading difference. Numerical evaluation of Eq. 11 can be seen in Table III for different speed

distributions. The table shows the speed values for different types of layered concepts. L360 is when the heading range per layer is $\alpha = 360°$. In the L180 concept the layers have heading ranges per layer of $\alpha = 180°$ and L90 with $\alpha = 90°$. The values do not vary significantly from the baseline conditions (all aircraft have equal speed). So it is not expected that the speed has any affect on the accuracy, but should be able to be adjusted by using the right $\bar{v}_{rel_h}$, if it causes inaccuracies.

The three distributions that were tested were uniform-, normal-, and bimodal distributions. Normal distribution to be closer to the baseline scenario where all the aircraft have the same speed, bimodal distribution to have two dominant speeds and uniform distribution is more spread over different speed settings. The probability density functions of the speed distributions can be seen in Figure 6.

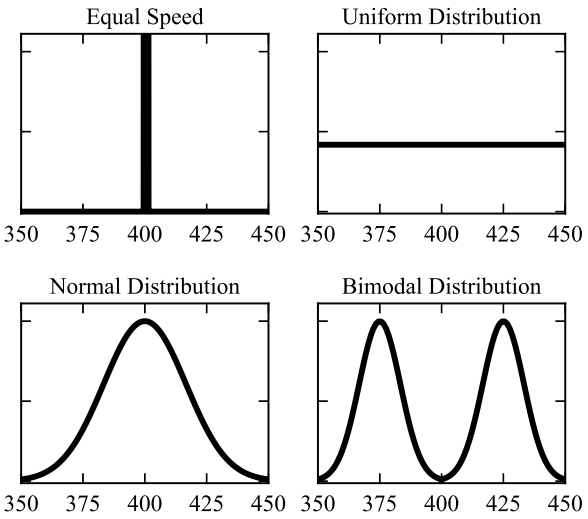

Figure 6. *The probability density functions for the four speed distributions used in the speed experiments.*

Table III
NUMERICALLY COMPUTED VALUES FOR $\bar{v}_{rel_h}$ FOR DIFFERENT SPEED DISTRIBUTION TYPES AND THE RELEVANT ACCURACIES.

Speed Distribution	UA/L360 [kts]	L180 [kts]	L90 [kts]
Equal	509 (100%)	370 (100%)	203 (100%)
Normal	507 (99.61%)	370 (100%)	205 (99.02%)
Bimodal	509 (100%)	373 (99.20%)	208(97.60%)
Uniform	512 (99.41%)	374 (98.93%)	210 (96.67%)

C. Altitude Distribution Adjustment

The model assumption for the altitude has two parts to it. First being the vertical density which affects the UA concept and the other being the number of combination of aircraft for the Layered concepts.

1) Unstructured Airspace: For UA, Eq. 2b shows that conflict probability is computed as the summation of two ratios; 1) the ratio between the volume searched for conflicts in the horizontal direction and the total volume, and 2) the ratio between the volume searched for conflicts in the vertical direction and the total volume. The first of these two ratios assumes a uniform distribution of aircraft cruising altitudes. However, if aircraft are not spread uniformly in the vertical direction, then it is logical that aircraft at busy altitudes experience more conflicts than aircraft in less dense altitudes. The effect of aircraft altitude on conflict probability, p_v, can be calculated as [8]:

$$p_v = \int_{alt_{min}}^{alt_{max}} P(h) \int_{h-d_{sep_v}}^{h+d_{sep_v}} P(z)dz \; dh \tag{12}$$

Here P is the probability density function for the altitude distribution, h is the altitude variable while z is the altitude variable for the other aircraft. When assuming uniform distribution, Eq. 12 becomes:

$$p_{v_{uniform}} = \frac{1}{H} \tag{13}$$

Eq. 13 was implicitly used in the derivation of the 3D conflict probability model given by Eq. 2b:

$$\begin{aligned} p_{2_{UA,3D}} =& \frac{4 \; d_{sep_h} d_{sep_v} \bar{v}_{rel_h} \; t_L}{A_{total}} \underbrace{\frac{1}{H}}_{p_{v_{uniform}}} \\ &+ \frac{\pi \; d_{sep_h}^2 \bar{v}_{rel_v} \; t_L}{A_{total}} \underbrace{\frac{1}{H}}_{p_{v_{uniform}}} \end{aligned} \tag{14}$$

Eq. 14 is equivalent to Eq. 2b. But when using an altitude distribution that is not uniform, the probability density function needs to be included in the model, like presented in Eq. 12. Now the conflict count model for unstructured airspace takes on the form as described in Eqs. 15:

$$C_{total_{UA,3D}} = \frac{N_{total}}{2} \left(N_{total} - 1\right) \; p_{2_{UA}} \tag{15a}$$

$$p_{2_{UA}} = \frac{4 \; d_{sep_h} d_{sep_v} \bar{v}_{rel_h} \; t_L}{A_{total}} p_v + \frac{\pi \; d_{sep_h}^2 \bar{v}_{rel_v} \; t_L}{A_{total}} p_v \tag{15b}$$

$$p_v = \int_{alt_{min}}^{alt_{max}} P(h) \int_{h-d_{sep_v}}^{h+d_{sep_v}} P(z)dz \; dh \tag{15c}$$

$$\bar{v}_{rel_h} = \frac{8v}{\alpha} \left(1 - \frac{2}{\alpha} \sin \frac{\alpha}{2}\right) \tag{15d}$$

$$\bar{v}_{rel_v} = v \sin(\gamma_{C/D})(1 - \epsilon^2) \tag{15e}$$

$$\epsilon = \frac{N_{cruise}}{N_{total}} \tag{15f}$$

When p_v was evaluated numerically for normal, bimodal and ranged uniform altitude distribution (see Figure 7), the corresponding values can be used to adjust the conflict count model, see Table IV where the p_v values and the predicted accuracies are presented. Once again, the 'accuracy' column in this table lists the accuracy of the analytical conflict count model that assumes uniform altitude distribution, regardless of the actual distributions.

Three altitude distributions were tested, normal-, bimodal-, and ranged-uniform. A normal distribution is used to investigate the effect of the case when the traffic is concentrated

around one altitude, the bimodal instead to describe concentration of the traffic around two altitudes spreading it more around. Often pilots prefer the upper airspace, that is why a ranged-uniform was chosen where the aircraft are uniformly distributed at higher altitudes. In Figure 7 the probability density functions for the altitude distributions are shown.

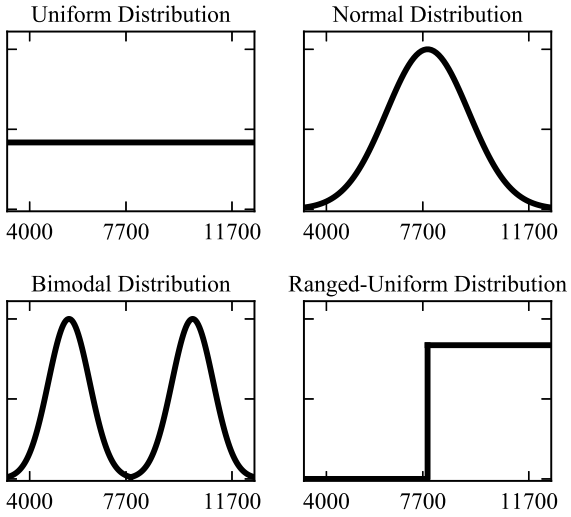

Figure 7. *The probability density functions for the four altitude distributions used in the altitude experiments.*

Table IV
NUMERICALLY COMPUTED VALUES FOR p_v.

Altitude Distribution	p_v	Accuracy
Uniform	0.171	100%
Normal	0.289	59.17%
Bimodal	0.289	59.17%
Ranged Uniform	0.342	50.00%

2) Layers: In the derivation of the Layers concept the number of combinations of aircraft is calculated differently for cruising aircraft, see Eq. 16. Here every layer needs to be considered individually and summed up to get the correct conflict count, see Eqs. 16a and 16b. If the aircraft are evenly spread over the layers (uniform altitude distribution), a simplification to the equation can be made, see Eq. 16c.

$$C_{layer_i} = \frac{N_{layer_i}}{2}(N_{layer_i} - 1)\ p_2 \tag{16a}$$

$$C_{Layers} = \sum_{1}^{L} \frac{N_{layer_i}}{2}(N_{layer_i} - 1)\ p_2 \tag{16b}$$

$$C_{Layers} = \frac{N_{Layers}}{2}(\frac{N_{Layers}}{L} - 1)\ p_2 \tag{16c}$$

When the conflict count models for a layered concepts is applied to a traffic scenario that has a non-uniform altitude distribution, the model is expected to have a low accuracy. If Eq. 16b is used instead of Eq. 16c to calculate the number of combinations of aircraft, then different altitude distributions can be considered. In such cases, the number of aircraft in each layer (N_{layer_i}) should be used. N_{layer_i} is found by creating a set of altitude samples for the various distributions being used, then counting the number of samples within each layer. Using this approach, the number of combinations of two aircraft were calculated for all altitude distributions and all values of N_{total} considered in this work, see Table V.

Table V
NUMBER OF COMBINATIONS OF TWO AIRCRAFT FOR DIFFERENT CRUISING ALTITUDE DISTRIBUTIONS FOR LAYERED AIRSPACES.

N_{total}	Uniform	Normal	Bimodal	Ranged Uniform
80	114	227 (50.22%)	207 (55.07%)	220 (51.82%)
302	1957	3734 (52.41%)	2418 (57.26%)	3960 (49.42%)
589	7655	14507 (52.77%)	13304 (57.54%)	15312 (49.99%)
1146	29069	54907 (52.94%)	50049 (58.08%)	58140 (50.00%)
1600	57000	107128 (53.21%)	98329 (57.97%)	113764 (50.10%)
Average Accuracy	100%	51.32%	57.38%	50.27%

D. Spatial Distribution Adjustment

The analytical model is assumed to have uniform spatial distribution, meaning that the density is the same throughout the airspace it is applied to. The conflict probability is described as the ratio between the volume searched by the conflict detection and the total volume of the airspace. If the traffic density is higher in one place, it stands to reason that the conflict probability is higher within the smaller area, which is referred to as hotspot in this paper.

If the model is applied to specifically the part of the airspace where the hotspot is, and then to the rest of the airspace, the model should give a more accurate conflict count. Figure 8 shows two examples of the two areas used to adjust the model to make it more accurate, with different hotspots, the larger being 55 nm and 40 nm. In Figure 8 there is also an example of the baseline scenario traffic density. Where the areas are marked by the black circles. The inner circle shows the hotspot and the outer circle shows the normal experiment area.

When splitting up the airspace the conflict have to be counted separately for each area. Because the model does not take into account conflicts between the two areas, they must be included as well. Eq. 17 shows the structure of the adjusted model. Where N_{Area_1} is the number of aircraft in the hotspot and N_{Area_2} is the number of aircraft in the rest of the airspace. The conflict probability differs for conflicts within the hotspot($p_{2,Area_1}$), outside the hotspot($p_{2,Area_1}$) and conflicts between aircraft inside and outside the hotspot($p_{2,Area_{1,2}}$).

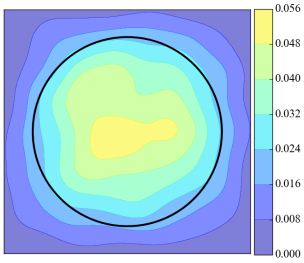

(a) *Baseline*

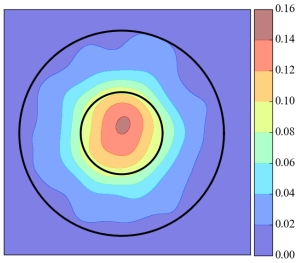

(b) *Hotspot 1, radius 55 nm*

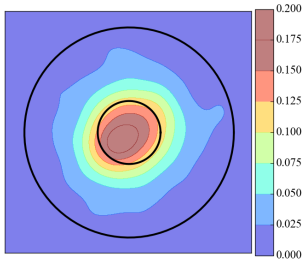

(c) *Hotspot 2, radius 40 nm*

Figure 8. *Traffic density heat maps of the experiment area and the hotspot areas.*

$$C_{total} = C_{Area_1} + C_{Area_2} + C_{Area_{1,2}} \tag{17a}$$

$$C_{Area_1} = \frac{N_{Area_1}}{2}(N_{Area_1} - 1)p_{2,Area_1} \tag{17b}$$

$$C_{Area_2} = \frac{N_{Area_2}}{2}(N_{Area_2} - 1)p_{2,Area_2} \tag{17c}$$

$$C_{Area_{1,2}} = N_{Area_1}N_{Area_2}p_{2,Area_{1,2}} \tag{17d}$$

This adjustments does not include numerical values as the adjustments for the other assumptions are based on. Here the analytical model, described in Section II, is used but applied to hotspot specifically, then to the rest of the airspace.

IV. Experiment Setup

Five fast-time simulation experiments are conducted to determine the accuracy of the conflict rate model. This chapter describes the design of these experiments. Four of the experiments are performed for different heading distributions, spatial distribution, altitude distributions and speed distributions, because these correspond to the four main scenario assumptions made during the derivation of the analytical models. An additional experiment is performed where all the model assumptions are respected. This experiment will be used as a baseline for comparison.

A. Simulation Development

1) Simulation Platform: For the simulations, the open-source ATM simulation platform BlueSky, is used. It is developed in the Python programming language at Delft University of Technology. More information on BlueSky is in [9].

2) Conflict Detection: The CD method used is called state-based conflict detection, where an aircraft's future position is predicted as a linear extrapolation of its position vector assuming constant speeds over a predefined look-ahead time. The conflict is detected when an aircraft's trajectory will violate another aircraft's protected zone as defined by minimum separation. The look-ahead time for CD was five minutes. The separation requirements for CD were 5 NM horizontally, and 1000 ft vertically.

3) Airspace Concepts and Concept Implementation: Four airspace concepts are tested, an unstructured airspace concept with no procedural restrictions and three types of Layered concepts, the concepts are summarized in Table VI. Each Layered concept has a defined heading range per each layer. Sometimes the concepts have more then one layer with the same heading range, this is called layer sets. Table VII shows the separation criteria, the height of each layer, and the lower and higher limit of the airspace.

Table VI
Airspace Concepts

Symbol	Name	Heading Range Per Layer, α	Number of Layer Sets, κ
UA	Unstructured Airspace	-	-
L360	Layers 360	360°	8
L180	Layers 180	180°	4
L90	Layers 90	90°	2

Table VII
Airspace Parameters

Horizontal Separation	Vertical Separation	Layer Height	Altitude Lower Limit	Altitude Upper Limit
5 nm	1000 ft	1100 ft	4000 ft	11700 ft

To implement the concepts, scenarios are modified such that they fit the concept's constraints. The horizontal routes for both UA and Layers concepts are made in the same way. For the unstructured concept, the cruising altitude for the flight is proportional to the flight distance, see Eq. 18a. For the Layers concept the heading as well as the distance determines the altitude, see Eq. 18b. [7]

$$h_{ua} = h_{min} + \frac{h_{max} - h_{min}}{d_{max} - d_{min}}(d - d_{min}) \tag{18a}$$

$$h_{lay} = h_{min} + \tau\left(\left\lfloor \frac{h_{max} - h_{min}}{d_{max} - d_{min}}\kappa \right\rfloor \frac{360°}{\alpha} + \left\lfloor \frac{\psi}{\alpha} \right\rfloor\right) \tag{18b}$$

The above equations describe how the altitude is selected with respect to the distance and heading. Here h is the altitude, d is the distance, ψ is the aircraft's heading, α is the heading range per layer and κ is the number of layer sets. The "$\lfloor ... \rfloor$" is the floor operator.

B. Traffic Scenarios

1) Testing Region and Flight Profiles: The simulation region is 400×400 nm. Origins are chosen based on the spatial distribution type, in most cases uniformly distributed across the whole region. Then the destination point will be chosen according to the heading and distance. The origin

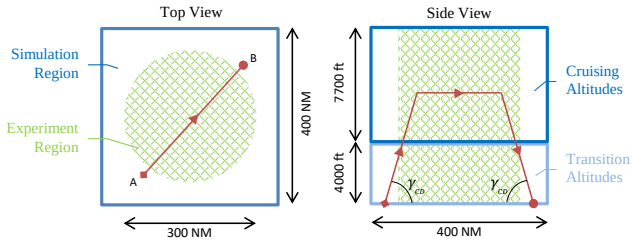

Figure 9. *Top and side view of the simulation environment, an example trajectory is shown. Taken from [7]*

and destination points can be located at any point within the simulation area.

Because the routes need to be within the simulation region, the traffic will be less dense near the edges of the simulation area, and the density will be zero on the edges. The results of the simulation will only be relevant in a specific zone within the simulation region. This is the region where the results will be analyzed in, a circle with a diameter of 300 nautical miles. Figure 9 shows a top and side view of the simulation region. It shows an example of a horizontal and a vertical route.

Aircraft will spawn at the lower boundary of the transition altitudes, see Figure 9, and climb up to their cruising altitude. All aircraft cruise distance. The aircraft will then descent to the destination point. All aircraft have the same climb and descent angle.

2) Scenario Generator: The scenario generator will choose semi-random values for heading, spawning points, distance and speed (only for speed experiments) relevant to the distribution type that is being tested. Using these, it will then compute the correct altitude and which layer is used for the Layers concepts, and choose an appropriate destination point within the simulation area that depends on the heading and distance. Figure 10 shows a flow chart of how the scenario generator works.

For a scenario generation which needs to have a specific spatial distribution the origin points and destination points needs to be specified within a certain area. This is so that the traffic will cross the middle of the area to create a hotspot. For example when creating a density hotspot in the center, the origin points need to be within a specific area determined within two circles, close to the edge of the simulation area. The destination points need to be within another area determined by two circles, close to the center. The sizes of the areas need to be specifically designed with respect to the minimum and maximum distance flown. Figure 11 show examples of origin and destination points plus one trajectory as an example. Because there is a minimum travel distance for aircraft in the simulations, the trajectory is forced though the center of the simulation area. This is caused by the areas which the origin and destination points are in and thus creates a density hotspot.

C. Independent variables

The independent variables of the five experiments performed are given below.

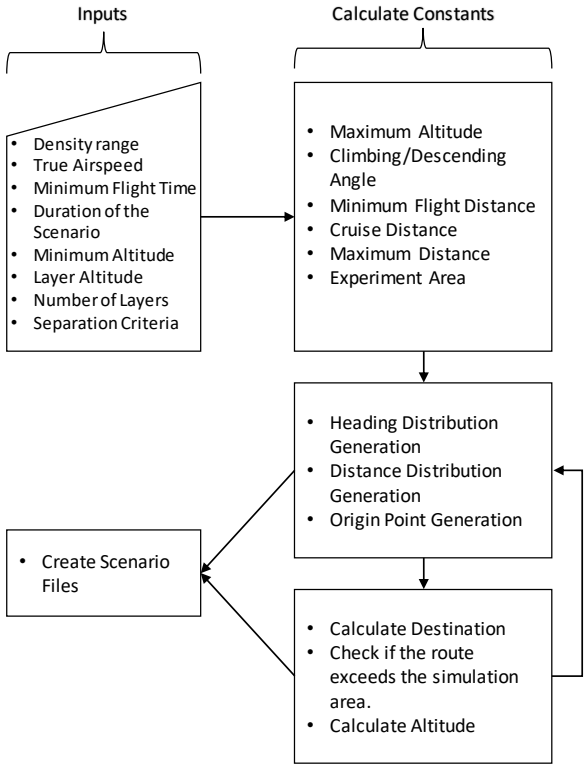

Figure 10. *A flow chart of the scenario generation.*

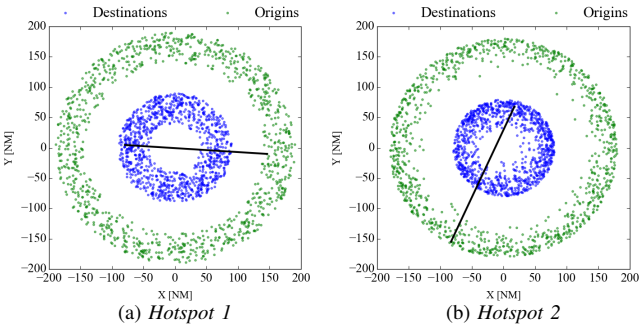

(a) *Hotspot 1* (b) *Hotspot 2*

Figure 11. *The origin (green) and destination (blue) points, with one example trajectory. To the left is the larger hotspot and to the right is the smaller hotspot.*

1) Baseline Experiment:

- Airspace concept: Unstructured Airspace, Layers 360, Layers 180, Layers 90.
- Traffic demand densities: 5 different densities, see Table VIII.

Total number of simulations to run:

- 4 concepts $\times$ 5 densities $\times$ 5 repetitions $=$ 100 simulations.

2) Heading Experiment: The heading experiment is to strictly check the effects of heading distributions other than uniform. It is not realistic that all aircraft have a uniformly distributed heading. The independent variables for the heading experiments are:

Table VIII
TRAFFIC DEMAND SCENARIOS (VALUES FOR SIMULATION REGION)

Density [AC/10000 nm^2]	Number of instantaneous AC
5	80
18	302
36	589
71	1146
100	1600

- Heading distribution, 3 distributions will be tested. Normal distribution, bimodal distribution and ranged normal distribution. See Figure 4.
- Airspace concept: Unstructured Airspace, Layers 360, Layers.
- Traffic demand densities: 5 different densities, see Table VIII.

Total number of simulations to run:

- 3 heading distributions $\times$ 2 concepts $\times$ 5 densities $\times$ 5 repetitions $=$ 150 simulations.

3) Speed Experiment: In the baseline scenario the airspeed is constant, but in this experiment it will vary between aircraft.

- Speed distribution: 3 distributions will be tested, normal distribution, bimodal distribution and uniform distribution. See Figure 6.
- Airspace concept: Unstructured Airspace, Layers 360, Layers 180, Layers 90.
- Traffic demand densities: 5 different densities, see Table VIII

Total number of simulations to run:

- 3 speed distributions $\times$ 4 concepts $\times$ 5 densities $\times$ 5 repetitions $=$ 300 simulations.

4) Altitude Variation Experiment: The altitude is modified by modifying the distance. The altitude distribution is more complicated than the other experiments, as for the Layers 180 and Layers 90 need to have the heading synchronized with the distance. The heading will only remain uniform for the unstructured airspace and Layers 360.

- Altitude distribution: 3 distributions will be tested, normal distribution, bimodal distribution and ranged-uniform. See Figure 7
- Airspace concept: Unstructured Airspace, Layers 360.
- Traffic demand densities: 5 different densities ranging, see Table VIII.

Total number of simulations to run:

- 3 altitude distributions $\times$ 2 concepts $\times$ 5 densities $\times$ 5 repetitions $=$ 150 simulations.

5) Spatial Experiment: This experiment's purpose is to see how the spatial distribution affects the accuracy of the conflict rate model. The spatial distribution is the distribution of aircraft's position within the airspace.

- Spatial distribution: 2 distribution will tested, where there are density hotspot in the middle of the airspace, of different sizes.
- Airspace concept: Unstructured Airspace, Layers 360, Layers 180, Layers 90.
- Traffic demand densities: 5 different densities, see Table VIII.

Total number of simulations to run:

- 2 spatial distribution $\times$ 4 concepts $\times$ 5 densities $\times$ 5 repetitions $=$ 200 simulations.

D. Dependent Variables

The goal is to compare the conflict count computed using the model with the conflict count logged during the simulations, so the two variables that are measured are the instantaneous number of conflict, and the instantaneous number of aircraft. The variables are logged in BlueSky while the simulation is running. To measure the accuracy, an additional parameter is introduced to the models, called the accuracy parameter (k value). See the basic model in Eq. 19.

$$C_{total_{UA}} = \frac{N_{total}}{2}(N_{total} - 1)\ p_2\ k \tag{19}$$

For the Layered concepts the fitting parameter is divided in 3 parts, k_{cruise} for two cruising aircraft conflicting, $k_{cruise-CD}$ for conflicts between cruising and climbing/descending aircraft and k_{CD} for conflicts between climbing/descending aircraft.

$$C_{total_{Lay}} = C_{cruise}k_{cruise} + C_{cruise-CD}k_{cruise-CD} + C_{CD}k_{CD} \tag{20}$$

Eqs. 19 and 20 are fitted to the simulation data using the least squares method where k is used as a fitting parameter. When the k is closer to 1, that means that the model is more accurate. If the parameter is less than 1, we can tell that the model is overestimating because the fitting parameter is less then 1 to scale it down. Also when k is larger than 1 we can tell that the model is underestimating and the fitting parameter is scaling up.

V. RESULTS

In this section the results for the four main experiments will be presented. The result from the baseline experiment is included for comparison with the results from the other experiments.

A. Heading Experiment

1) Effect of heading distribution on conflict count: Figures 12 and 13 show that the number of conflicts is highest when aircraft headings were uniformly distributed. The normal distribution and ranged uniform distribution, are similar but the bimodal distribution is closer to the uniform distribution. The expected horizontal relative velocity, in Table II, is very close for uniform distribution and bimodal distribution, and again close for normal-, and ranged-uniform distribution, and thus the results from the simulations were as expected.

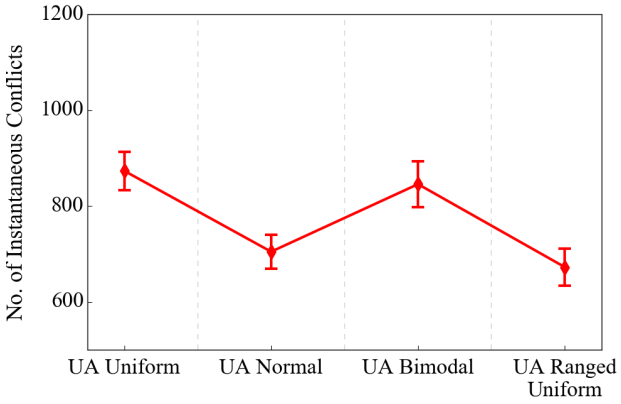

Figure 12. *Heading Experiment - The total number of instantaneous conflicts for the largest density being tested for Unstructured Airspace.*

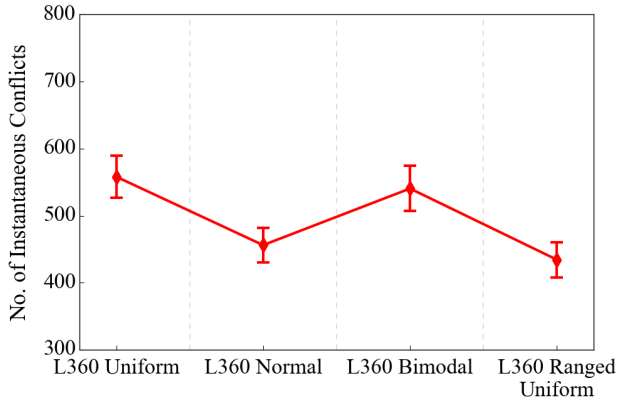

Figure 13. *Heading Experiment - The total number of instantaneous conflicts for the largest density being tested for the Layers 360 concept.*

2) Effect of heading distribution on model accuracy: The results from the experiments were fitted with both the analytical models and the adjusted models. The model accuracies of the analytical model are in Table IX, where the baseline scenario is the uniformly distributed heading. The accuracies of the normal-, and ranged-uniform distribution decrease, but the bimodal distribution does not cause much inaccuracies. The ranged-uniform has the worst accuracy, most likely because the relative horizontal velocity is the furthest away from the value that the baseline scenario has. Table II shows how the accuracies were predicted based on the difference in expected horizontal relative velocity. The accuracy results, for the analytical model, turned out as expected.

The accuracies using the numerically computed values to adjust the model are presented in Table X. The accuracy of the models generally increase. This is the case for both UA and Layered airspaces. The only case where there is a slight dip in accuracy is for the bimodal distribution. The reason for this decrease in accuracy is most likely that simulations are of course a stochastic process. In general the numerical adjustments worked really well when applied to the model.

Table IX
HEADING: BASELINE k VALUES AND ACCURACY.

		Baseline Uniform	Normal	Bimodal	Ranged Uniform
UA	k	1.024 (97.6%)	0.812 (76.8%)	1.004 (99.5%)	0.768 (69.9%)
L360	k_{cruise}	1.004 (99.5%)	0.779 (71.7%)	0.997 (99.7%)	0.735 (64.0%)
	$k_{cruise-CD}$	0.900 (88.9%)	0.761 (68.6%)	0.870 (85.0%)	0.725 (62.1%)
	k_{CD}	0.812 (76.9%)	0.676 (52.2%)	0.739 (64.7%)	0.628 (40.8%)

Table X
HEADING: ADJUSTED k VALUES AND ACCURACY.

		Baseline Uniform	Normal	Bimodal	Ranged Uniform
UA	k	1.024 (97.6%)	0.982 (98.1%)	1.041 (96.0%)	0.974 (97.3%)
L360	k_{cruise}	1.004 (99.5%)	1.005 (99.4%)	1.045 (95.6%)	1.012 (98.8%)
	$k_{cruise-CD}$	0.900 (88.9%)	0.924 (91.8%)	0.902 (89.2%)	0.924 (91.8%)
	k_{CD}	0.812 (76.9%)	0.865 (84.4%)	0.773 (70.7%)	0.855 (83.1%)

B. Speed Experiment

1) Effect of speed distribution on conflict count: The conflict count per number of instantaneous aircraft is presented in Figures 14, 15, 16 and 17. The figures show that the conflict count does not vary much between speed distributions. When the expected horizontal relative velocity was calculated for different speed distributions, the numerical values were all really similar for every distribution type, to this was predicted.

The reason why the results overlap for all speed conditions is because the average speed is the same in for all tested cases. This means that the conflict count models are insensitive to the shape of the speed distribution, and are only affected by the value the average speed in an airspace volume of interest.

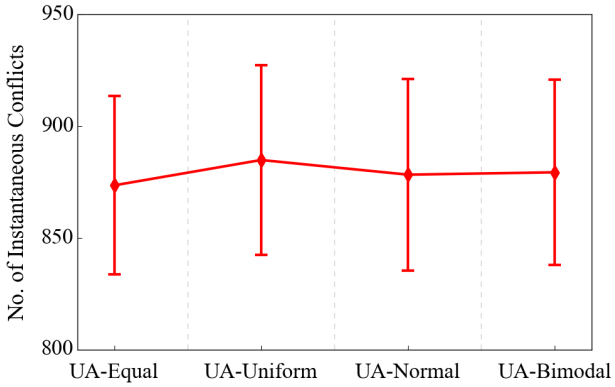

Figure 14. *Speed Experiment - The total number of instantaneous conflicts for the largest density being tested for Unstructured Airspace.*

2) Effect of speed distribution on model accuracy: Table IX shows the accuracies when the analytical model is fitted with the simulation results. The accuracies do not vary much from

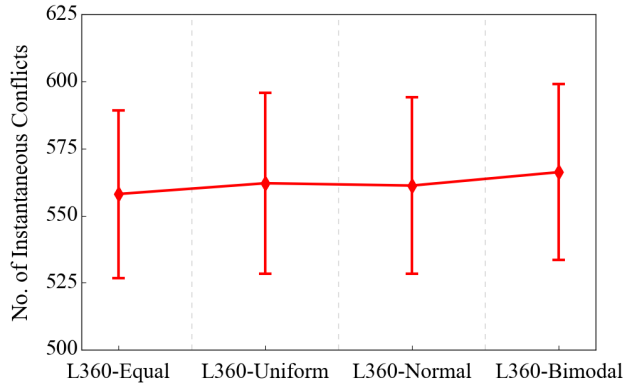

Figure 15. *Speed Experiment - The total number of instantaneous conflicts for the largest density being tested for the Layers 360 concept.*

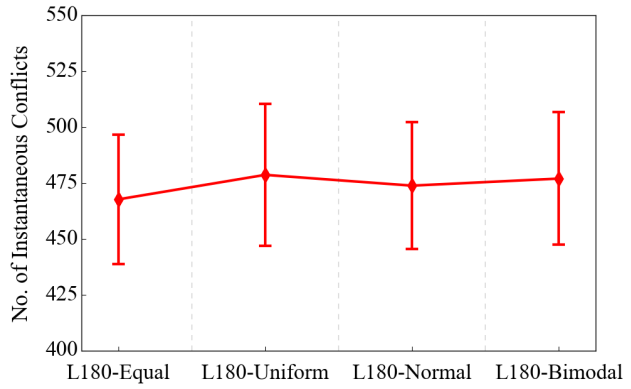

Figure 16. *Speed Experiment - The total number of instantaneous conflicts for the largest density being tested for the Layers 180 concept.*

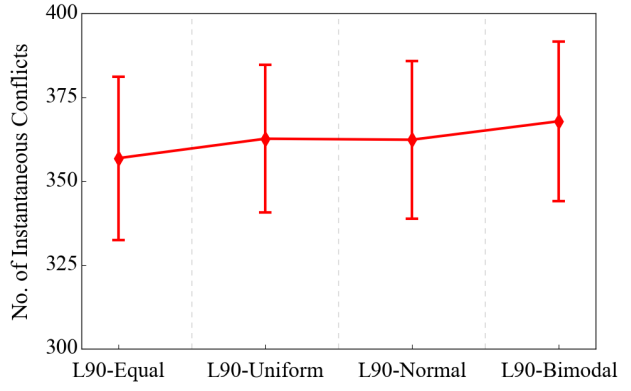

Figure 17. *Speed Experiment - The total number of instantaneous conflicts for the largest density being tested for the Layers 90 concept.*

the baseline scenario, which is where the speed distribution is equal.

The accuracies from the adjusted model is in Table XII. Using the numerically computed values still leads to good accuracies, they do not change much, but some get better and some get worse. This is mostly because of small changes in the expected horizontal relative velocity. Because $\bar{v}_{rel_h}$ does not change much, as can be seen in Table III, the accuracies were not expected to change much.

Table XI
SPEED: BASELINE k VALUES AND ACCURACY.

		Baseline Equal	Uniform	Normal	Bimodal
UA	k	1.024 (97.6%)	1.026 (97.4%)	1.026 (97.3%)	1.020 (97.9%)
L360	k_{cruise}	1.004 (99.5%)	0.997 (99.7%)	1.006 (99.3%)	1.003 (99.6%)
	$k_{cruise-CD}$	0.900 (88.9%)	0.898 (88.7%)	0.902 (89.2%)	0.907 (89.7%)
	k_{CD}	0.812 (76.9%)	0.850 (82.4%)	0.856 (83.2%)	0.860 (83.8%)
L180	k_{cruise}	0.995 (99.5%)	1.002 (99.7%)	1.005 (99.4%)	1.010 (98.9%)
	$k_{cruise-CD}$	0.897 (88.5%)	0.908 (89.9%)	0.901 (89.0%)	0.900 (88.9%)
	k_{CD}	0.814 (77.2%)	0.844 (81.6%)	0.829 (79.4%)	0.846 (81.8%)
L90	k_{cruise}	0.946 (94.3%)	0.960 (95.8%)	0.967 (96.6%)	0.974 (97.4%)
	$k_{cruise-CD}$	0.894 (88.1%)	0.891 (87.8%)	0.896 (88.4%)	0.896 (88.4%)
	k_{CD}	0.813 (77.1%)	0.837 (80.5%)	0.839 (80.8%)	0.855 (83.1%)

Table XII
SPEED: ADJUSTED k VALUES AND ACCURACY.

		Baseline Equal	Uniform	Normal	Bimodal
UA	k	1.024 (97.6%)	1.022 (97.7%)	1.029 (97.0%)	1.019 (98.0%)
L360	k_{cruise}	1.004 (99.5%)	0.992 (99.2%)	1.009 (99.0%)	1.001 (99.8%)
	$k_{cruise-CD}$	0.900 (88.9%)	0.895 (88.3%)	0.905 (89.5%)	0.906 (89.6%)
	k_{CD}	0.812 (76.9%)	0.846 (81.8%)	0.859 (83.6%)	0.859 (83.7%)
L180	k_{cruise}	0.995 (99.5%)	0.991 (99.1%)	1.007 (99.2%)	1.003 (99.6%)
	$k_{cruise-CD}$	0.897 (88.5%)	0.905 (89.5%)	0.904 (89.3%)	0.899 (88.8%)
	k_{CD}	0.814 (77.2%)	0.841 (81.1%)	0.832 (79.9%)	0.845 (81.7%)
L90	k_{cruise}	0.946 (94.3%)	0.928 (92.3%)	0.960 (95.8%)	0.949 (94.7%)
	$k_{cruise-CD}$	0.894 (88.1%)	0.888 (87.4%)	0.899 (88.7%)	0.895 (88.3%)
	k_{CD}	0.813 (77.1%)	0.833 (80.0%)	0.842 (81.2%)	0.854 (83.0%)

C. Altitude experiment

1) Effect of altitude distribution on conflict count: Figures 18 and 19 show that varying the altitude distribution changes the number of instantaneous conflict. It can be noted that a uniform altitude distribution causes the least number of conflicts. This suggests that the analytical model accuracy should be underestimating for the other altitude distributions.

2) Effect of altitude distribution on model accuracy: Table XIII shows the accuracies where the model was fitted with the data using the analytical model that is derived for a uniform altitude distribution scenario and the adjusted k values using

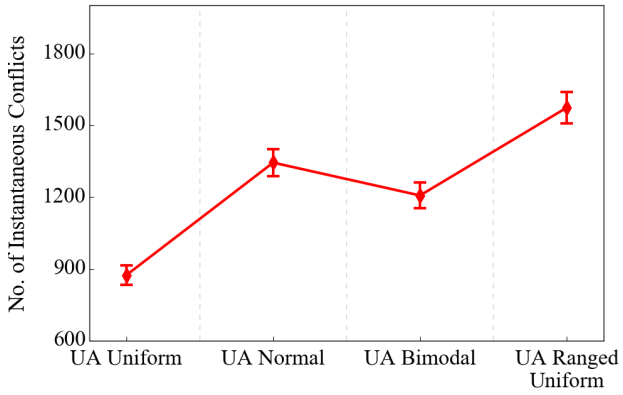

Figure 18. *Altitude Experiment - The total number of instantaneous conflicts for the largest density being tested for Unstructured Airspace.*

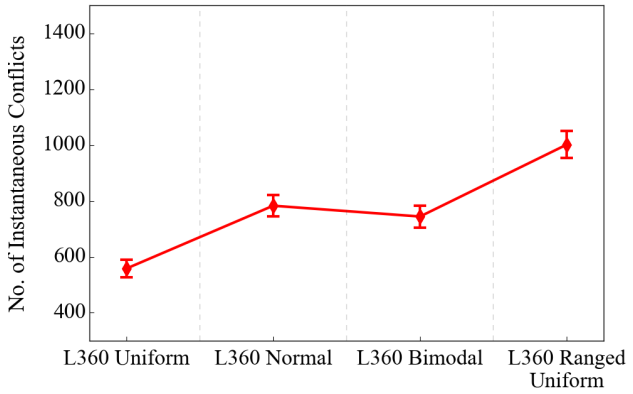

Figure 19. *Altitude Experiment - The total number of instantaneous conflicts for the largest density being tested for the Layers 360 concept.*

the numerical conflict count model. The baseline scenario has the uniform distribution. The accuracies were affected severely, the bimodal distribution was affected the least but very inaccurate still, but the other two distributions have very similar accuracies. For the layered concepts the ranged-uniform distribution had the worst accuracy. When the aircraft are distributed uniformly over half the altitude, it is expected that the conflicts will be twice as many. This was the results of the Layered concept experiments.

Table XIV shows the accuracy when the data is fitted with the adjusted model. When the values in Table IV for the UA, and Table V are the values used for the Layered concept. The accuracies are greatly improved when the adjustments are applied. In the Layered concept the $k_{cruise-C/D}$ and $k_{C/D}$ parameters are not changed, that is because the altitude distribution only affects the cruising aircraft. The accuracies work well for all scenarios, and the analytical model is applicable with the numerical adjustments.

D. Spatial Experiment

1) Effects of spatial distribution on conflict count: Figures 20, 21, 22 and 23 show the conflict count for the largest number of instantaneous aircraft for the baseline scenario and a

Table XIII
ALTITUDE: BASELINE k VALUES AND ACCURACY.

		Baseline Uniform	Normal	Bimodal	Ranged Uniform
UA	k	1.024 (97.6%)	1.569 (63.7%)	1.416 (70.6%)	1.576 (63.4%)
L360	k_{cruise}	1.004 (99.5%)	1.664 (60.0%)	1.573 (63.5%)	2.041 (48.9%)
	$k_{cruise-CD}$	0.900 (88.9%)	0.936 (93.2%)	0.911 (90.3%)	0.914 (90.6%)
	k_{CD}	0.812 (76.9%)	0.870 (85.1%)	0.827 (79.1%)	0.766 (69.5%)

Table XIV
ALTITUDE: ADJUSTED k VALUES AND ACCURACY.

		Baseline Uniform	Normal	Bimodal	Ranged Uniform
UA	k	1.024 (97.6%)	1.102 (90.6%)	0.994 (99.4%)	0.957 (95.5%)
L360	k_{cruise}	1.004 (99.5%)	0.881 (86.6%)	0.894 (88.2%)	1.015 (98.4%)
	$k_{cruise-CD}$	0.900 (88.9%)	0.936 (93.2%)	0.911 (90.3%)	0.914 (90.6%)
	k_{CD}	0.812 (76.9%)	0.870 (85.1%)	0.827 (79.1%)	0.766 (69.5%)

scenario with a density hotspot. The conflict count is increased very significantly when the density is larger in one area.

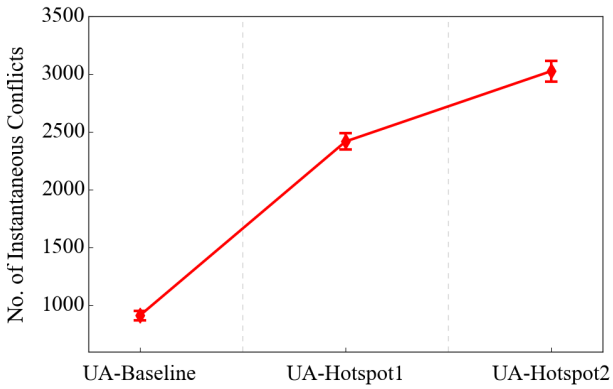

Figure 20. *Spatial Experiment - The total number of instantaneous conflicts for the largest density being tested for Unstructured Airspace.*

2) Effects of spatial distribution on model accuracy: In Table XV are the values when the simulation data is fitted with the baseline conflict count model. In general the accuracies are very low for the hotspot scenarios, except for aircraft that are climbing/descending. Table XVI shows the accuracy values when the conflict count form the simulations are fitted with the adjusted model. The accuracies are improved in all cases, and are even more accurate than the baseline model. This means that the model can be applied to different areas when dealing with a hotspot.

VI. DISCUSSION

This paper investigated the effect of traffic scenario related assumptions on the accuracy of analytical conflict count models for unstructured and layered airspace designs. Additionally,

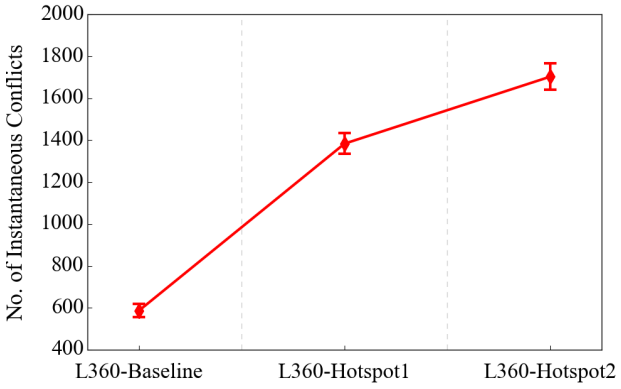

Figure 21. *Spatial Experiment - The total number of instantaneous conflicts for the largest density being tested for the Layers 360 concept.*

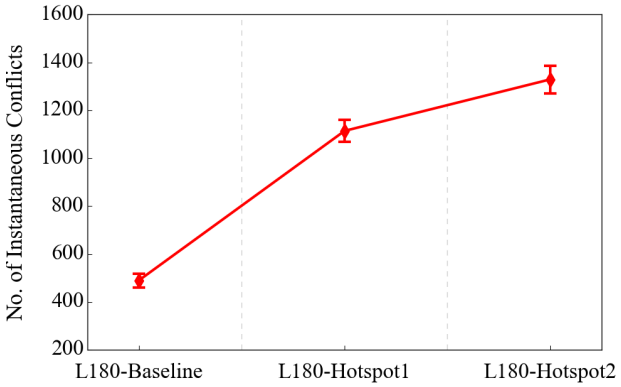

Figure 22. *Spatial Experiment - The total number of instantaneous conflicts for the largest density being tested for the Layers 180 concept.*

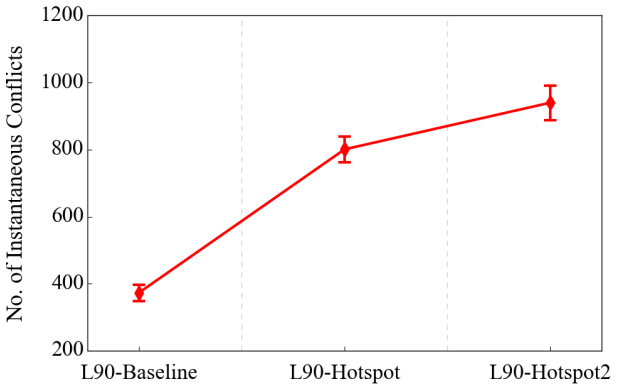

Figure 23. *Spatial Experiment - The total number of instantaneous conflicts for the largest density being tested for the Layers 90 concept.*

numerical methods were proposed as a means to improve model accuracies when traffic scenario assumptions are violated. The proposed methods were tested using 5 different fast-time simulation experiments. This section discusses the results of these experiments in relation to the main research questions of this study.

Table XV
SPATIAL: BASELINE k VALUES AND ACCURACY.

		Baseline Uniform	Hotspot 1	Hotspot 2
UA	k	1.025 (97.6%)	1.724 (57.9%)	2.077 (48.1%)
L360	k_{cruise}	1.004 (99.5%)	2.080 (48.0%)	2.575 (38.8%)
	$k_{cruise-CD}$	0.900 (88.9%)	0.561 (21.7%)	0.558 (20.8%)
	k_{CD}	0.812 (76.9%)	1.041 (96.0%)	1.114 (89.7%)
L180	k_{cruise}	0.995 (99.5%)	2.178 (45.9%)	2.616 (38.2%)
	$k_{cruise-CD}$	0.897 (88.5%)	0.563 (22.5%)	0.562 (22.2%)
	k_{CD}	0.814 (77.2%)	1.051 (95.0%)	1.121 (89.1%)
L90	k_{cruise}	0.946 (94.3%)	2.479 (40.3%)	2.972 (33.6%)
	$k_{cruise-CD}$	0.894 (88.1%)	0.585 (29.1%)	0.582 (28.3%)
	k_{CD}	0.813 (77.1%)	1.076 (92.8%)	1.141 (87.5%)

Table XVI
SPATIAL: ADJUSTED k VALUES AND ACCURACY.

		Baseline Uniform	Hotspot 1	Hotspot 2
UA	k	1.025 (97.6%)	0.906 (89.6%)	1.017 (98.2%)
L360	k_{cruise}	1.004 (99.5%)	1.035 (96.6%)	1.067 (93.6%)
	$k_{cruise-CD}$	0.900 (88.9%)	0.810 (88.7%)	0.824 (78.7%)
	k_{CD}	0.812 (76.9%)	0.752 (68.0%)	0.843 (81.5%)
L180	k_{cruise}	0.995 (99.5%)	1.083 (92.2%)	1.084 (92.2%)
	$k_{cruise-CD}$	0.897 (88.5%)	0.813 (77.1%)	0.829 (79.5%)
	k_{CD}	0.814 (77.2%)	1.049 (95.3%)	0.848 (82.2%)
L90	k_{cruise}	0.946 (94.3%)	1.232 (81.1%)	1.233 (81.0%)
	$k_{cruise-CD}$	0.894 (88.1%)	0.845 (81.6%)	0.851 (82.6%)
	k_{CD}	0.813 (77.1%)	1.073 (93.1%)	0.860 (83.8%)

A. Do the traffic scenario assumptions affect the accuracy of the analytical conflict count models?

Like mentioned before, the derivation of the model make certain assumptions. The heading distribution is assumed to be uniform. The speed is assumed to be equal for all aircraft. Aircraft are assumed to be spread evenly through all flight levels (uniform altitude distribution). The airspace that the model is being applied to, is assumed to have uniform density (uniform spatial distribution).

The heading distribution affects the expected horizontal relative velocity($\bar{v}_{rel_h}$). The analytical mode uses the baseline value for $\bar{v}_{rel_h}$ for all scenarios. The accuracy is affected the least when using bimodal heading distribution because the angle between two aircraft is more likely to be larger for a bimodal heading distribution than for a normal or ranged-uniform distributions expected relative velocity. The $\bar{v}_{rel_h}$

value is much lower for the normal distribution, and for the ranged-uniform. Those values are close to each other which is reflected in the results of the experiment. The normal distribution gives slightly better results than the ranged-uniform, but that is because $\bar{v}_{rel_h}$ is slightly greater.

The speed is another factor in computing the expected horizontal relative velocity. The results of the simulations do not show that the shape of the speed distribution has any significant effect on the expected horizontal relative velocity, as long as the average speed is the same. The results from non of the distribution that were being tested, stood out as different from the other. As the values for $\bar{v}_{rel_h}$ were all very similar, the speed distribution was not expected to affect the accuracies much, which proved to be the case.

The altitude distribution affects the unstructured and layered airspace differently. For the UA model, the uniform altitude distribution allows the conflict probability (p_2) to be expressed in terms of ratio between volume searched by the CD and the total volume of the airspace. But when the altitude distribution is not uniform the vertical part of the volume needs to be compensated for. The ranged-uniform altitude distribution was expected to have 50% accuracy because only half of the airspace is being used, but the actual accuracy is a bit higher. This is because the altitude distribution in the simulations affects mostly cruising aircraft. In the simulations the aircraft are being generated at a fixed time interval and all aircraft have the same climb rate, so climbing/descending aircraft still have a mostly uniform altitude distribution. The normal-, and bimodal distributions, were expected to have very close accuracies, because they have very similar p_v values (see Table V). Still the simulation results show that they differ some.

However the altitude distribution for layered concept affects the number of possible combinations of two aircraft. Because the height of each layer is larger than the vertical separation criteria, there is no chance of overlapping with an aircraft flying in a different altitude. The conflict count of each layer is computed as if it was a small airspace with only a single available flight level. The results for cruising-climbing/descending conflicts and climbing/descending conflicts were similarly accurate as the baseline scenario. The accuracies for the cruising conflicts were however much smaller. For the ranged-uniform distribution here, we can see that the accuracy is about half as accurate as the fully uniform distribution. Like stated earlier, only half of the altitudes are being used, so it is logical that there will be twice as many conflicts.

For the spatial distribution experiment, the accuracy was effected very much. The number conflicts were much higher than the baseline model suggested for UA and cruising aircraft in the layered concepts. Since all the cruising aircraft have to pass through the hotspot, the conflict probability is much higher for those aircraft. However, regarding conflict between cruising and climbing/descending aircraft, the model was overestimating, but conflicts for only climbing/descending aircraft were actually more accurate than for the baseline scenario.

To summarize, the heading distribution does affect the accuracy of the analytical conflict count model. The varying speed does not seem to have much affect on the accuracy. The results for the altitude distributions show that when the aircraft are not spread evenly across all the altitudes, it has a significant affect on the accuracy. The spatial distribution has very large effect on the accuracy.

B. Which assumption has the largest effect on the accuracy?

Of the scenarios tested in this thesis, the hotspot in spatial distribution experiment causes the largest inaccuracies. When the altitude distribution is assumed to be uniform, it has much larger effect on the accuracy than the heading distribution, considering the traffic scenarios used in this research. While the speed distribution does not affect the model accuracy that much, it has the smallest effect.

C. Can numerical adjustments improve the accuracy of the models when the assumptions are violated?

In short, yes, the accuracies are improved by using the numerical values.

For the heading distribution, the adjustment that was applied showed very a good accuracy when the adjusted model was fitted with results from the experiments. When the numerically computed expected horizontal relative velocities (from Table II) are used to adjust the model, the accuracy for the normal-, and ranged-uniform distribution are improved greatly. But for the bimodal distribution the accuracy is decreases slightly. This might be because the simulations are stochastic and the difference in the accuracies is not very large. As stated earlier the accuracy for the bimodal distribution was already quite good so changes to the model did not affect the accuracy severely. In general, the conflict count model's flexibility is improved by using this adjustment.

Although the results from the speed experiments were quite accurate, the numerically computed values for the $\bar{v}_{rel_h}$ from Table III were used for adjustment. This improved some of the accuracies on a very small scale, while decreasing the accuracies of others. This change is minimal, and because the numerical values for $\bar{v}_{rel_h}$ were so close to the value used for the analytical model, this was expected. In the case of the speed assumption, an adjustment is not necessary but is still an option.

The values in Table IV are used to improve the inaccuracies for a non-uniform altitude distribution in unstructured airspace. The values are used as a part of the ratio between the volume searched by the CD and the total volume (as described in Section III). For normal and bimodal distributions, the values are the same. This is because the bimodal distribution is a distribution with two normal curves with half the size of the 'regular' normal distribution. When the values are derived the curves are integrated and it makes sense that they would yield the same value.

When the number of combinations is calculated for every layer instead of assuming the same number of aircraft in each layer. When the adjustment was applied, it resulted in improved accuracies for cruising aircraft. The other k parameters for layered airspace were unaffected, because the adjustment is not applied there.

The method to improve the accuracy for different spatial distributions is not really based on using numerically computed

values like the other methods, but by applying the baseline model differently it may be improved. This method improves the accuracies for the scenario used in this paper. However, the application may have to be adjusted to the scenario that is being used. For example the airspace may have to be split up in more than two parts, which increases the number of terms in the equation.

D. Additional Considerations

The numerical methods presented in this paper to cope with traffic scenario assumptions have been tested for each assumption individually. In reality, it is likely that multiple aspects of traffic scenarios vary simultaneously; for example, both heading and altitude distributions are non-uniform for oceanic traffic. For such cases, the numerical adjustments for each individual traffic property can be combined, as long as the distribution shapes are known.

Some improvements can be made on the spatial distribution adjustment, by including the probability density function. This should be approached in a similar way as the altitude distribution adjustment is made, but for latitudinal and longitudinal distribution.

Although this research aims to investigate assumptions made in previous studies, there are still some assumptions made here. It is assumed that there is no effect from weather or terrain, and perfect aircraft state information is used for conflict detection. Although, climbing and descending aircraft are included, the scope of this research is limited to en-route airspace operations.

VII. Conclusion

The goal of this research was to study the effect of traffic scenario properties on the accuracy of analytical conflict count models for unstructured and layered airspace designs. The conflict count models have been derived assuming uniform heading and altitude distribution, an equal speed and the same density throughout the experiment area. Five experiments were performed: Four which addresses these assumptions and one which meets the assumptions, which is then used for comparison. Numerical adjustments to the models were made to compensate for the error caused by deviating by the ideal traffic scenario for the model. Then the accuracies of the analytical models without the adjustments were determined as well as the accuracies of the adjusted models. The following conclusions can be drawn:

- The analytical conflict count models are able to predict the shape of the relationship between the number of instantaneous conflicts and the instantaneous number of aircraft for all traffic scenario properties, but the accuracy decreases as the scenario assumptions are broken.
- The heading distribution affects the accuracy significantly.
- If all aircraft are assumed to have the same speed, it does not affect the accuracy significantly.
- Assuming a uniform altitude distribution causes large inaccuracies when the traffic scenario does not have a uniform altitude distribution.
- The accuracy for a traffic scenario with uneven traffic density can be improved by applying the analytical model to different specific sections of the airspace.
- The spatial distribution has a largest effect on the accuracy of the analytical model.
- The accuracy can be improved by augmenting the analytical models with numerically computed values of the number of combinations of aircraft, or the conflict probability between two aircraft, depending on the scenario assumption that is violated.

References

[1] "Eurocontrol annual report," 2015.
[2] J. M. Hoekstra, R. C. J. Ruigrok, and R. Van Gent, "Free flight in a crowded airspace?" *Progress in Astronautics and Aeronautics*, vol. 193, pp. 533–546, 2001.
[3] M. Tra, "The effect of a layered airspace concept on conflict probability and capacity," 2016, MSc Thesis.
[4] E. Sunil, J. Ellerbroek, and J. M. Hoekstra, "Analysis of airspace structure and capacity for decentralized separation using fast-time simulations," *Journal of Guidance, Control and Dynamics*, vol. 40, pp. 38–51, 2017.
[5] M. R. Jardin, "Analytical relationships between conflict counts and air-traffic density," *Journal of Guidance, Control and Dynamics*, vol. 28, pp. 1150–1156, 2005.
[6] J. M. Hoekstra, J. Maas, M. Tra, and E. Sunil, "How do layered airspace design parameters affect airspace capacity and safety?" in *ICRAT confrence*, 2016.
[7] E. Sunil, J. Ellerbroek, J. Hoekstra, and J. Maas, "Three-dimensional conflict count models for unstructured and layered airpsace designs," Delft University of Technology.
[8] S. Endoh, "Aircraft collision models," MIT Department of Aeronautics and Astraonautics, Tech. Rep., 1982.
[9] J. M. Hoekstra and J. Ellerbroek, "Bluesky atc simulator project: an open data and open source approach," in *Research Gate*, 2016.

Part II

Scientific Paper Appendix

Appendix A

A-1 Heading Experiment

A-1-1 Fitting validation

Figures A-1 to A-8 show the validation for the fitting. Where the first two densities are used to fit the curve and the rest of the line is drawn with that fitting to see if if follows the data points for the higher densities.

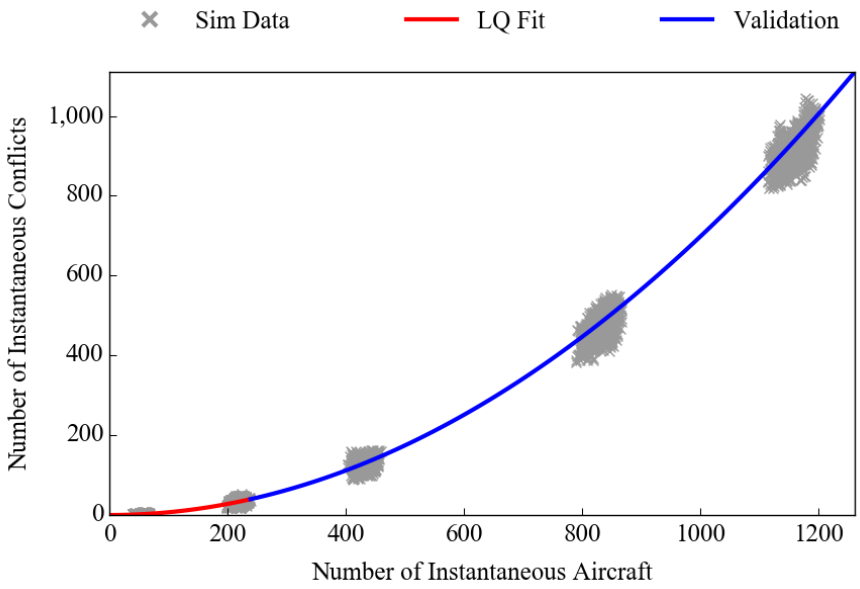

Figure A-1: Fitting validation for the UA, using uniform heading distribution.

Layers 360

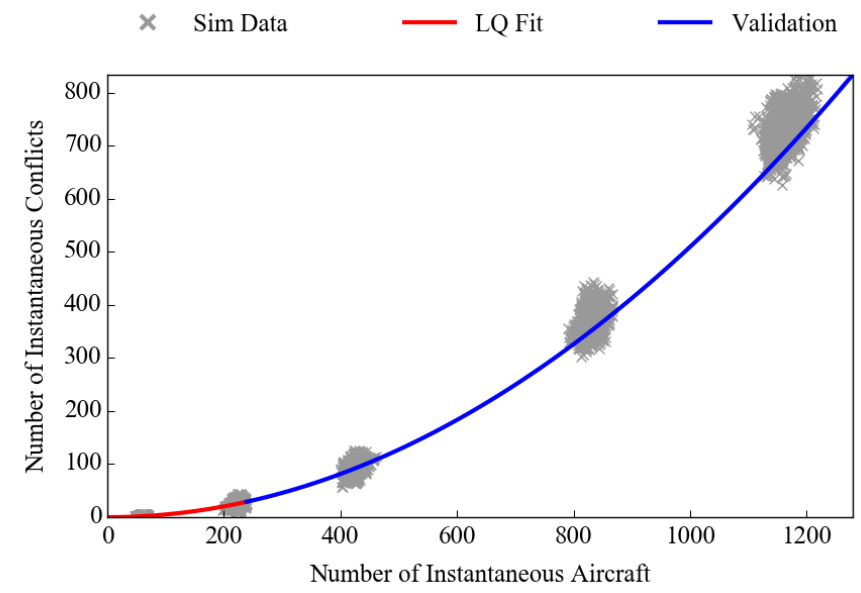

Figure A-2: Fitting validation for the UA, using normal heading distribution.

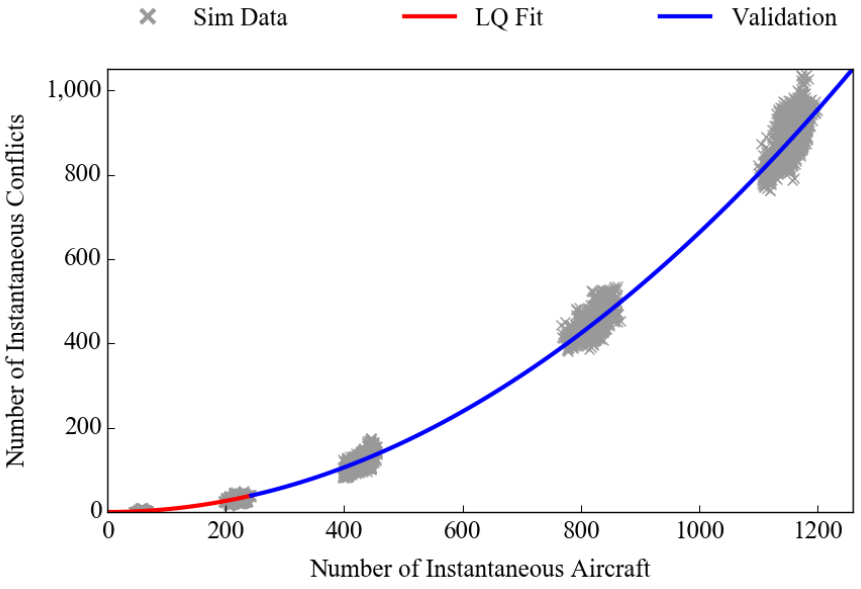

Figure A-3: Fitting validation for the UA, using bimodal heading distribution.

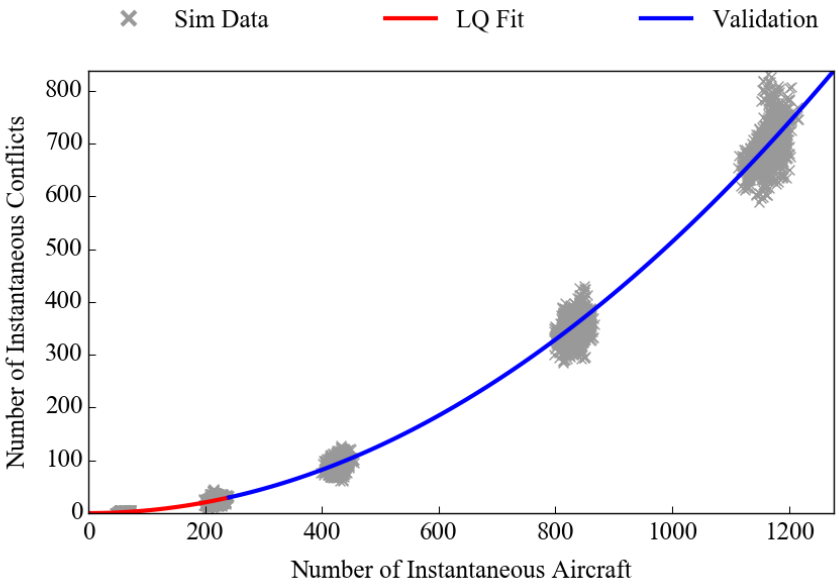

Figure A-4: Fitting validation for the UA, using ranged-uniform heading distribution.

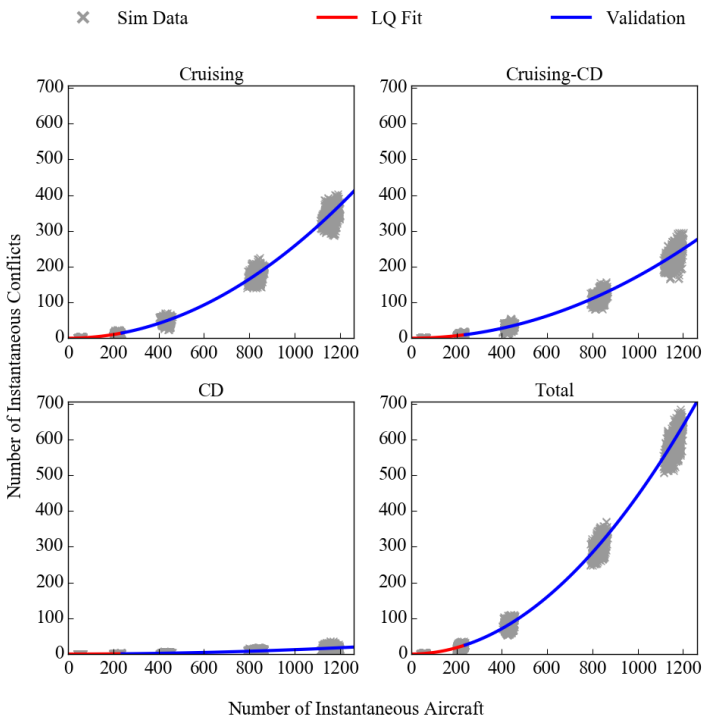

Figure A-5: Fitting validation for the Layers 360, using uniform heading distribution.

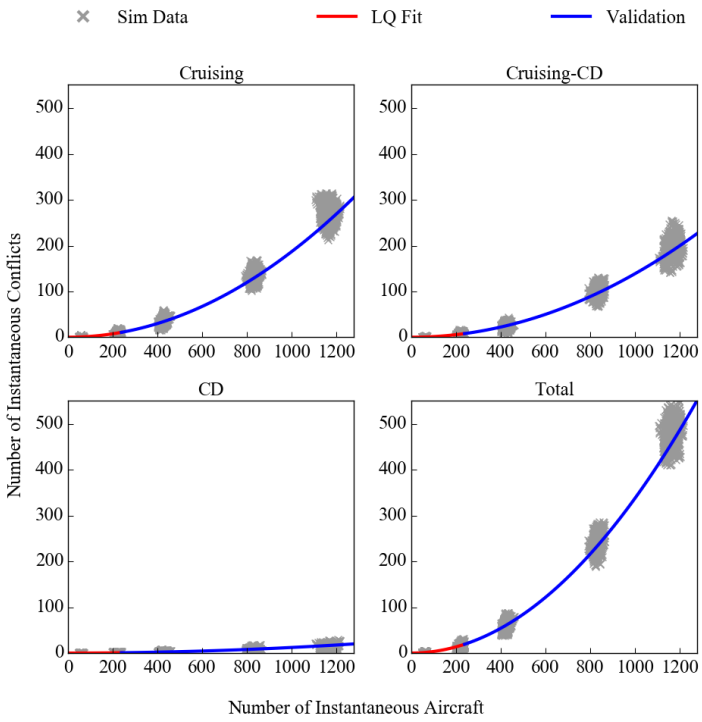

Figure A-6: Fitting validation for the Layers 360, using normal heading distribution.

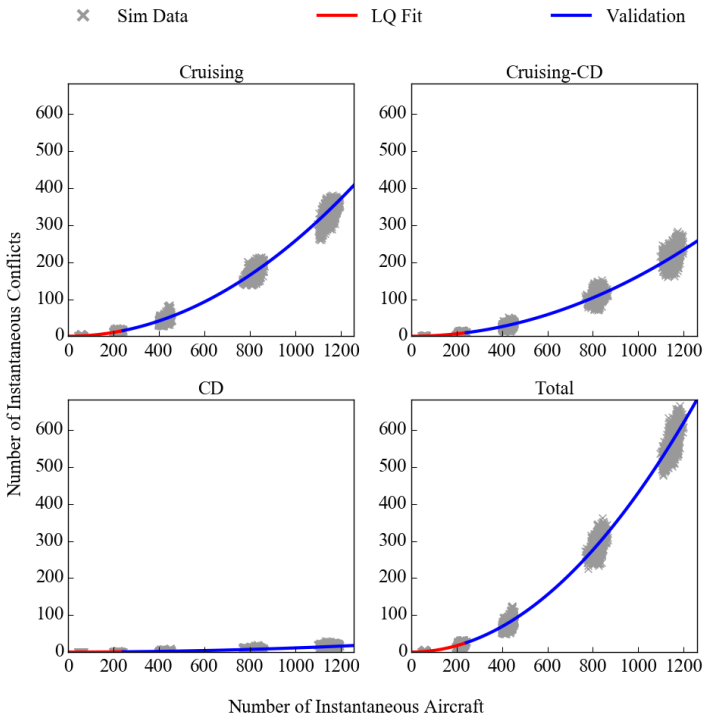

Figure A-7: Fitting validation for the Layers 360, using bimodal heading distribution.

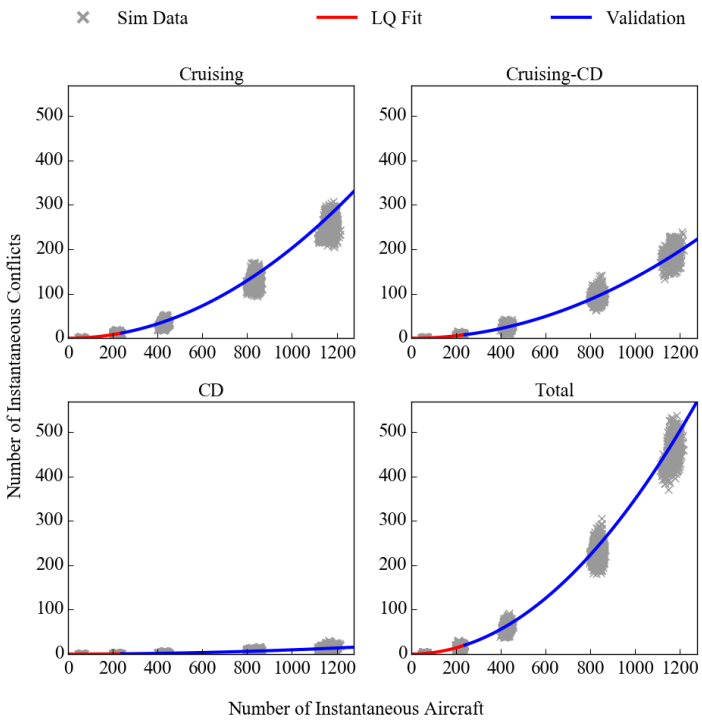

Figure A-8: Fitting validation for the Layers 360, using ranged-uniform heading distribution.

A-1-2 Number of conflicts affected by heading distribution

The total number of conflicts are shown in Figures A-9 and A-10. Figure A-11 shows the number of conflicts between two cruising aircraft. Figure A-12 shows the number of conflict between a cruising aircraft and an aircraft that is climbing or descending. Figure A-13 shows the number of conflicts for two aircraft that are both either cruising or climbing.

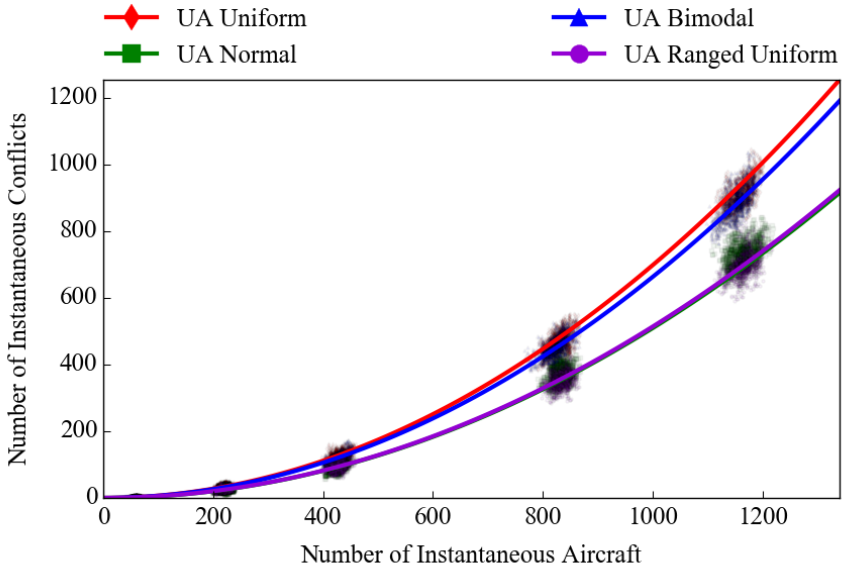

Figure A-9: The total number of conflicts for the UA, in the heading experiment.

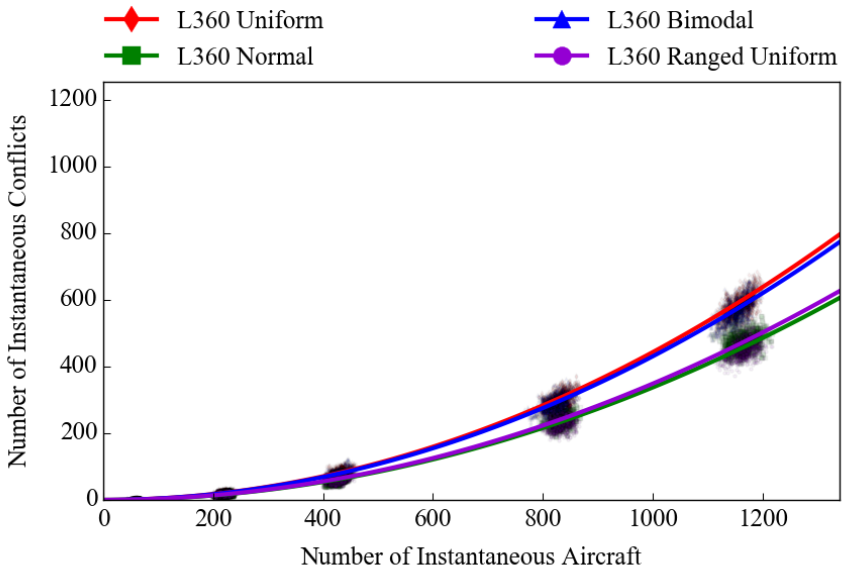

Figure A-10: The total number of conflicts for the Layers 360, in the heading experiment.

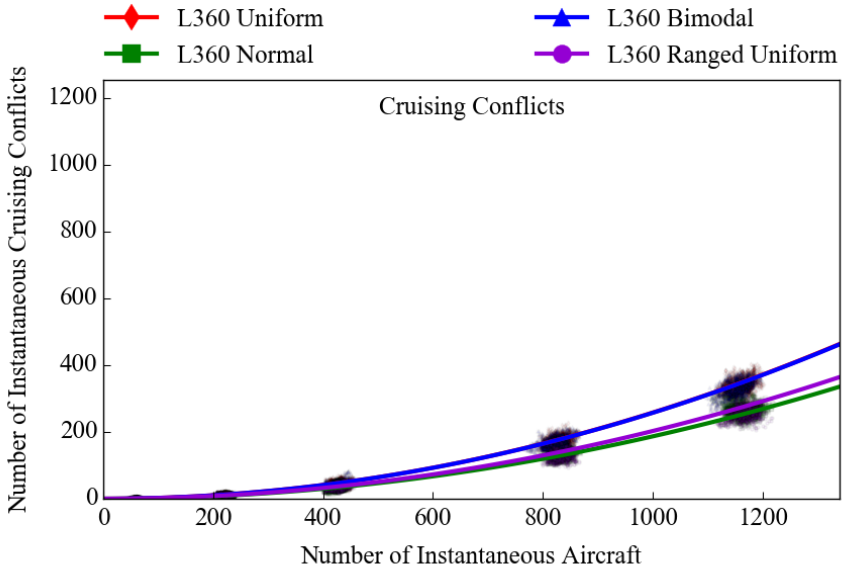

Figure A-11: The number of cruising conflicts for the Layers 360, in the heading experiment.

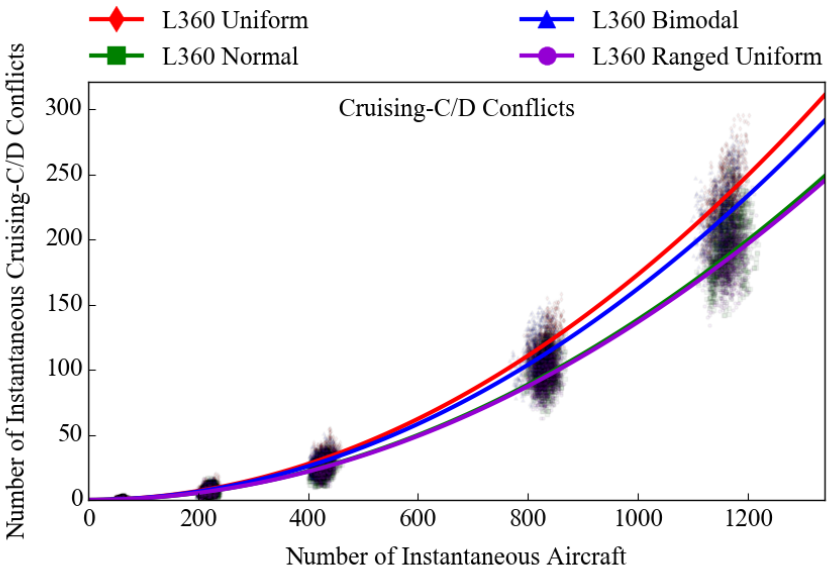

Figure A-12: The number of cruising-climbing/descending conflicts for the Layers 360, in the heading experiment.

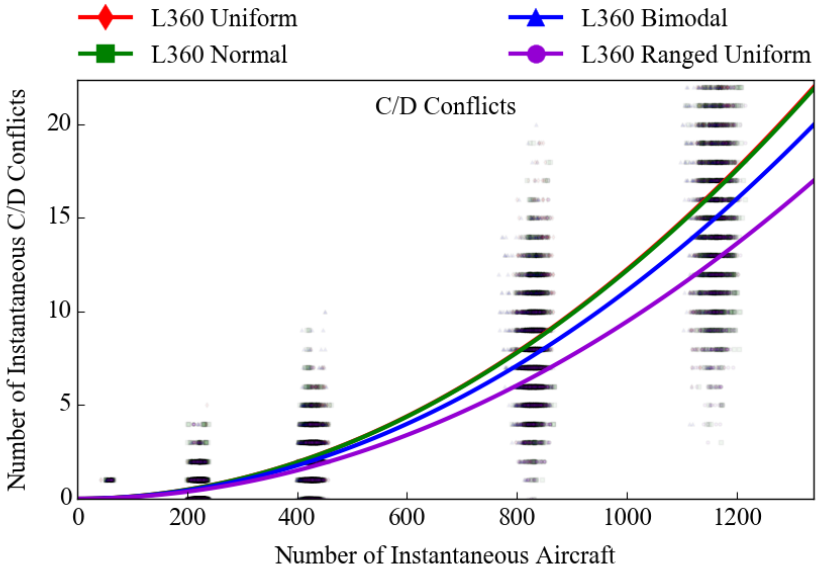

Figure A-13: The number of climbing/descending conflicts for the Layers 360, in the heading experiment.

A-2 Speed Experiment

A-2-1 Fitting validation

Figures A-14 to A-29 show the validation for the fitting. Where the first three densities are used to fit the curve and the rest of the line is drawn with that fitting to see if if follows the data points for the higher densities.

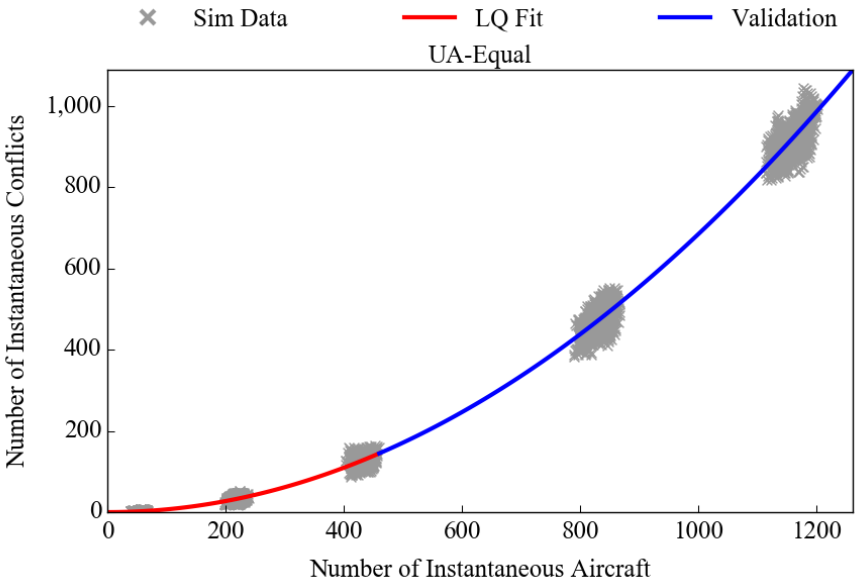

Figure A-14: Fitting validation for the UA, using equal speed distribution.

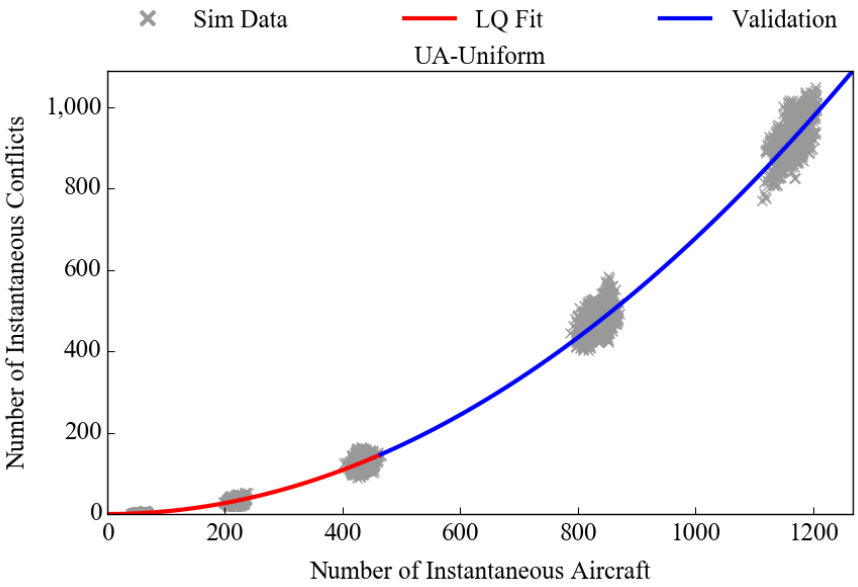

Figure A-15: Fitting validation for the UA, using uniform speed distribution.

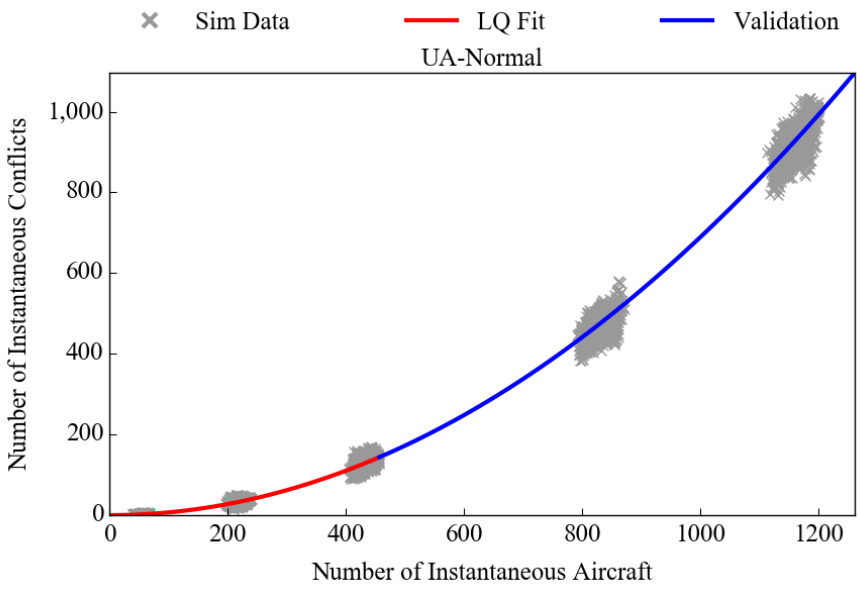

Figure A-16: Fitting validation for the UA, using normal speed distribution.

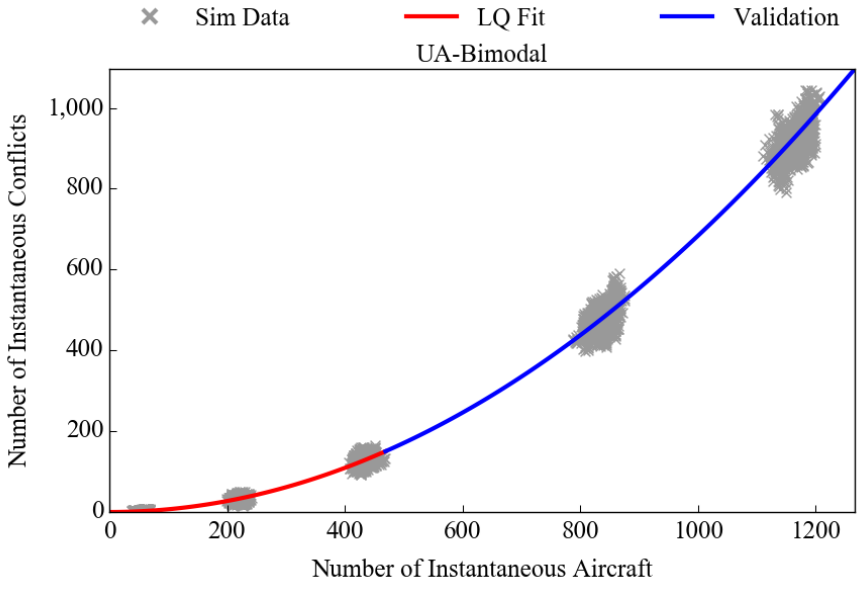

Figure A-17: Fitting validation for the UA, using bimodal speed distribution.

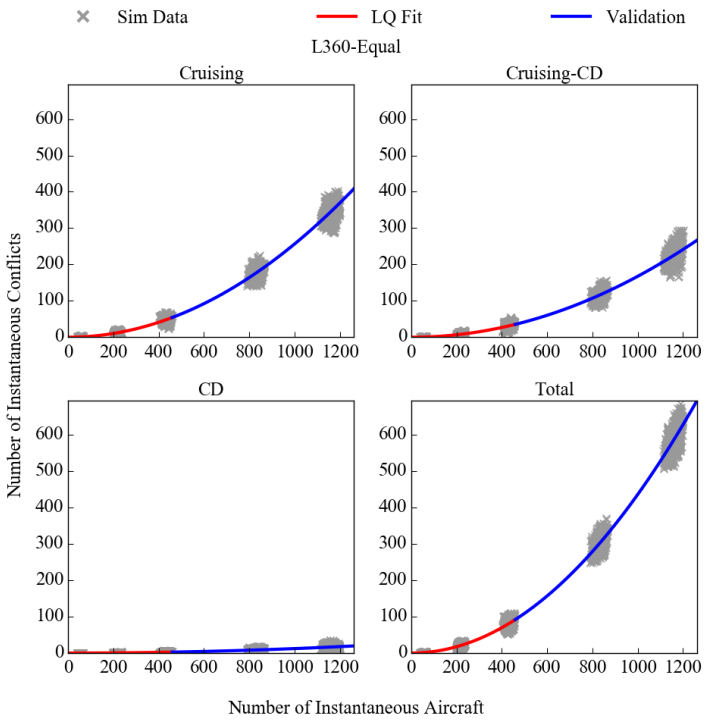

Figure A-18: Fitting validation for the Layers 360, using equal speed distribution.

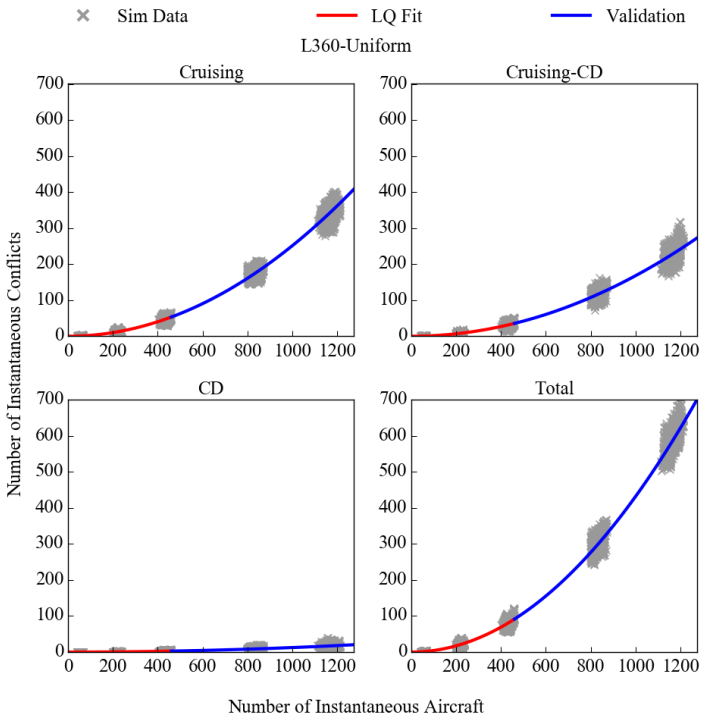

Figure A-19: Fitting validation for the Layers 360, using uniform speed distribution.

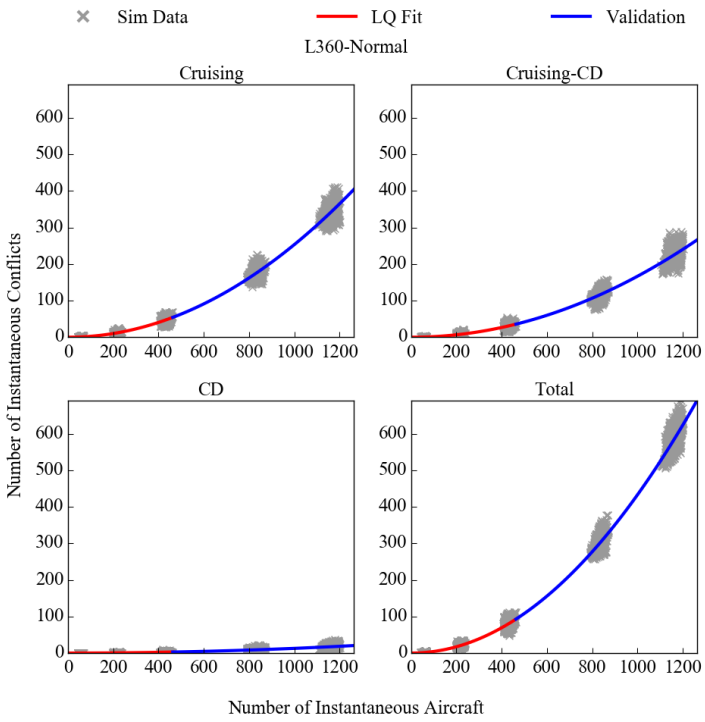

Figure A-20: Fitting validation for the Layers 360, using normal speed distribution.

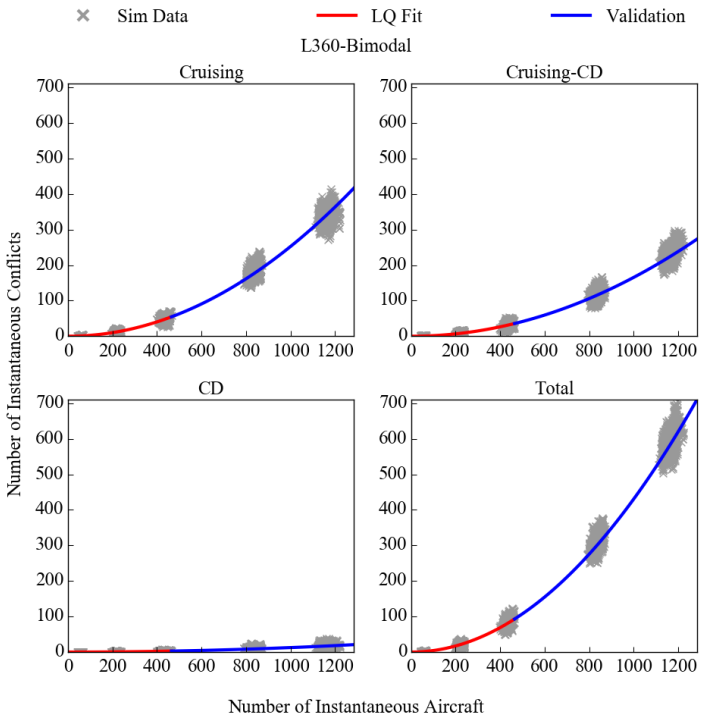

Figure A-21: Fitting validation for the Layers 360, using bimodal speed distribution.

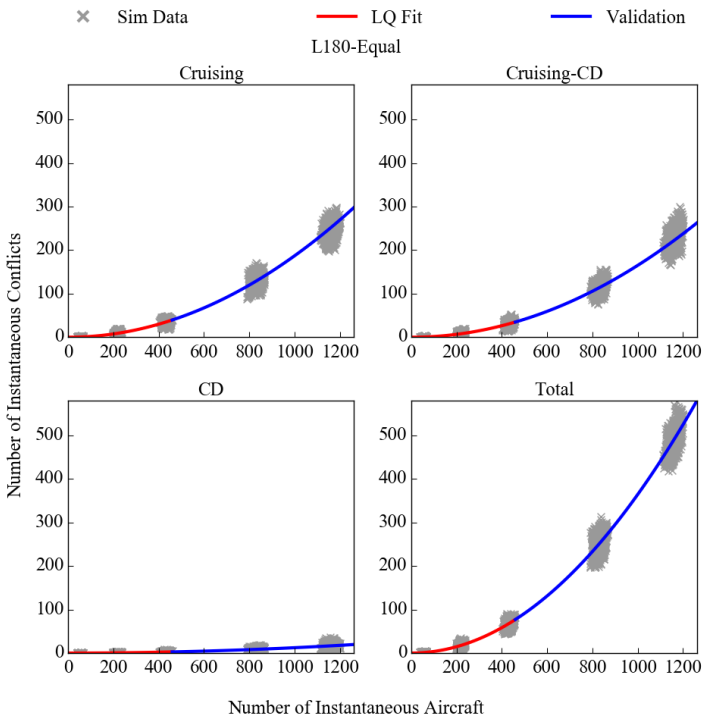

Figure A-22: Fitting validation for the Layers 180, using equal speed distribution.

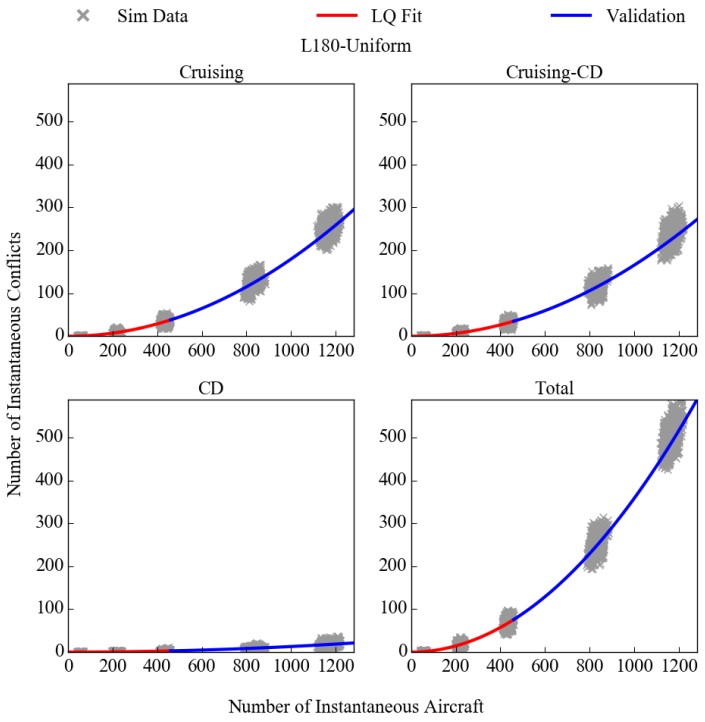

Figure A-23: Fitting validation for the Layers 180, using uniform speed distribution.

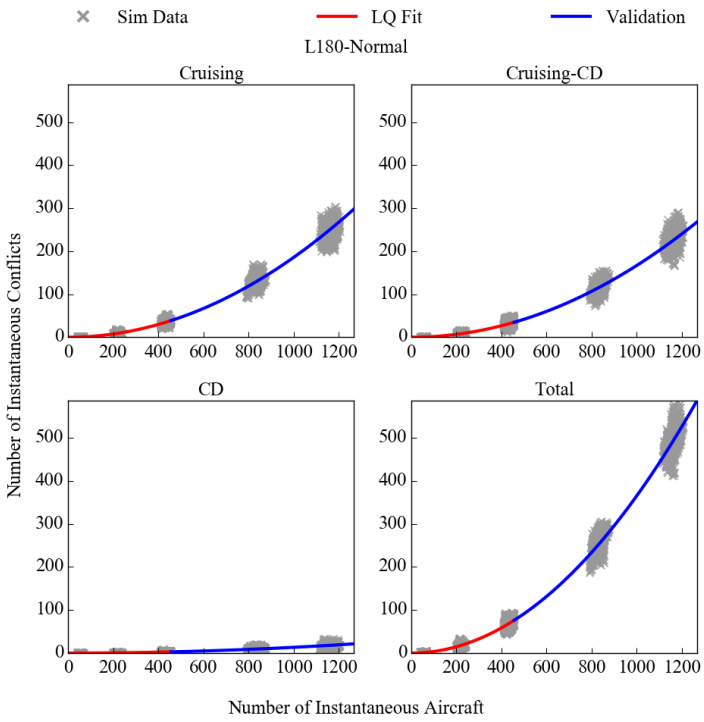

Figure A-24: Fitting validation for the Layers 180, using normal speed distribution.

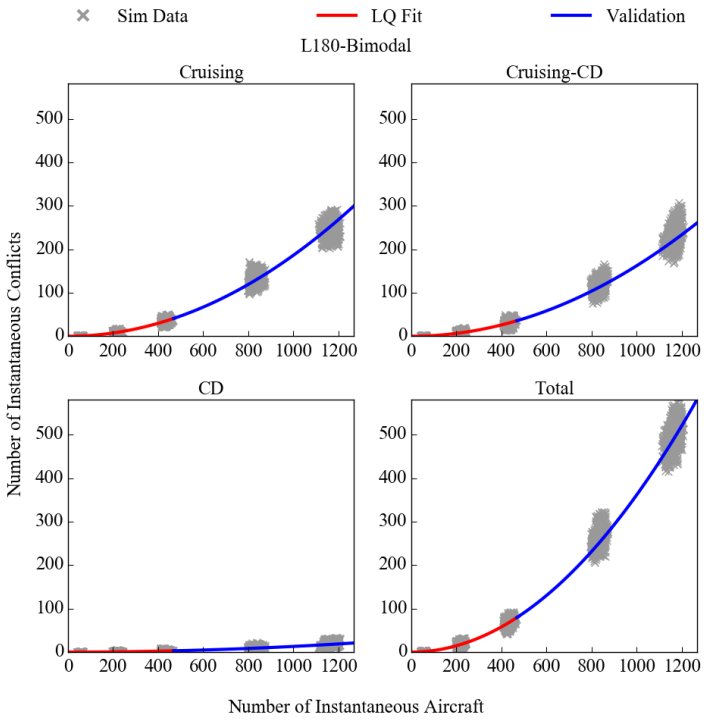

Figure A-25: Fitting validation for the Layers 180, using bimodal speed distribution.

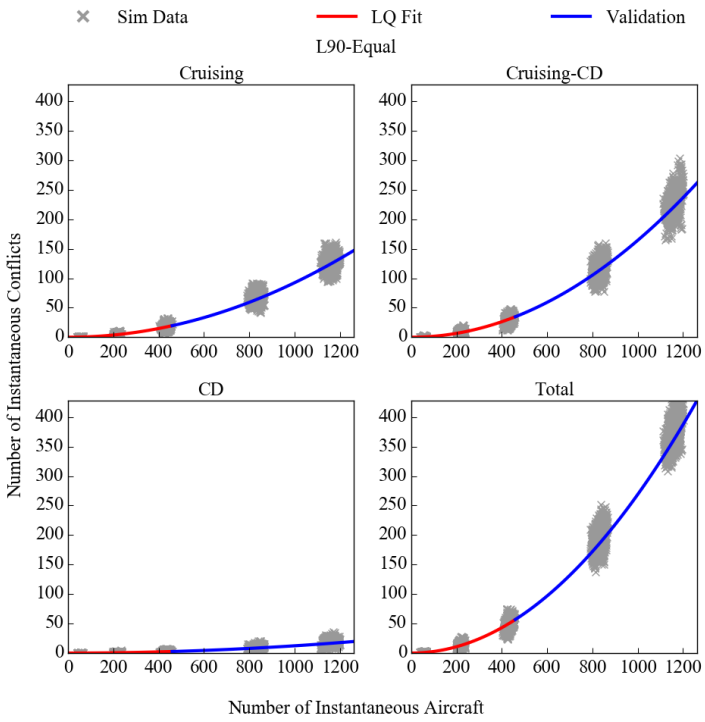

Figure A-26: Fitting validation for the Layers 90, using equal speed distribution.

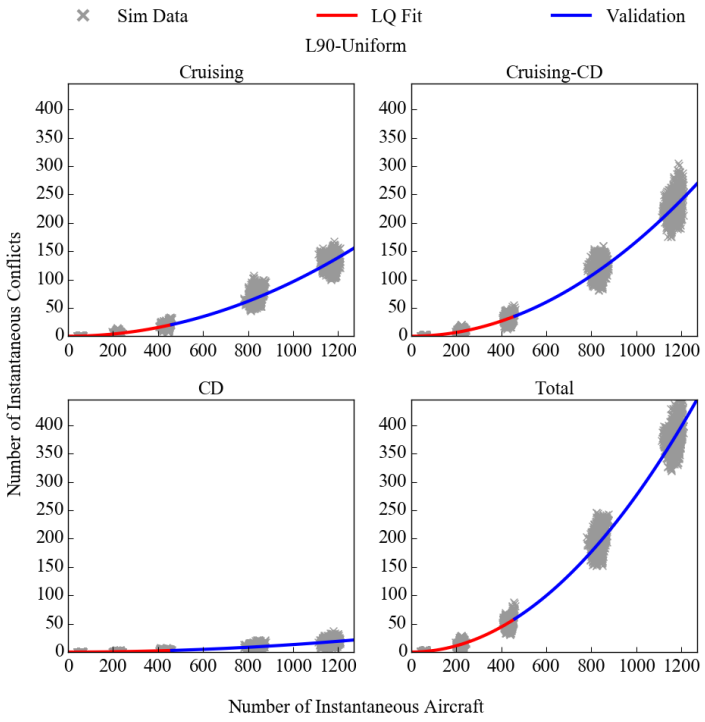

Figure A-27: Fitting validation for the Layers 90, using uniform speed distribution.

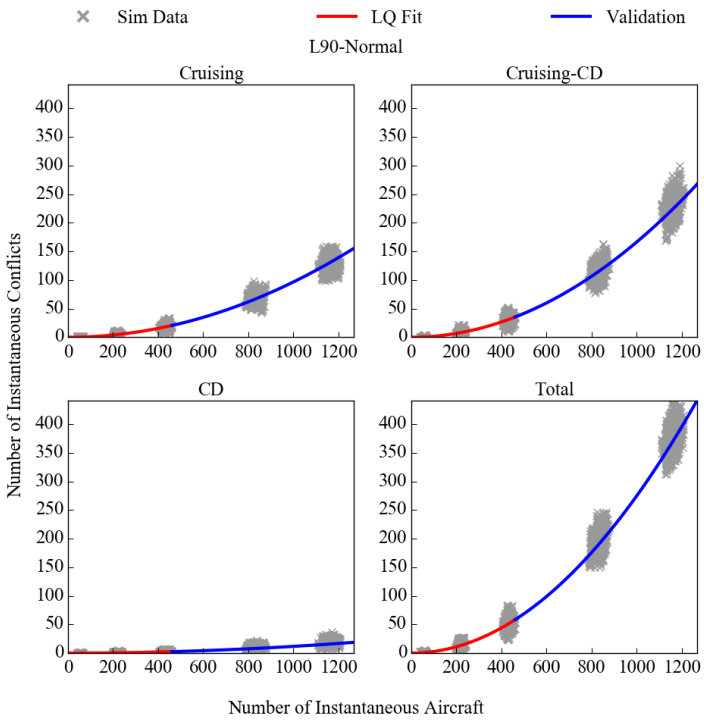

Figure A-28: Fitting validation for the Layers 90, using normal speed distribution.

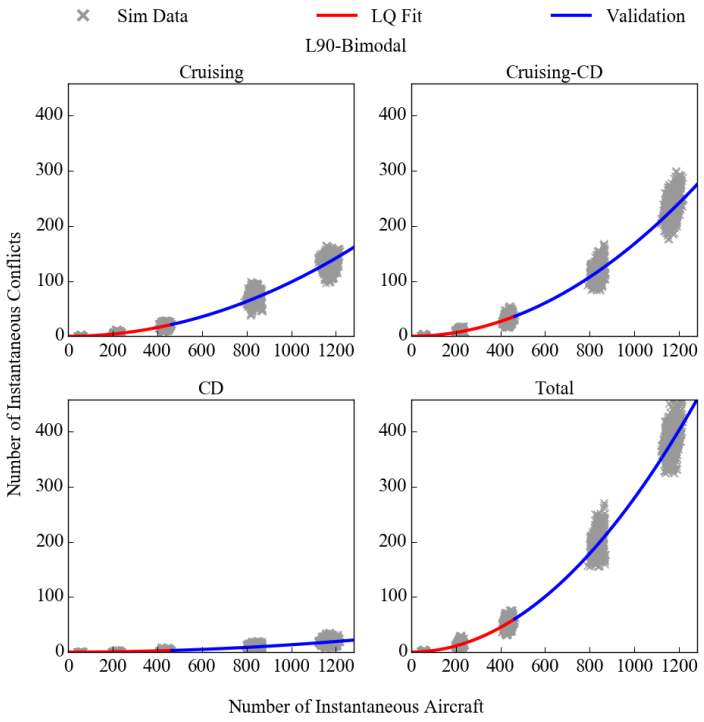

Figure A-29: Fitting validation for the Layers 90, using bimodal speed distribution.

A-2-2 Number of conflicts affected by speed distribution

The total number of conflicts are shown in Figures A-30, A-31, A-35 and A-39. Figure A-32, A-36 and A-40 shows the number of conflicts between two cruising aircraft. Figure A-33, A-37 and A-41 shows the number of conflict between a cruising aircraft and an aircraft that is climbing or descending. Figure A-34, A-38 and A-42 shows the number of conflicts for two aircraft that are both either cruising or climbing.

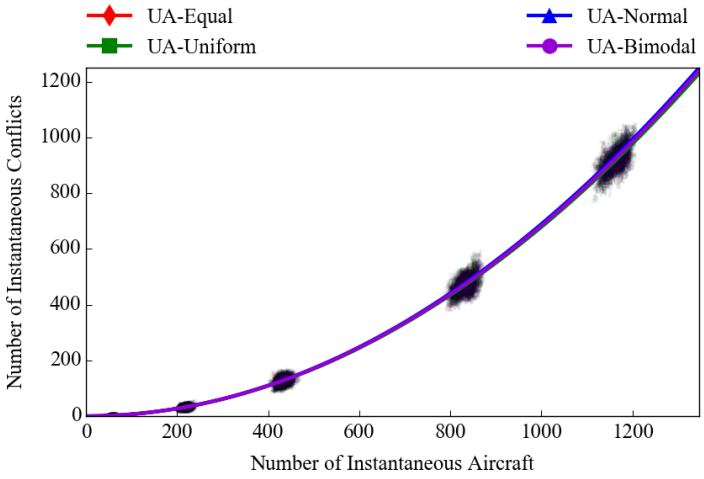

Figure A-30: The total number of conflicts for the UA, in the speed experiments.

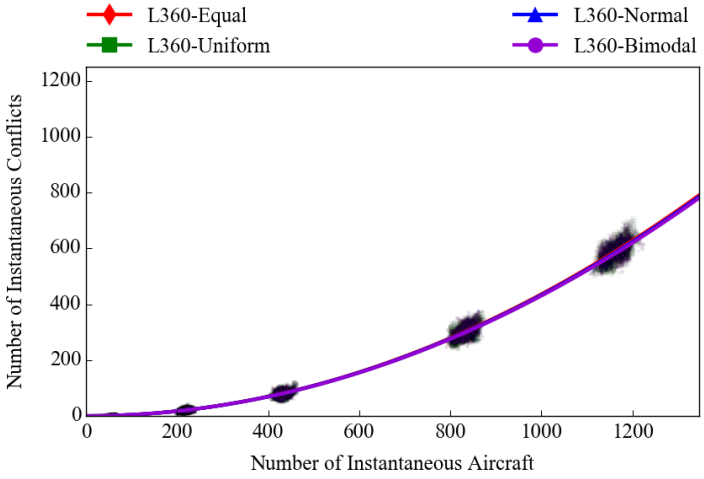

Figure A-31: The total number of conflicts for the L360, in the speed experiments.

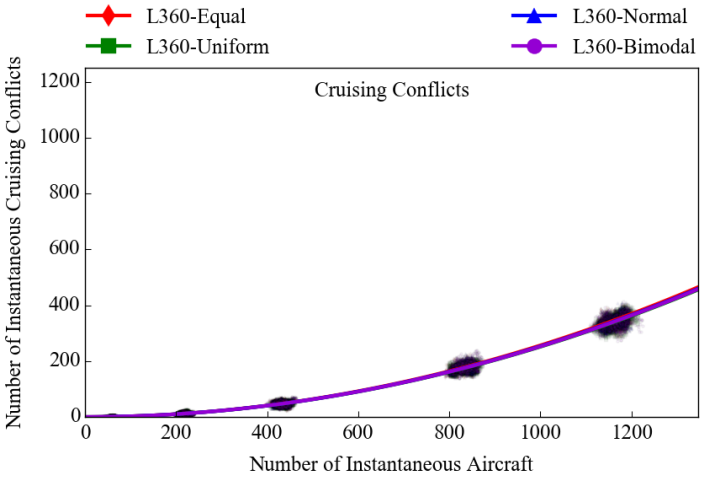

Figure A-32: The number of cruising conflicts for the L360, in the speed experiments.

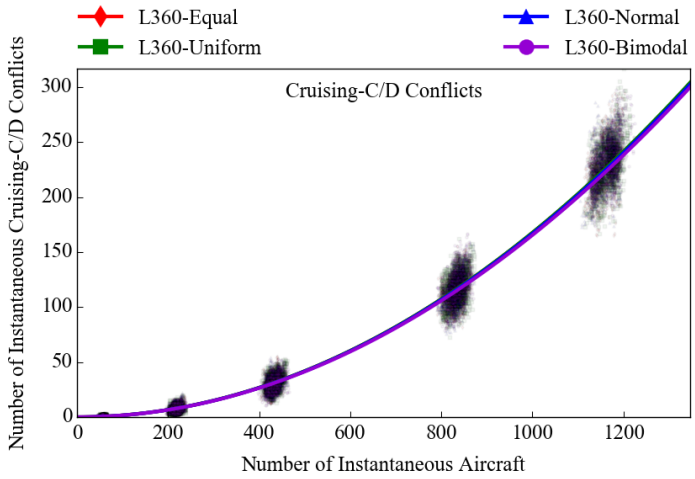

Figure A-33: The number of cruising-C/D conflicts for the L360, in the speed experiments.

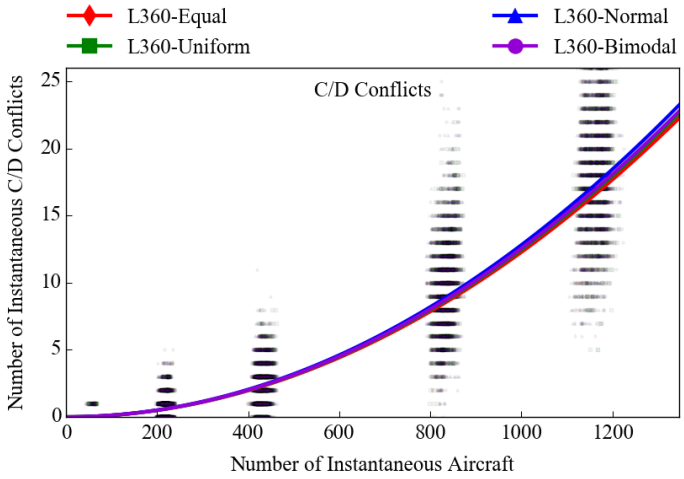

Figure A-34: The number of cruising-C/D conflicts for the L360, in the speed experiments.

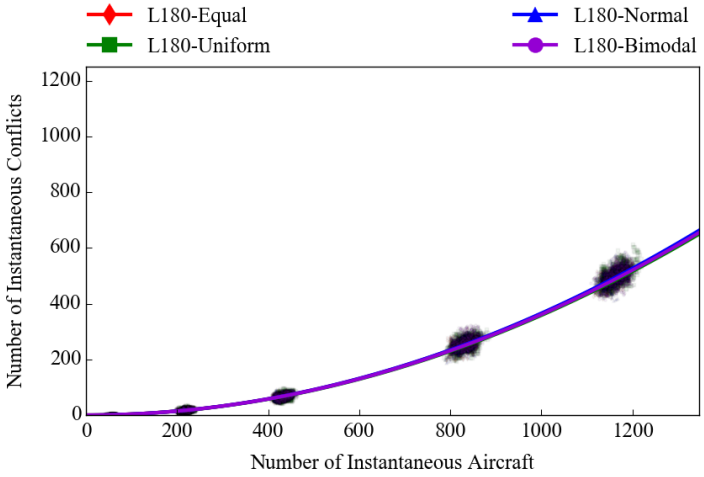

Figure A-35: The total number of conflicts for the L180, in the speed experiments.

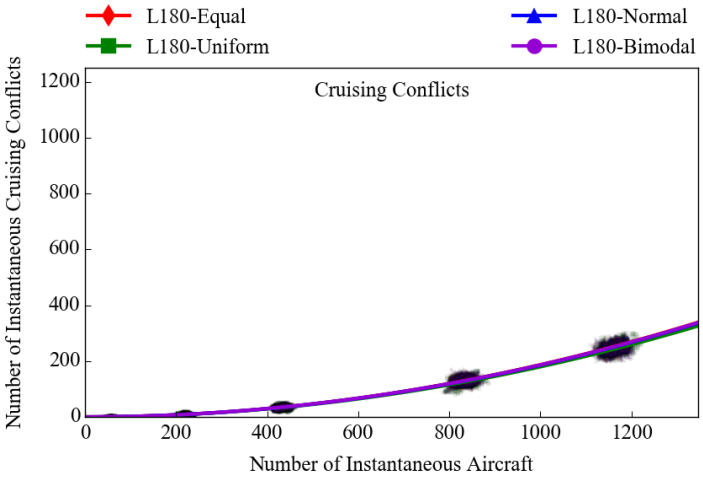

Figure A-36: The number of cruising conflicts for the L180, in the speed experiments.

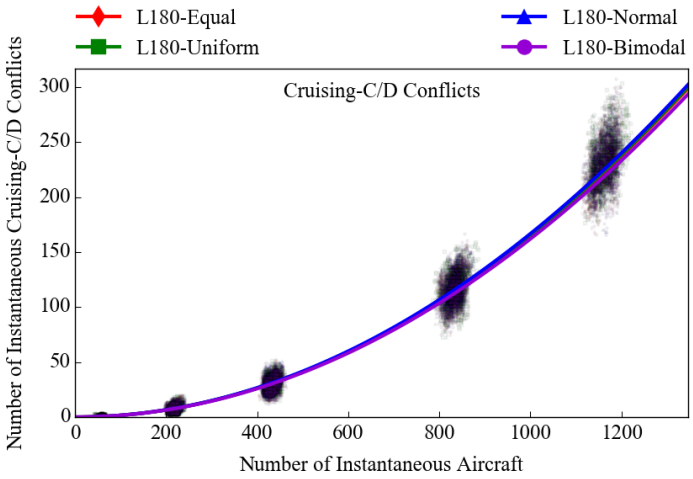

Figure A-37: The number of cruising-C/D conflicts for the L180, in the speed experiments.

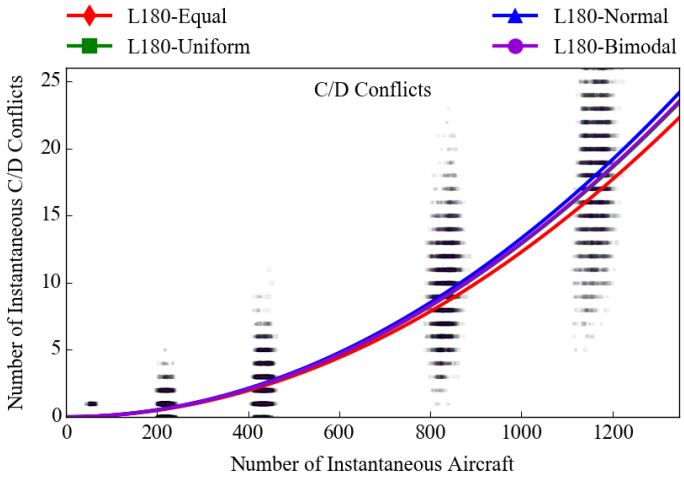

Figure A-38: The number of cruising-C/D conflicts for the L180, in the speed experiments.

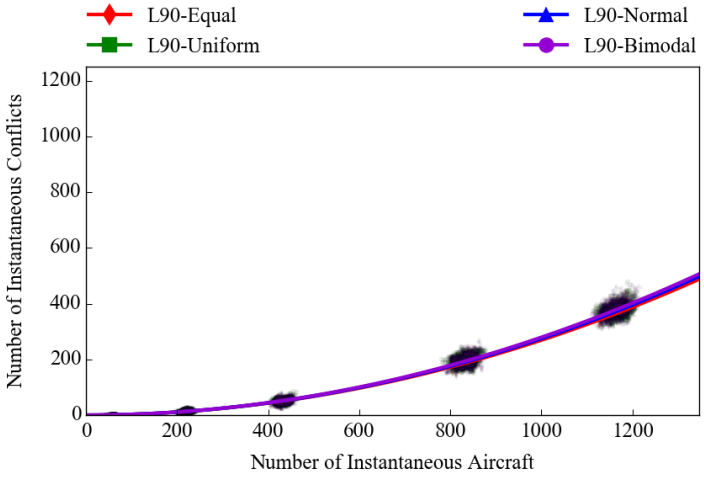

Figure A-39: The total number of conflicts for the L90, in the speed experiments.

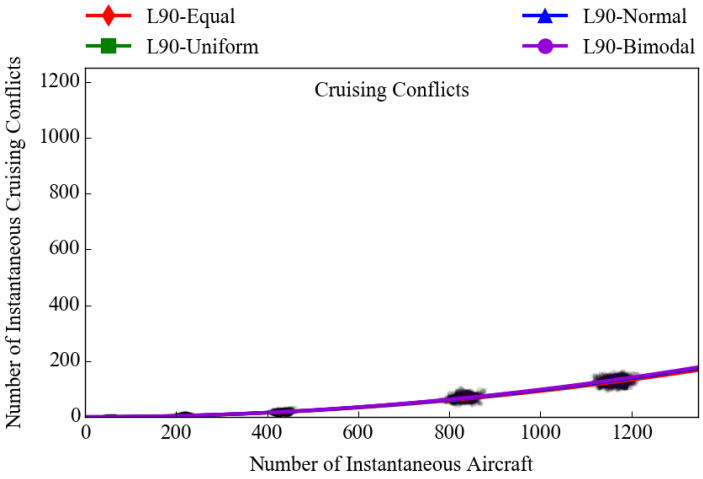

Figure A-40: The number of cruising conflicts for the L90, in the speed experiments.

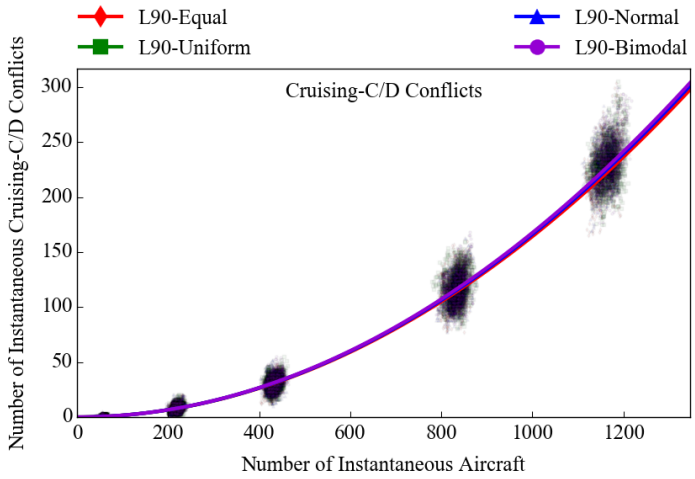

Figure A-41: The number of cruising-C/D conflicts for the L90, in the speed experiments.

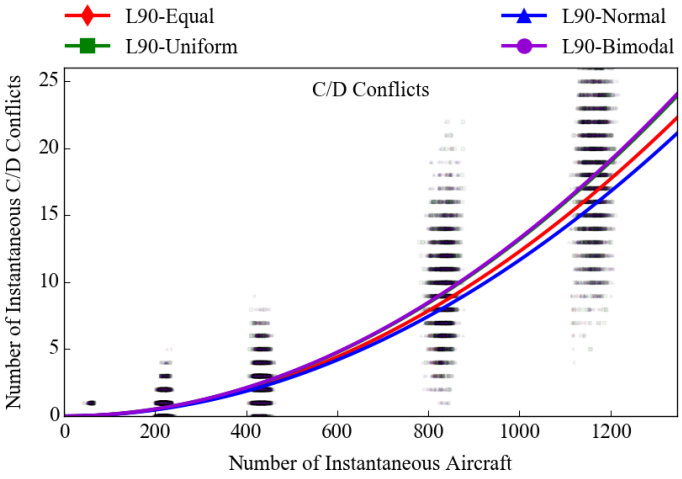

Figure A-42: The number of cruising-C/D conflicts for the L90, in the speed experiments.

A-3 Altitude Experiments

A-3-1 Fitting validation

Figures A-43 to A-50 show the validation for the fitting. Where the first two densities are used to fit the curve and the rest of the line is drawn with that fitting to see if if follows the data points for the higher densities.

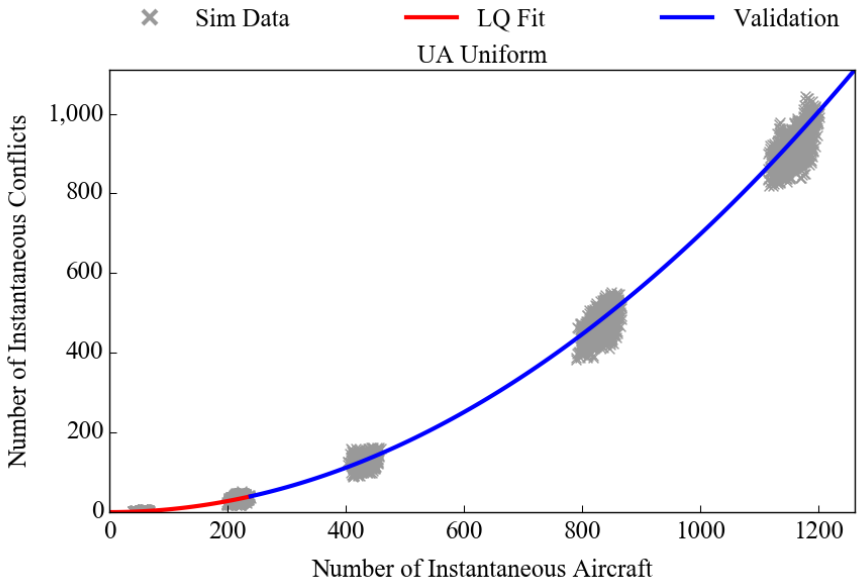

Figure A-43: Fitting validation for the UA, using uniform altitude distribution.

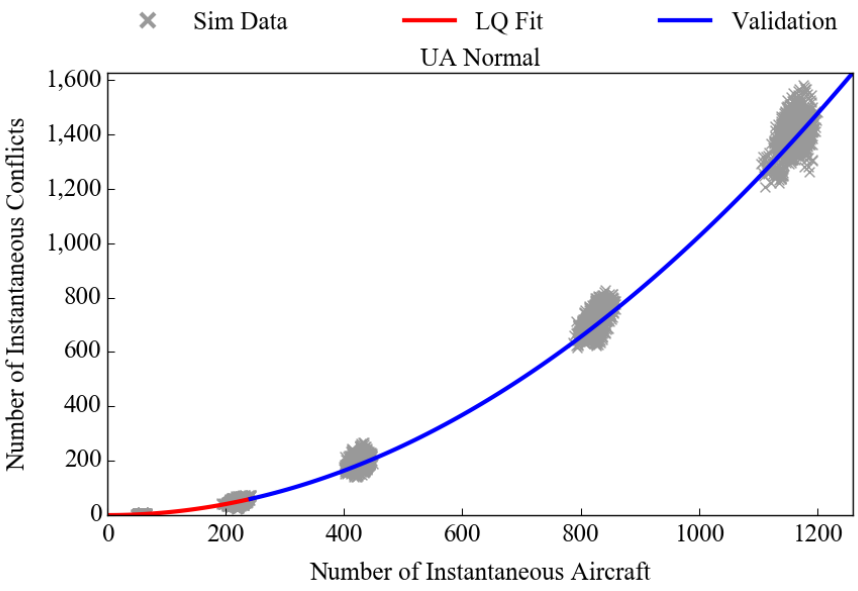

Figure A-44: Fitting validation for the UA, using normal altitude distribution.

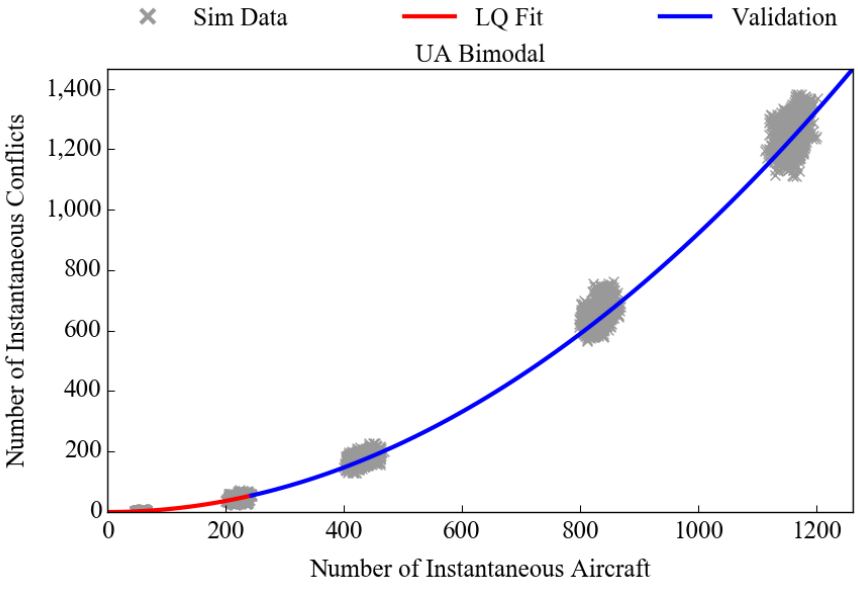

Figure A-45: Fitting validation for the UA, using bimodal altitude distribution.

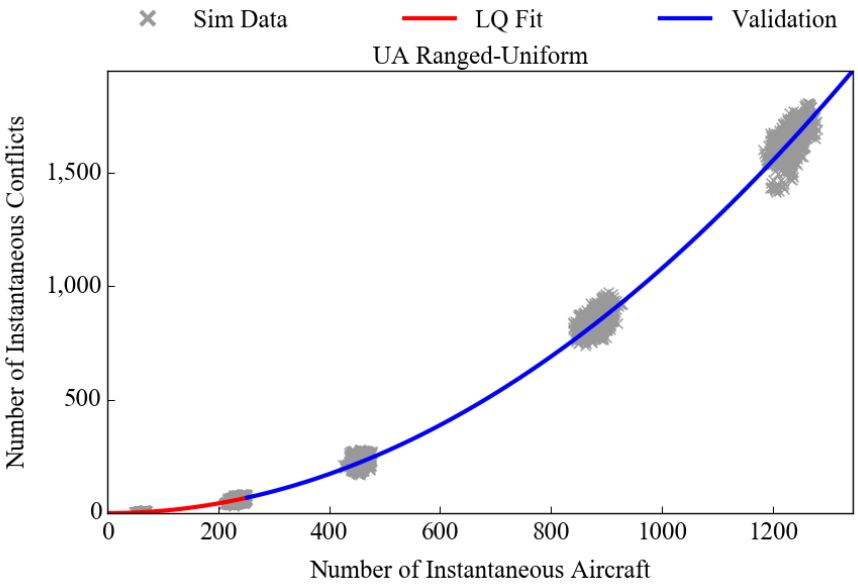

Figure A-46: Fitting validation for the UA, using ranged-uniform altitude distribution.

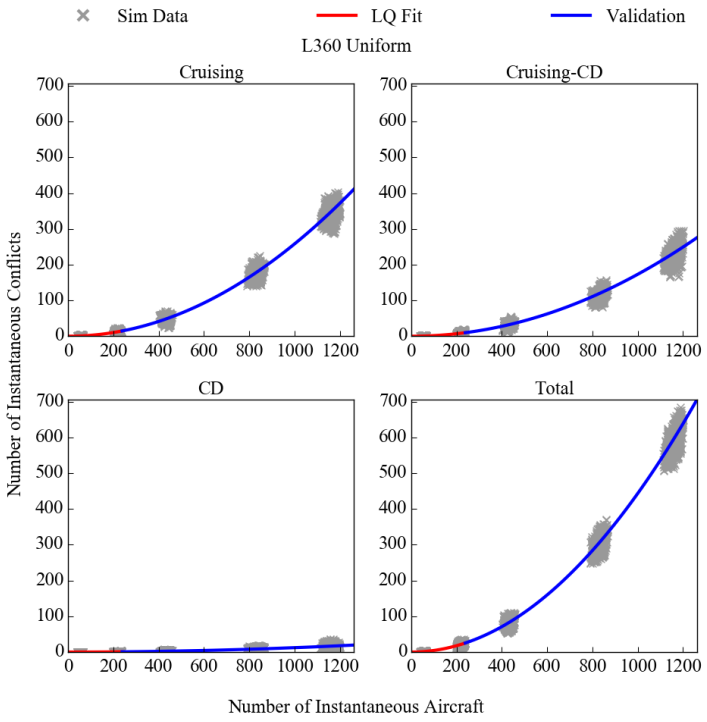

Figure A-47: Fitting validation for the Layers 360, using uniform altitude distribution.

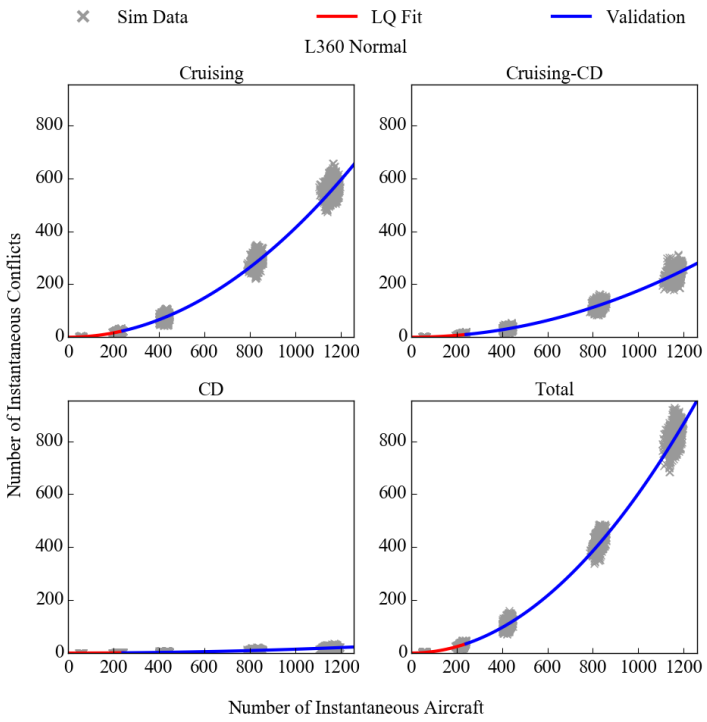

Figure A-48: Fitting validation for the Layers 360, using normal altitude distribution.

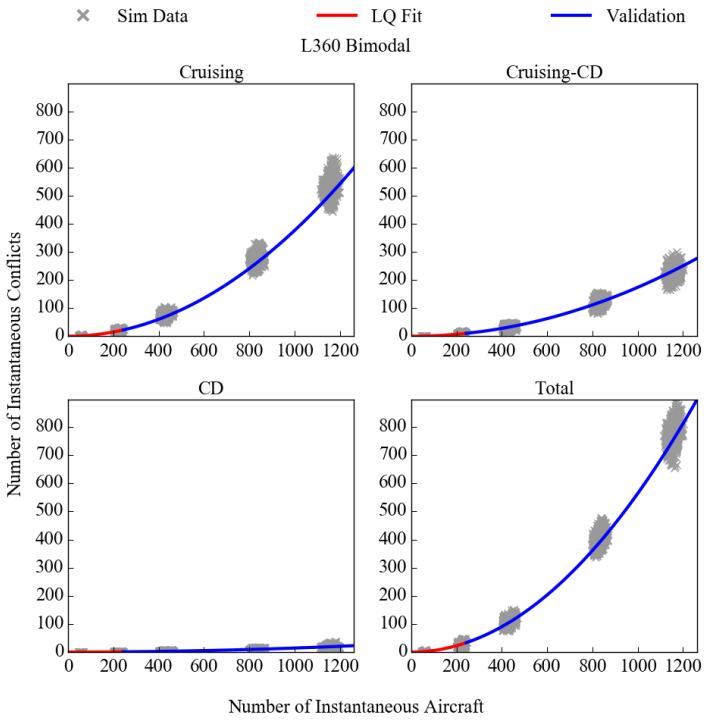

Figure A-49: Fitting validation for the Layers 360, using bimodal altitude distribution.

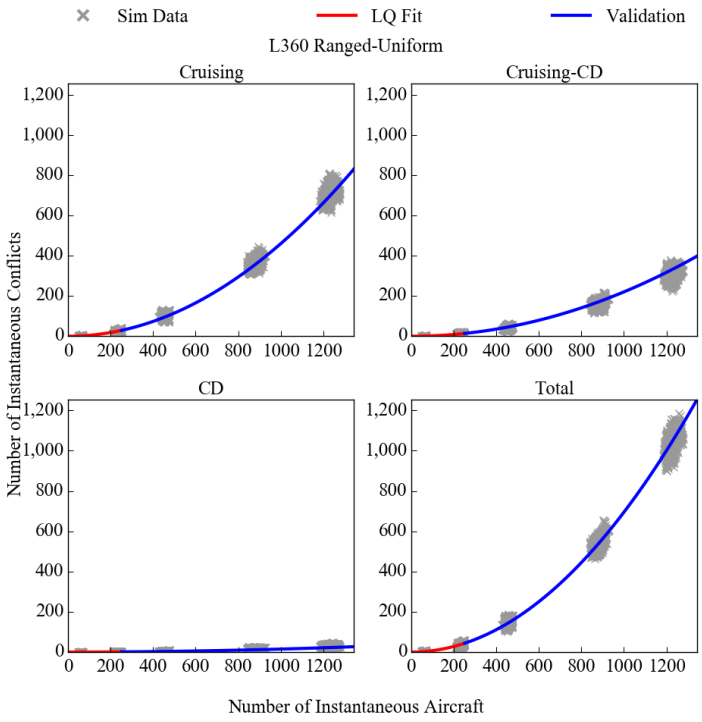

Figure A-50: Fitting validation for the Layers 360, using ranged-uniform altitude distribution.

A-3-2 Number of conflicts effected by altitude distribution

The total number of conflicts are shown in Figures A-51 and A-52. Figure A-53 shows the number of conflicts between two cruising aircraft. Figure A-54 shows the number of conflict between a cruising aircraft and an aircraft that is climbing or descending. Figure A-55 shows the number of conflicts for two aircraft that are both either cruising or climbing.

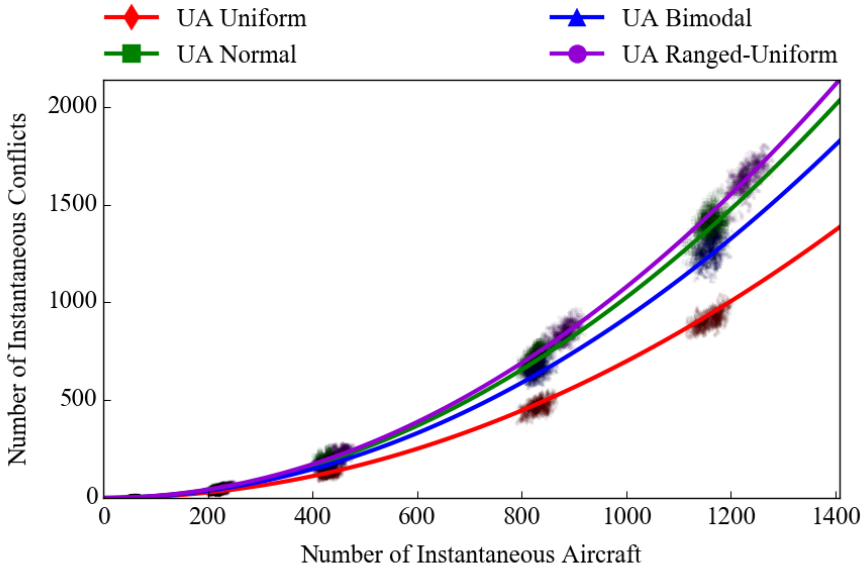

Figure A-51: The total number of conflicts for the UA, in the altutude experiment.

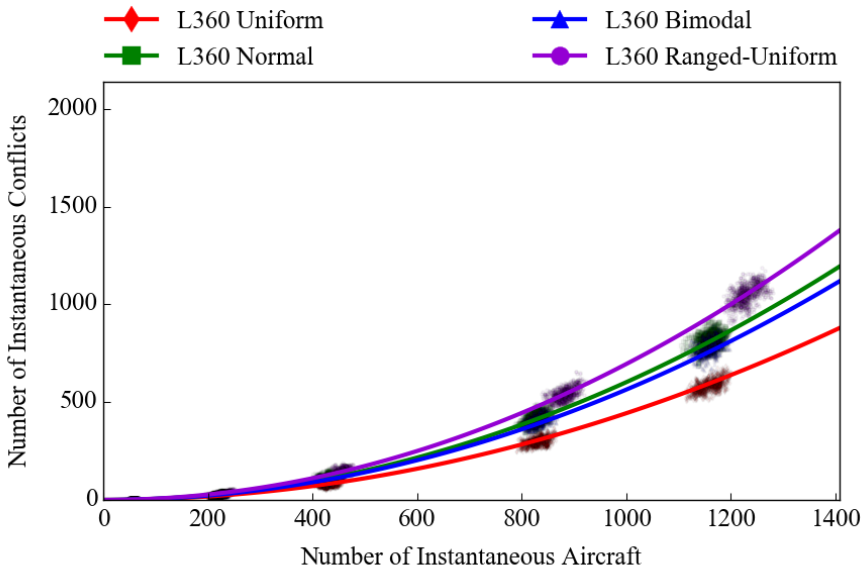

Figure A-52: The total number of conflicts for the Layers 360, in the altutude experiment.

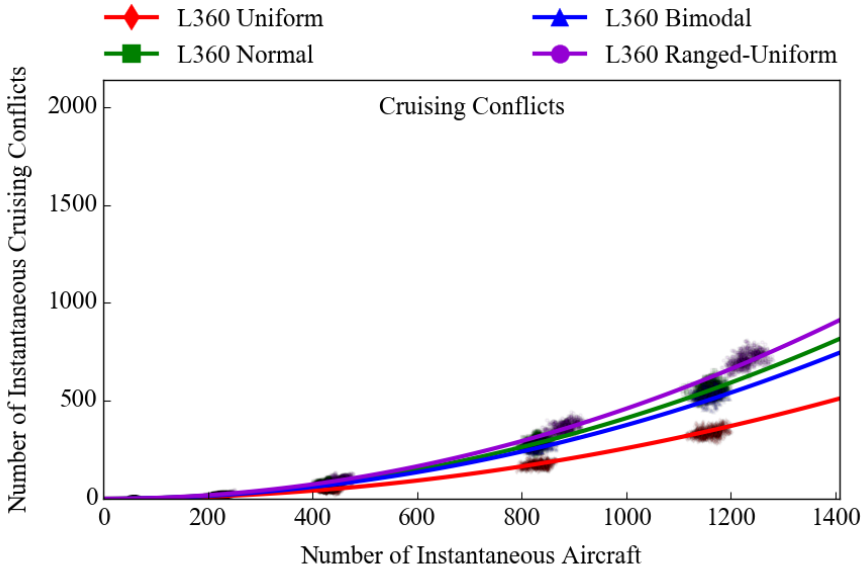

Figure A-53: The number of cruising conflicts for the Layers 360, in the altutude experiment.

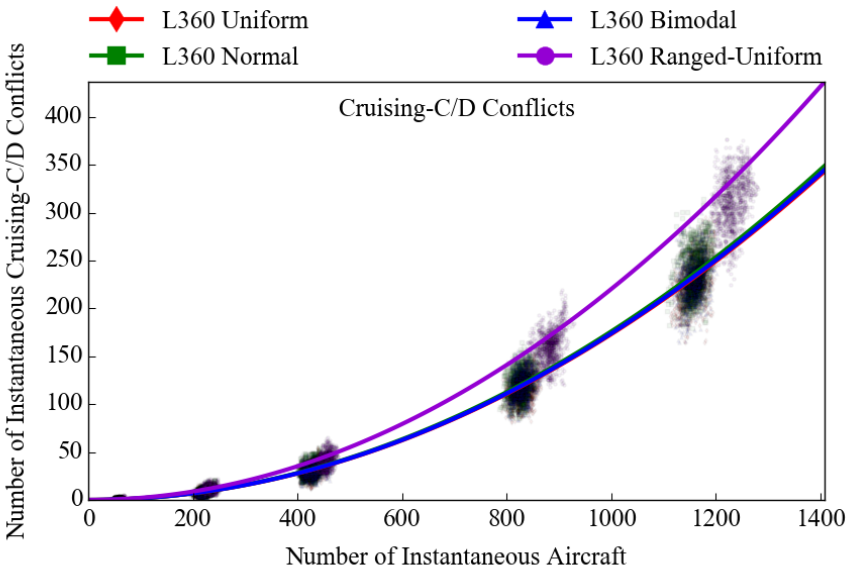

Figure A-54: The number of cruising-climbing/descending conflicts for the Layers 360, in the altutude experiment.

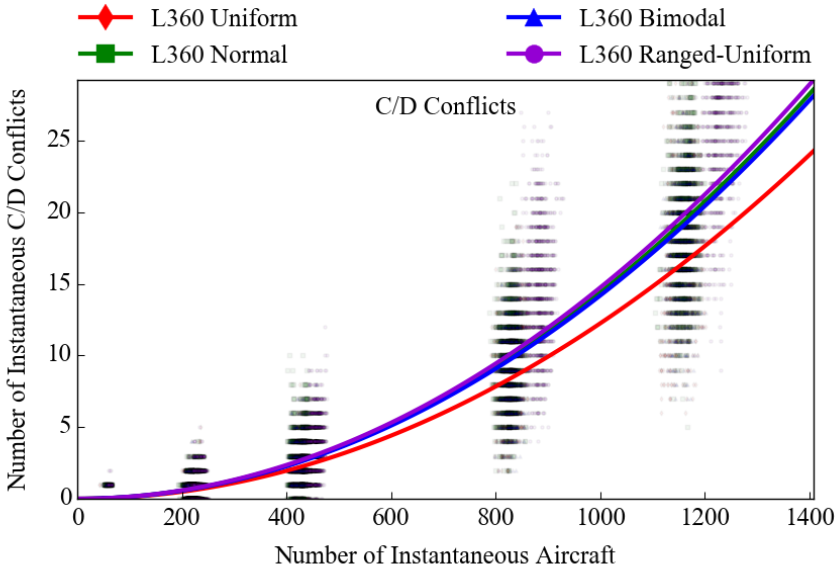

Figure A-55: The number of climbing/descending conflicts for the Layers 360, in the altutude experiment.

A-4 Spatial experiment

A-4-1 Fitting validation

Figures A-56 to A-67 show the validation for the fitting. Where the first three densities are used to fit the curve and the rest of the line is drawn with that fitting to see if if follows the data points for the higher densities.

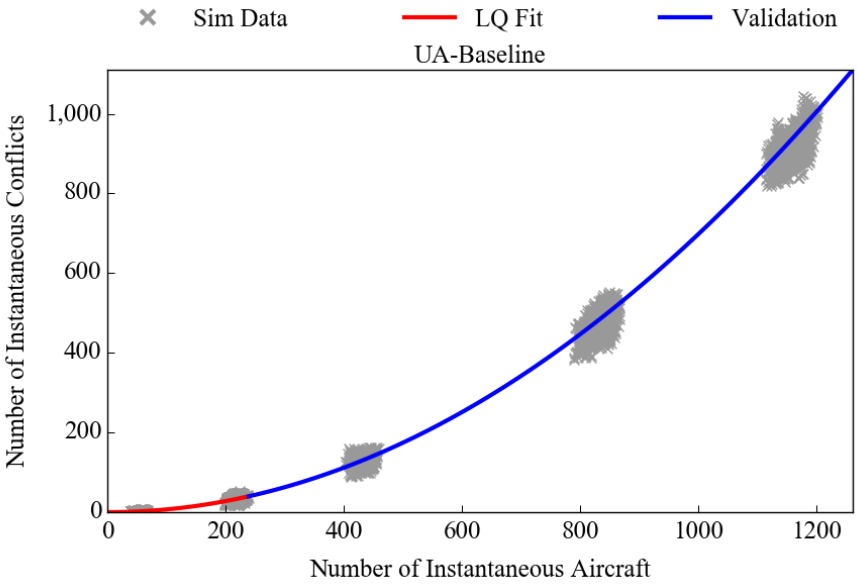

Figure A-56: Fitting validation for the UA, using the baseline spatial distribution.

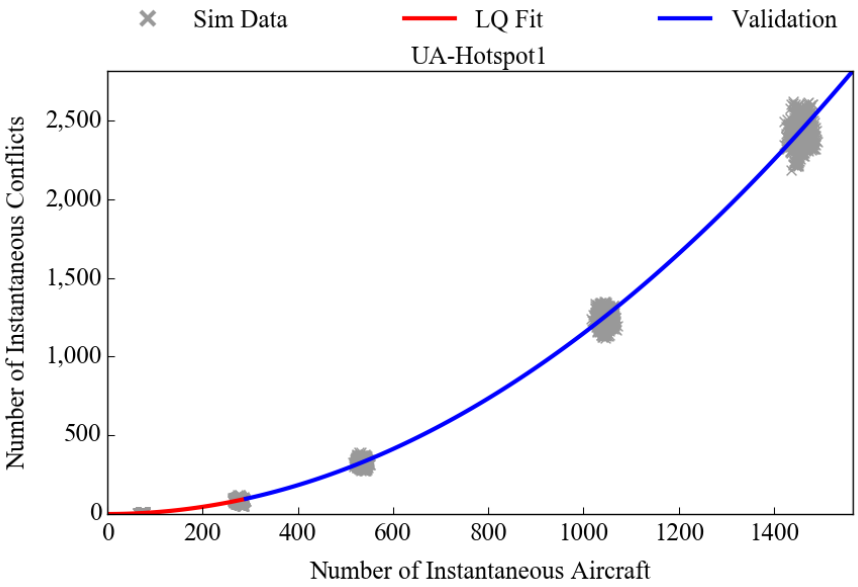

Figure A-57: Fitting validation for the UA, when there is the larger density hotspot.

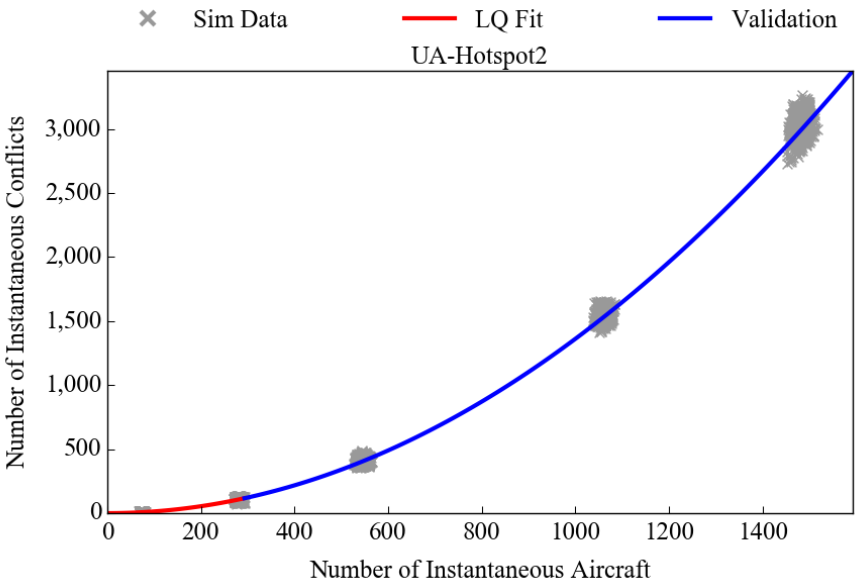

Figure A-58: Fitting validation for the UA, when there is the smaller density hotspot.

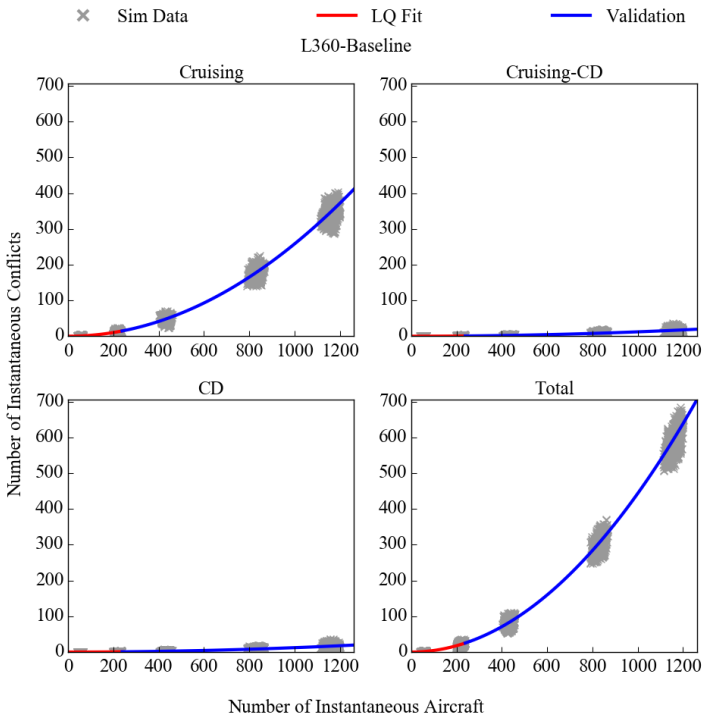

Figure A-59: Fitting validation for the Layers 360, using the baseline spatial distribution.

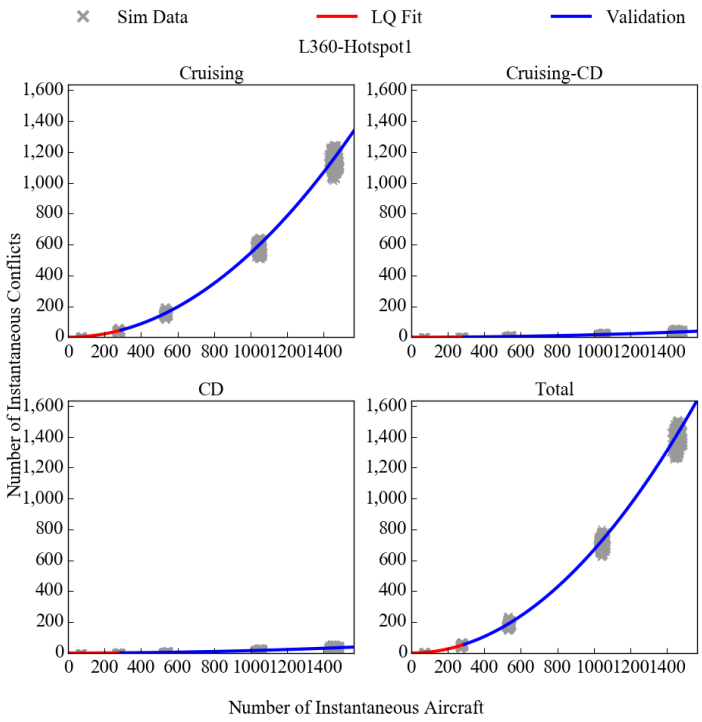

Figure A-60: Fitting validation for the Layers 360, when there is the larger density hotspot.

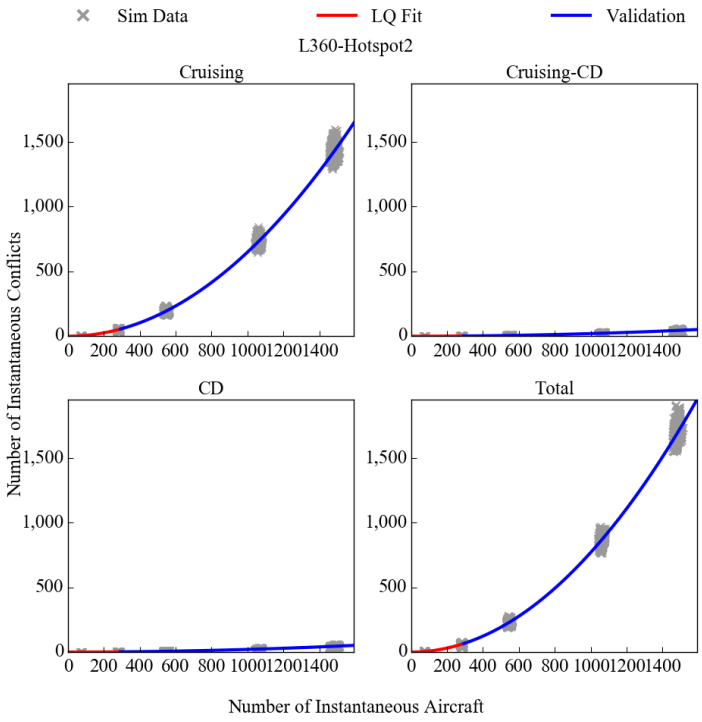

Figure A-61: Fitting validation for the Layers 360, when there is the smaller density hotspot.

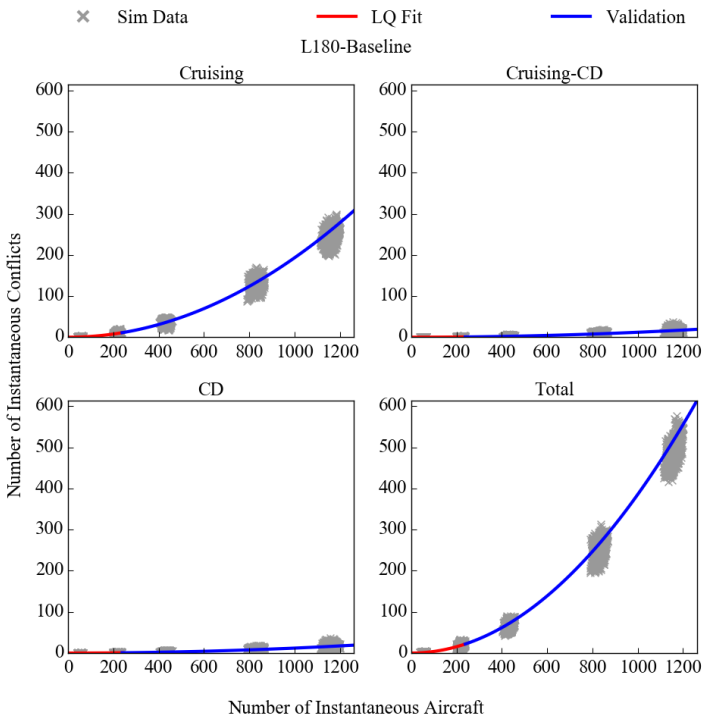

Figure A-62: Fitting validation for the Layers 180, using the baseline spatial distribution.

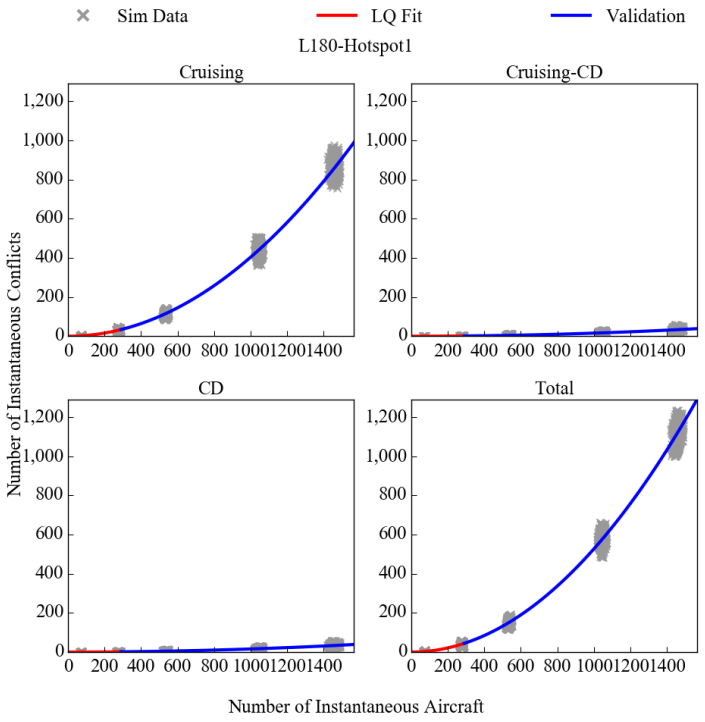

Figure A-63: Fitting validation for the Layers 180, when there is the larger density hotspot.

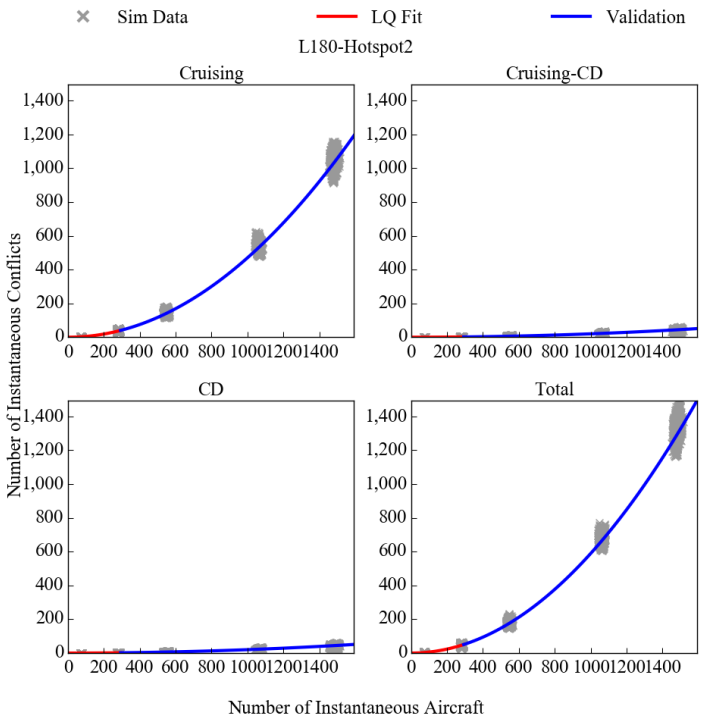

Figure A-64: Fitting validation for the Layers 180, when there is the smaller density hotspot.

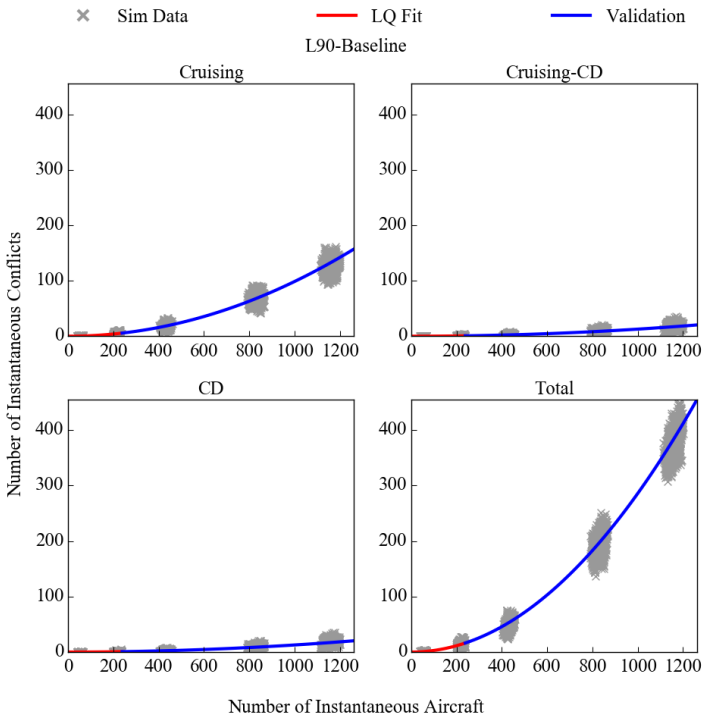

Figure A-65: Fitting validation for the Layers 90, using the baseline spatial distribution.

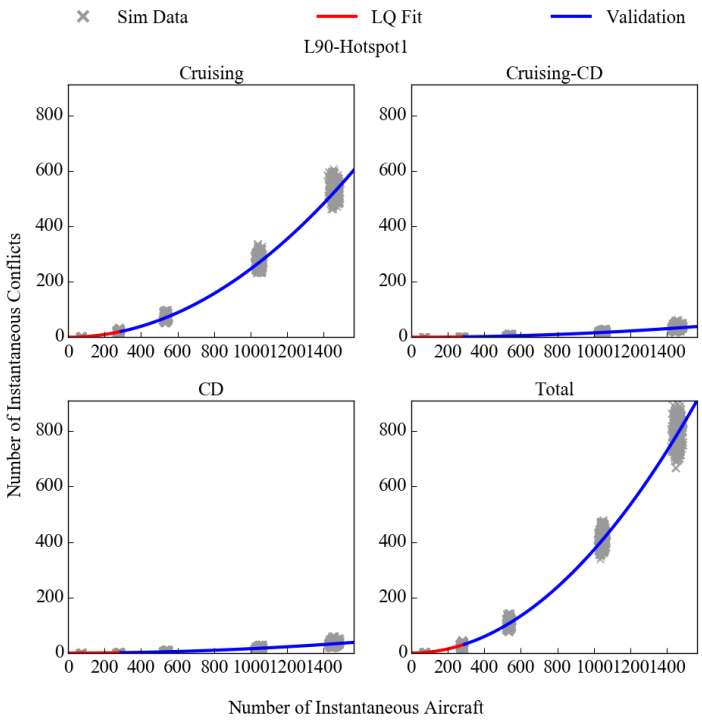

Figure A-66: Fitting validation for the Layers 90, when there is the larger density hotspot.

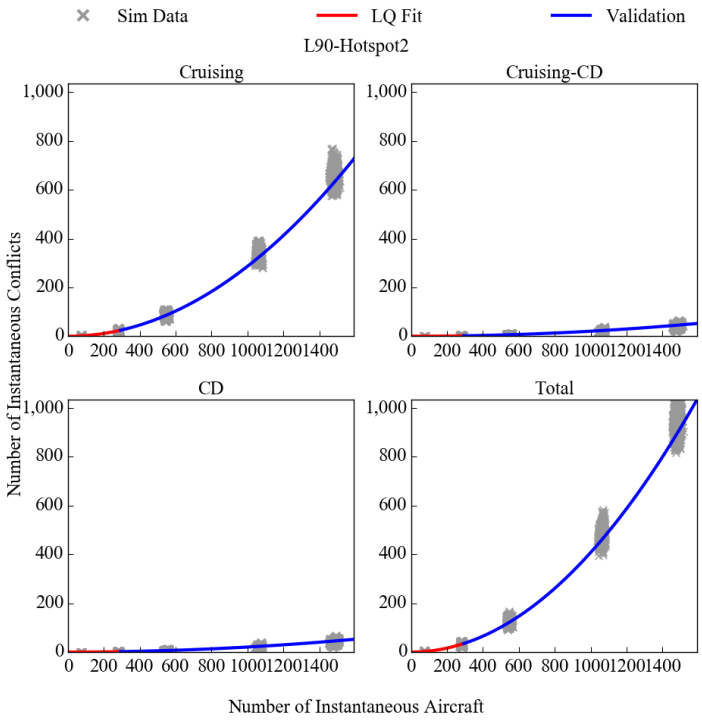

Figure A-67: Fitting validation for the Layers 90, when there is the smaller density hotspot.

A-4-2 Number of conflicts affected by spatial distribution

The total number of conflicts are shown in Figures A-68, A-69, A-73 and A-77. Figure A-70, A-74 and A-78 shows the number of conflicts between two cruising aircraft. Figure A-71, A-75 and A-79 shows the number of conflict between a cruising aircraft and an aircraft that is climbing or descending. Figure A-72, A-76 and A-80 shows the number of conflicts for two aircraft that are both either cruising or climbing.

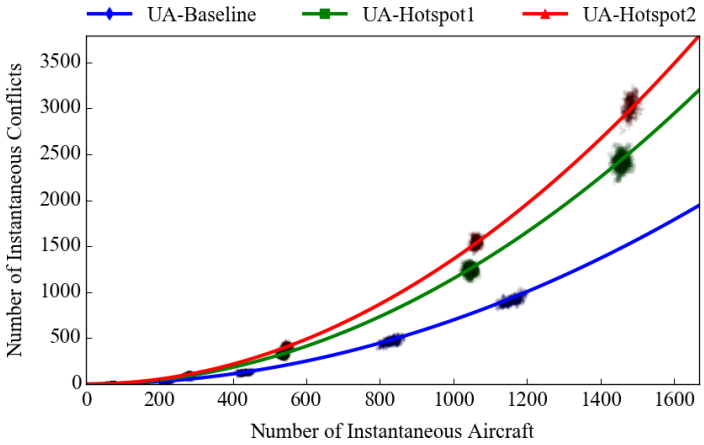

Figure A-68: The total number of conflicts for the UA, in the spatial experiments.

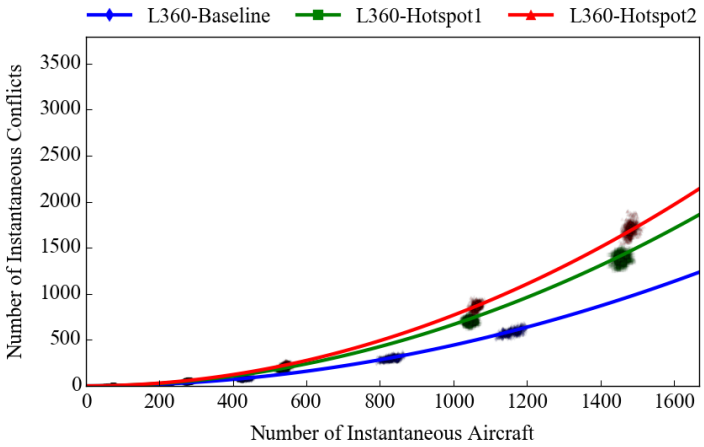

Figure A-69: The total number of conflicts for the L360, in the spatial experiments.

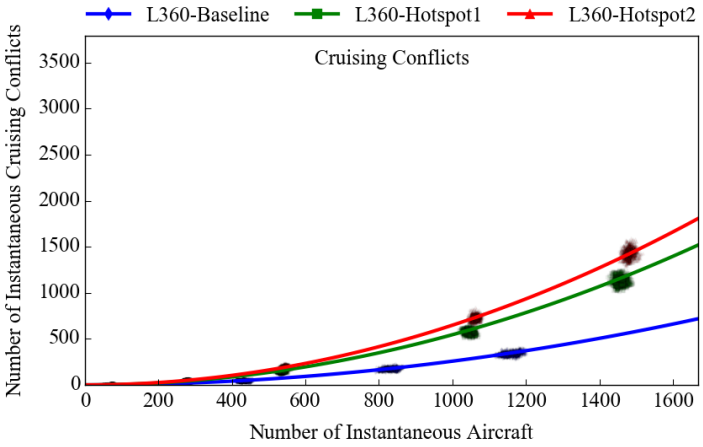

Figure A-70: The number of cruising conflicts for the L360, in the spatial experiments.

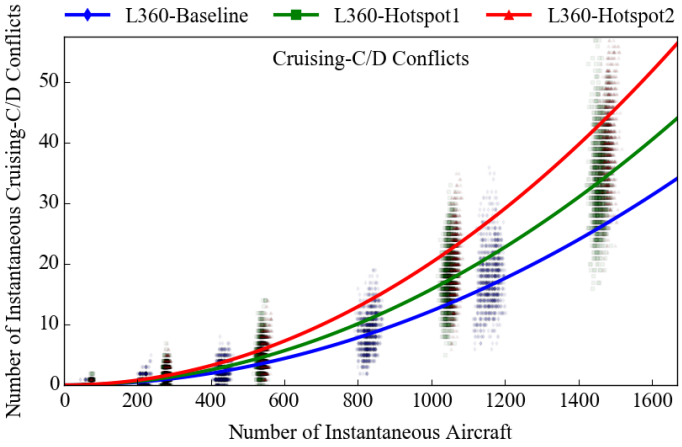

Figure A-71: The number of cruising-C/D conflicts for the L360, in the spatial experiments.

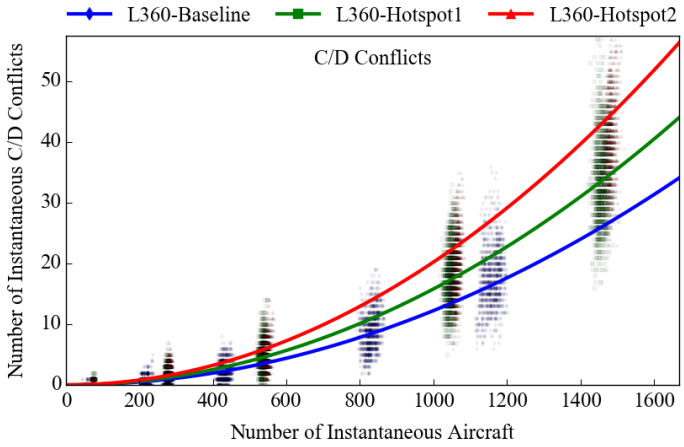

Figure A-72: The number of cruising-C/D conflicts for the L360, in the spatial experiments.

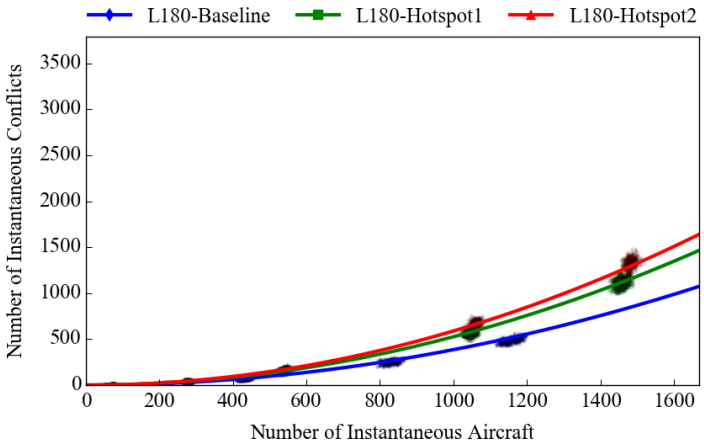

Figure A-73: The total number of conflicts for the L180, in the spatial experiments.

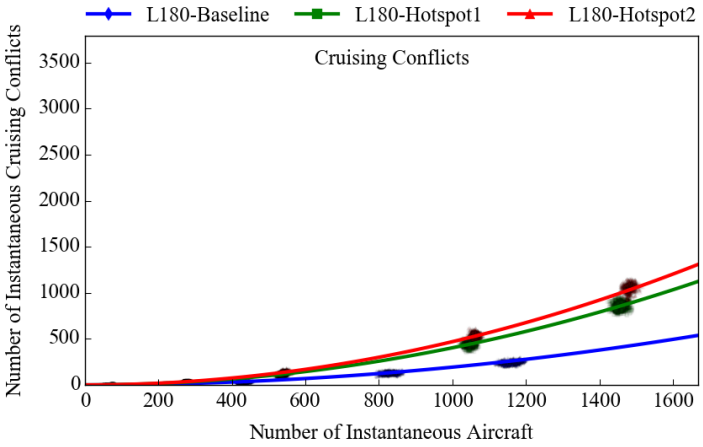

Figure A-74: The number of cruising conflicts for the L180, in the spatial experiments.

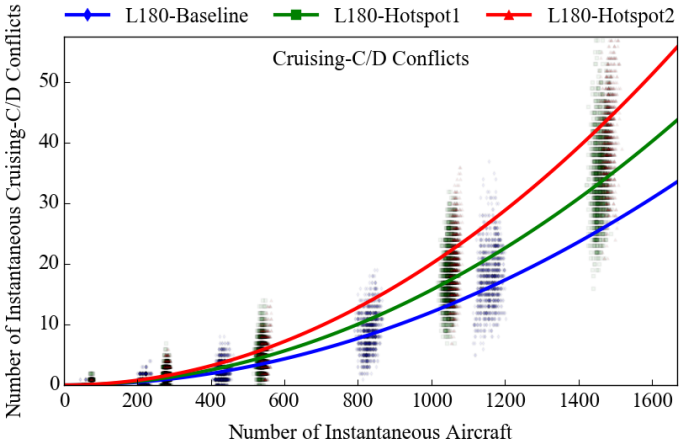

Figure A-75: The number of cruising-C/D conflicts for the L180, in the spatial experiments.

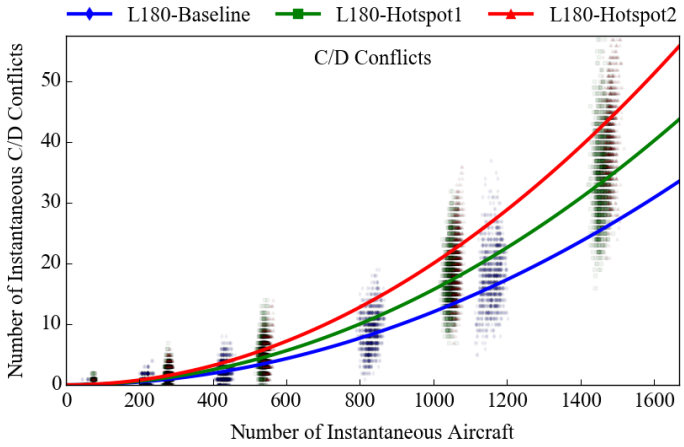

Figure A-76: The number of cruising-C/D conflicts for the L180, in the spatial experiments.

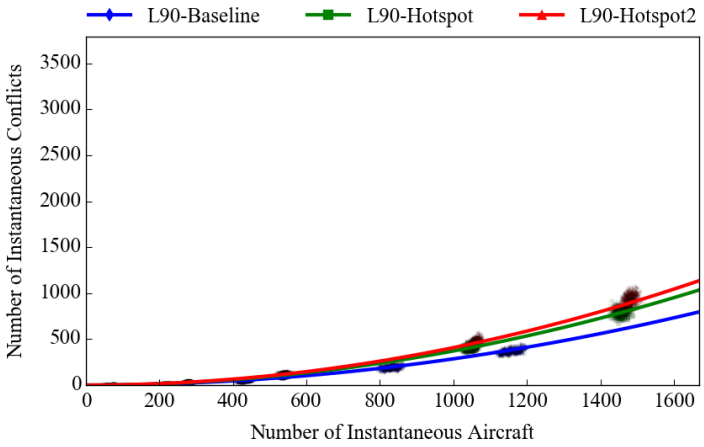

Figure A-77: The total number of conflicts for the L90, in the spatial experiments.

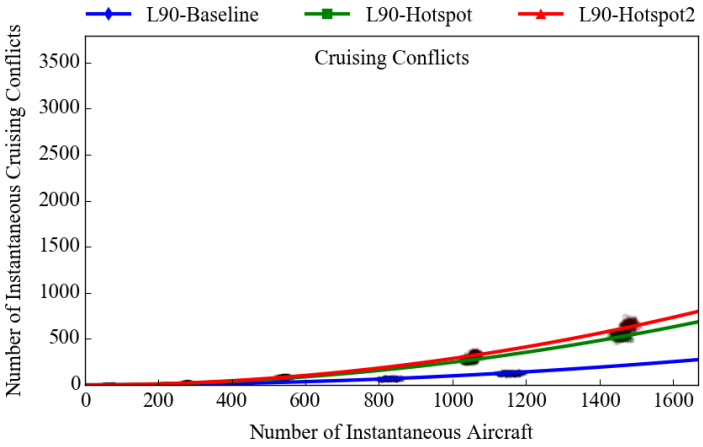

Figure A-78: The number of cruising conflicts for the L90, in the spatial experiments.

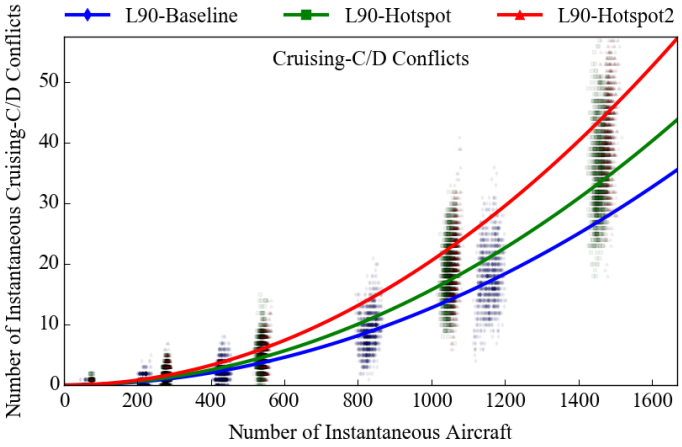

Figure A-79: The number of cruising-C/D conflicts for the L90, in the spatial experiments.

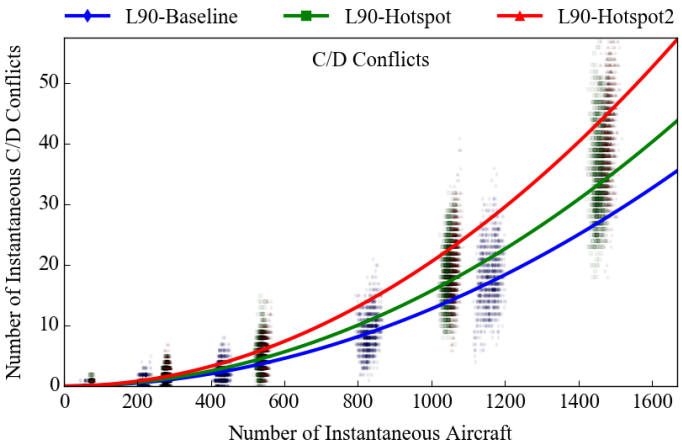

Figure A-80: The number of cruising-C/D conflicts for the L90, in the spatial experiments.

Part III

Preliminary Report [Already graded]

Chapter 1

Introduction

Air traffic has always been increasing and is predicted to keep growing even further. With the rapid increase in air traffic, either improvement in current Air Traffic Management (ATM) system or new ATM system is needed to keep up with demand. In order to create a system that will ensure safe separation between aircraft, any new concepts need to be researched thoroughly before being deployed. There are many options that have been proposed, some believe that a so called decentralized airspace may be a good solution. A decentralized strategy is when the responsibility of maintaining safe separation between aircraft is moved from the ATC to the cockpit.

1-1 Background

After World War I, the development of aviation technology, aircraft manufacturing and pilot training took a leap. Air traffic had increased a lot and thus there was a need to manage the traffic. ATM began in the 1920's, after rapid growth in flights, air traffic rules and airways were established with the Air Commerce Act of 1926 (*NACTA - A History of Air Traffic Control*, n.d.), which is the foundation of the control concepts used today.

In the second World War new routes were designed according to new technology such as radar, which made surveillance possible so the Air Traffic Control (ATC) could plan for incoming flights. In the war the jet engine was developed, and in 1958, the first passenger jet plane was introduced. The increase in traffic from 1958 to 1977 was more then 1000% (*NACTA - A History of Air Traffic Control*, n.d.) and ATC became even more crucial to maintain safety. Radar helped the Air Traffic Controller (ATCo) to monitor inbound traffic for airports and later, traffic along airways. Radar was strictly ground based and could not be used in the cockpit.

The need for improved surveillance technology increased with the growth in air traffic, to both improve flexibility and capacity of the airspace. The Automatic Dependent Surveillance - Broadcast (ADS-B) has been developed, an on-board surveillance system, where aircraft broadcast their states and receives information about other aircraft's states. This means that

the ADS-B system makes air to air surveillance possible and offers improvement in air to ground surveillance. The knowledge of the location, heading and speed of other aircraft may enable the pilots to maintain separation between aircraft.

The current traffic control system is a centralized type of ATM. Centralized mode of operation is when the control strategy is based on one or more central nodes which the traffic is controlled from. The focus is to maintain order and smooth traffic flow, which results in more stability but less efficiency when considering high density scenarios.

1-1-1 Traffic Growth

When using radar surveillance, traffic usually makes use of airway navigation. Airways are still in use today as they still have benefits for the ATCo, such as stability and predictability. However there are some drawbacks as well. Airways are not optimal routes for many flights, and is thus less efficient than direct routing. With increased traffic, airways may become a bottleneck which causes time delays. The delays may cause nuisance to passengers and can be very costly for the airlines in fuel consumption in lower altitudes.

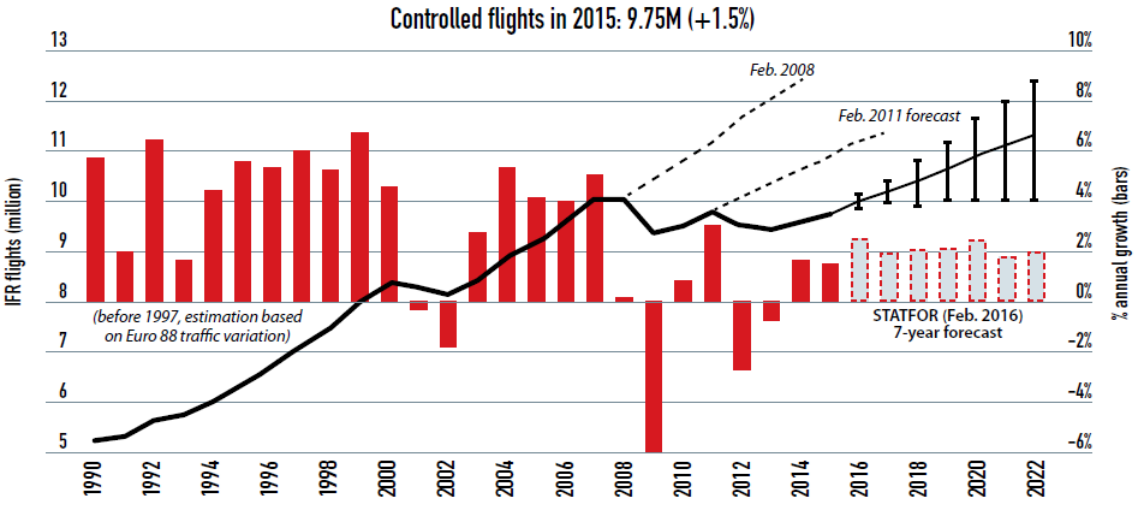

Figure 1-1: Traffic growth and predictions for the future. (*Eurocontrol Annual Report*, 2015)

Air traffic demand is always increasing as may be seen on Figure 1-1, except when something out of the ordinary happens, for example in the financial crisis of 2008 or when air traffic was down due to volcanic ashes. The number of controlled flights increased 1.5% from 2014 to 2015, and the prediction for the next 7 years is around 2.2% annually according to the Eurocontrol annual report 2015 (*Eurocontrol Annual Report*, 2015). Delays in flights increased by 23% between 2014 and 2015 but Eurocontrol's Performance Review Committee has expressed concerns with increased delays when traffic starts to grow more.

With increased traffic and delays, there are bound to be some issues with the capacity of the airspace. The solution to these issues would be either to reinforce the current system which is what has been done in the past. But this solution has limits like the workload of the controllers. Another solution would be to introduce a new system, like the decentralized control concepts.

1-2 Decentralized Airspace

As mentioned previously, decentralized airspace is when the task of separating aircraft is in the hands of the pilots. The separation is maintained with the help of the Airborne Separation Assurance System (ASAS), which predicts potential losses of separation (conflicts), and then suggest a maneuver to resolve the conflict, referred to as Conflict Detection (CD) & Conflict Resolution (CR). The CD has a limit on how far in the future it predicts a conflict, that time is called the look-ahead time. (Hoekstra, Gent, & Ruigrok, 2002)

Most researches related to decentralized airspace are either about CD & CR or about the structure of the airspace. Different structure concepts have been proposed in previous research, see Figure 1-2, obtained from (Sunil et al., 2017), where the concepts are compared in terms of efficiency, safety and stability. In this thesis the main focus is about the structure of the airspace, where structure is defined as the number of constrained degrees of freedom of aircraft motion.

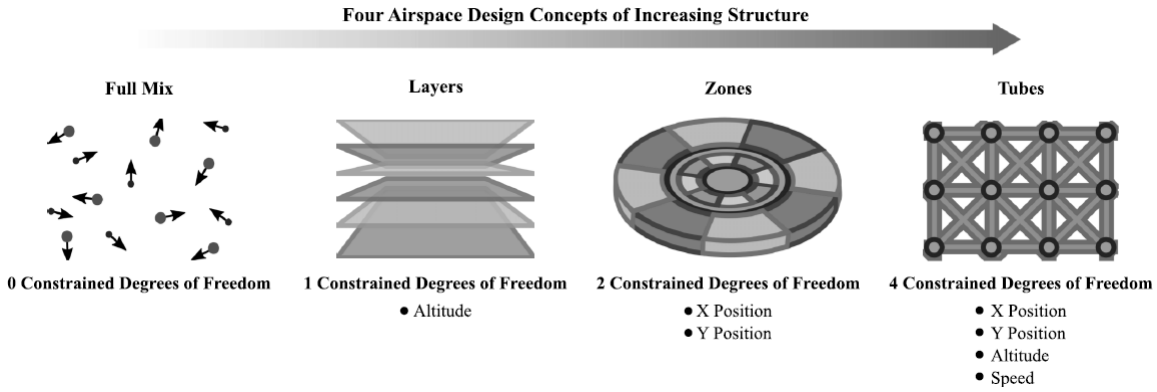

Figure 1-2: Four proposals for structure, with constrains increasing from left to right.(Sunil et al., 2017)

1-3 Previous Research on Decentralized Airspace Structure

Studies have been conducted on different structure concepts. When the 4 concepts shown in Figure 1-2 were compared, the Layers concept had the best results, according to (Sunil et al., 2017). The Layers concept has an altitude constraint, where the aircraft are sorted in altitude layers. The layer which the aircraft are assigned to is dependent on the heading of the aircraft. The concept may be considered as an extension of the hemispheric rule, where eastbound and westbound traffic fly on different altitude bands. The idea behind the concept is that it is suppose to prevent conflicts as distributing traffic over flight levels lowers the amount of conflicts, and similar headings per altitude layer should decrease the probability of conflicts. The heading range can vary, a good visualization for a 45° range, can be seen in Figure 1-3. Different airspace concepts are often compared with an unstructured airspace, sometimes referred to as Full Mix. Unstructured airspace does not impose any constraints, except for physical constraints such as terrain and weather.

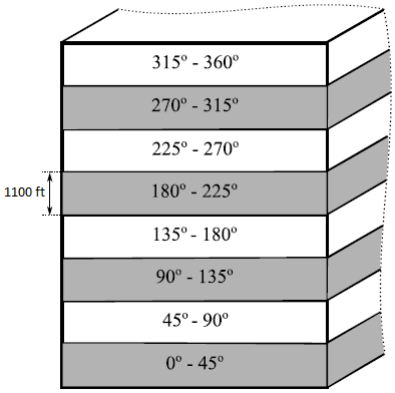

Figure 1-3: Representation of the Layers 45 concept. Where the altitude between layers is 1100 ft and the heading ranges are of the size 45°. (Sunil et al., 2017)

Conflict rate is a metric that may be used for determining the intrinsic safety of an airspace. It is the number of conflicts between aircraft per unit time. In literature (Hoekstra, Ruigrok, & Van Gent, 2001), the conflict rate for a single aircraft and for the whole airspace were modeled. The inputs of the model are the number of instantaneous aircraft and the conflict probability. In (Jardin, 2005) the conflict probability is described as proportional to the ratio between the aircraft covers in the sector (area defined by the separation criteria and the distance flown), and the total area of the airspace.

However this does not take the relative velocity into account. In (Hoekstra, Maas, Tra, & Sunil, 2016) the relative velocity factor was added to the model, as well as an expansion for the Layers concept. The number of layers has been taken into account, and the relative velocity as well as the probability distribution function for the heading differences are included in the derivation of conflict rate. The conflict rate model was expanded further to apply to climbing and descending aircraft in (Tra, 2016) where the ratio of the volume searched by the CD and the total volume of the airspace is utilized for the conflict probability. However the vertical relative velocity was not taken into account, which has been done in (Sunil, n.d.), which has yet to be published.

The conflict rate model takes into account certain assumptions about traffic scenario properties. A *traffic scenario* is a certain setting of traffic structure, it defines the heading and routes for all aircraft in the airspace. The routes include origin point, destination, cruising altitude and the speed. The assumptions are applied for both the Layers concept and unstructured airspace. When deriving the model that included the relative velocity, it was assumed that the heading distribution is uniform and the speed is constant (Hoekstra et al., 2016). The simulations previously performed in (Tra, 2016), had a uniform spacial distribution and uniform distribution of aircraft over the flight levels. In Tra's MSc thesis he validates the model within these following assumptions. Summarizing the assumptions regarding traffic scenarios were used in previous work:

1. The heading angle of aircraft within the simulation area is uniformly distributed.
2. Density is the same over the whole experiment area (spatial distribution is uniform).
3. Traffic is evenly distributed over flight levels.

4. All aircraft have equal airspeed.

But are these assumptions likely to be a realistic scenario?

1-4 Research Objective and Questions

As stated in the previous section, the conflict rate models have been validated, but only when the traffic scenario meets the assumptions. In this study, the traffic scenario is changed by adjusting the distribution setting of scenario properties (heading, altitude, location, and speed). In practice, traffic scenarios are rarely uniformly distributed for the properties mentioned or have the same speed for all aircraft. Thus the model has to be validated for different scenarios to investigate a larger range of scenarios. Examining the assumptions should show how the conflict rate model will react to differently structured traffic scenarios, and determine if the model can be applied to traffic scenarios that don't meet all the assumptions.

The objective of this research is to: *Study the sensitivity of conflict rate models for unstructured and layered airspace designs, when the underlying modeling assumptions related to traffic scenario properties are varied from their ideal (i.e., uniform) distributions.* For example, if only uniformly distributed west-bound heading is used instead of being uniformly distributed over all headings, or the altitude is normally distributed but not uniformly. To reach the objective, this study will try to answer the following research questions and sub-questions:

- What is the effect on the accuracy for the conflict rate model for unstructured airspace and the Layers concept, when the assumptions made in the derivation of the model are not respected?
    1. How dependent is the conflict rate model on uniform heading distribution?
    2. How accurate is the conflict rate model when the traffic is not evenly spread over the flight levels?
    3. What is the accuracy of the model when some area of the airspace is much denser than the rest of the airspace?
    4. Will the model still work if aircraft speeds are not not homogeneous?
- Which traffic scenario property affects the model the most?

1-5 Research Approach

The research is split into two parts, preliminary thesis and main thesis. In the preliminary part, the preparatory work is done for the main thesis, where hypotheses are formed, traffic scenarios are designed and the approach to the experiment is decided. The first step is to do a literature review on relevant subjects.

The goal of the literature review is to investigate and present the state of CD, various decentralized airspace concepts and to fully analyze the conflict rate model derivation. In this study, only CD without CR is applied for the aim is to observe intrinsic safety with the

conflict rate. CR might create more conflict which are not accounted for in the conflict rate model. The conflict rate model is the main focus of the literature study, the model is derived and the equations described in detail.

Next is testing the accuracy of the conflict rate model by analyzing the derivation of the equations of the model. Each property of the scenario affects a certain part of the model, and are then examined individually and in some cases re-derived to fit the corresponding traffic scenario property. Hypotheses on how each scenario property affects the model are made in Chapter 3. To prove or disprove the hypotheses, experiments will be performed. Traffic scenarios are designed to specifically break one assumption at a time but all the other assumptions stay respected. Figure 1-4 is a flowchart of the steps taken in the preliminary thesis phase.

In the main thesis phase, multiple fast-time simulations will be performed where aircraft are generated according to the traffic scenarios that are to be tested. Then the number of conflicts will be counted without any conflict resolution, and the conflict rate determined. The conflict rate from the simulations and from the model will be compared and the accuracy of the model will be determined. Figure 1-5 lists the steps that are to be taken in the main phase of the research.

1-6 Research Scope

Although this thesis aims to expand the scope of previous research, there are still some assumptions that are being applied. It is assumed that there is 0 wind, and no weather or terrain to constrain the traffic. The ADS-B is assumed to have no imperfections. These assumptions could affect the model accuracy but the objective is to investigate the accuracy regarding the traffic scenario. If these assumptions are not included it is difficult to see if the inaccuracies are caused by the traffic scenario, or some other effects. Another assumption is that only en-route airspace is considered, because procedures are different outside of en-route.

1-7 Outline

The thesis is split up into two parts, preliminary and main thesis. Included in the preliminary thesis is the literature review, which can be found in Chapter 2, where the state of the art is investigated and the conflict rate model is described in detail. The design of traffic scenarios is discussed in Chapter 3. Here the scenarios, that are to be tested in the simulations, are designed and hypotheses are formed, based on the equations of the conflict rate models. In Chapter 4, the simulation platform is discussed, the experiment design is presented, dependent and independent variables are also listed. The preliminary thesis will be summarized in Chapter 5.

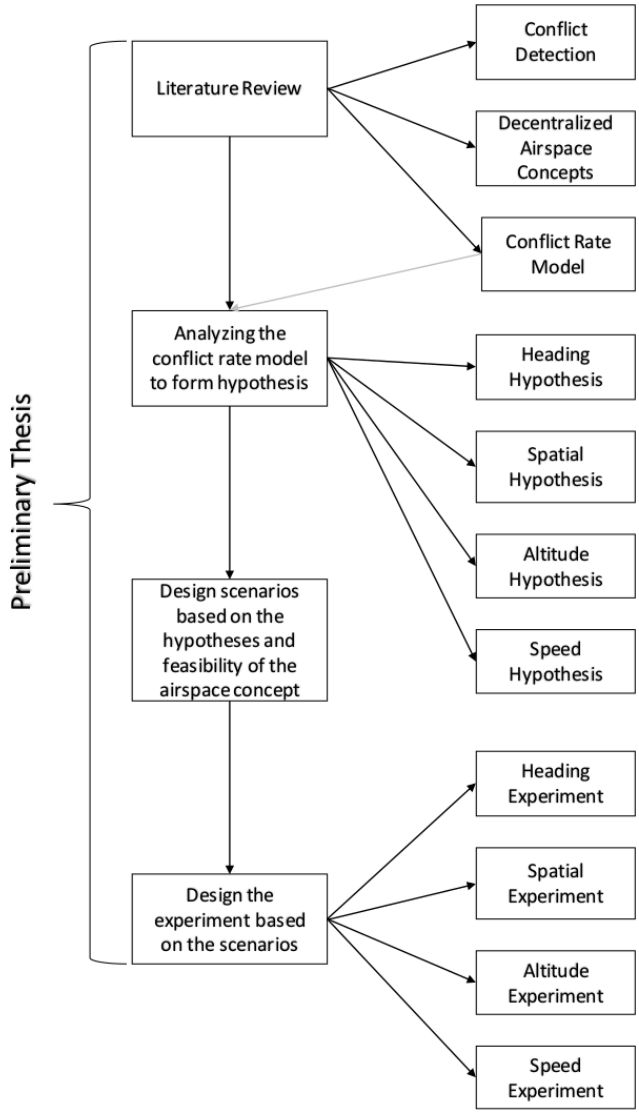

Figure 1-4: The steps taken in the preliminary phase of the research.

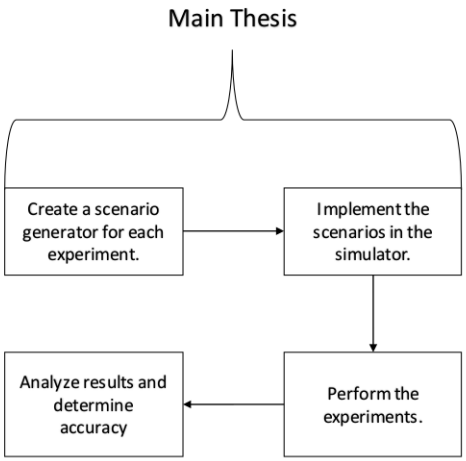

Figure 1-5: The steps taken in the main phase of the research.

Chapter 2

Literature Review

This chapter goes into conflict detection (CD) and describes various decentralized airspace concepts, most notably the Layers concept and an unstructured airspace. The background of conflict rate models is also discussed and the corresponding equations derived.

2-1 Conflict Detection

First it is important to clearly define what a *conflict* is. Conflict is an event when there is a potential loss of minimum separation between two aircraft. When ensuring separation of aircraft, a minimum distance between aircraft is set, typically 5 nm horizontally and 1000 ft vertically, forming a kind of protected zone around the aircraft. The minimum separation is a design criteria of the airspace, and can be set at different values, for examples, some airspaces have 10 nm as the horizontal minimum. When an aircraft intrudes another aircraft's protected zone it is called *loss of separation* or *intrusion*.

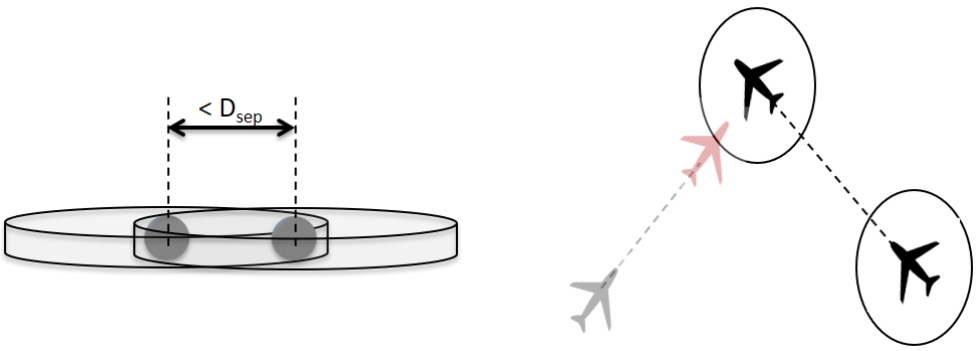

(a) Demonstration of an intrusion.

(b) Demonstration of a conflict.

Figure 2-1: Taken from (Sunil, 2017)

To obtain state data from the other aircraft, the advanced surveillance technology called ADS-B (Hicok & Lee, 2002) is used. Any user within range and proper equipment can receive ADS-B data from broadcasting aircraft. When an aircraft is equipped with ADS-B it broadcasts its information, such as heading and velocity to other aircraft. Thus ADS-B enables an aircraft's pilots to receive surveillance information and detect future conflicts. The process of detecting conflicts is called CD, where the possible future location of the aircraft is linearly extrapolated from the aircraft's current speed and heading. Much progress has been made in development of CD, and many algorithms have been developed (Kuchar & Yang, 2000). Only CD, without CR, will be used in this research because the interest is only in the abilty of an airspace design, by itself, to prevent conflicts.

2-2 Decentralized Airspace Concepts

In a decentralized concept, the separation maintenance falls into two sub-tasks: CD and CR. In (Hoekstra et al., 2016) mentions a third option to maintain separation, conflict prevention. This is not actually a task but more like a design component of the airspace. An airspace might be designed in such a way that less conflict will occur. Airways and using semi-circular rule for heading and altitudes are two examples of conflict prevention. Different airspace design concepts can make conflicts less likely, an example is the Layers concept.

Unstructured Airspace

Unstructured airspace is when aircraft have full control over their own routing. The trajectories they take can be based on optimality. The only constraints are physical constraints like weather, terrain or restricted airspace. Unstructured airspace is often referred to as Free Flight, or Full Mix concepts. The concept was designed to allow direct routing, as it was thought to be more efficient if the airlines could self-optimize (RTCA, 1995). In literature (Clari, Ruigrok, & Hoekstra, 2000) it is concluded that direct routing benefits outweigh the costs related to ASAS.

Layers

In the Layers concept, heading-height rules are used to fix an aircraft's altitude based on its heading. Height rules do not apply to climbing or descending aircraft. The altitude is the only constraints in the Layers concept. Each layer has a heading range assigned to a specific flight level. The heading range is a design parameter which can be adjusted. According to (Tra, 2016), there are fewer conflict with smaller heading range. A visualization can be seen on Figure 1-3. Limiting the aircraft to heading ranges and distributing the traffic between flight levels, lowers the relative velocity between them, resulting in less conflict probability. This increase of safety comes at a slight cost of efficiency though according to (Sunil et al., 2017).

Other Airspace Concepts

In (Sunil et al., 2017) two more concepts are proposed called zones and tubes. Zones separate traffic based on travel direction, similar as the Layers concept, but using a horizontal segmentation, of airspace using predefined paths. These paths are sets rings or along the radial of the zone, see in Figure 2-2a. Aircraft can choose paths in the zone, combining the rings and radials for a trajectory. The Zones concept has no vertical segmentation of the airspace, so the aircraft can choose the optimal altitude. The purpose of the Tube concept is to increase predictability of the traffic. The concept consists of predefined routes connected by nodes, see Figure 2-2b. The Tubes concept has time-based separation while other decentralized airspaces such as the Zones, Layers and unstructured airspace use self separation.

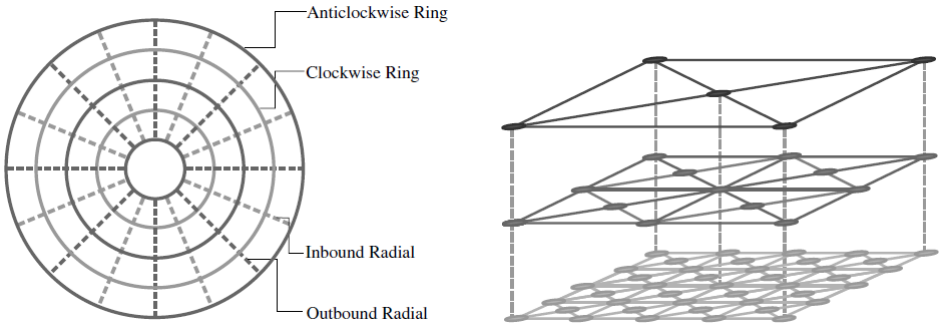

(a) Top view of the Zones concept.

(b) Isometric view of the Tubes concept.

Figure 2-2: A visualization of the Tubes and Zones.(Sunil et al., 2017)

The Layers concept had overall the best results in (Sunil et al., 2017), as a concept with constraints that could prove beneficial. A strict horizontal constraints may result in a mismatch between the airspace structure and the traffic demand. The efficiency for the Layers is a slightly worse than the unstructured airspace, called Full Mix in (Sunil et al., 2017). However the Layers has the best results for stability and safety.

Another type of Layers concept is in use under VFR conditions, where eastbound and westbound traffic are separated by 1000 ft. Where eastbound traffic travels at odd numbered flight levels and westbound traffic at even numbered flight levels. Other implementations of height rules have been studied and can be a type of Layers concept, (Eurocotrol, 2004), (Leiden, Peters, & Quesada, 2009), (Irvine & Hering, 2007) and (Ford, 1983).

2-3 Conflict Rate Model

Conflict rate is the number of conflicts per unit time (Hoekstra et al., 2016) and can be used as a metric for intrinsic safety. In this work, intrinsic safety is defined as the safety that is provided by the airspace design/structure by itself, i.e., safety without tactical CR. There are two ways to measure conflict rate. One where experiments are needed, which can be time consuming and takes computing power. Other is using a theoretical approach, where conflict rate models are used to estimate the conflict rate.

The expected conflict rate is estimated as the product of the number of possible combination of two aircraft, and the conflict probability. The number of possible combinations of aircraft is the maximum number of conflict possible in the airspace, but that is not a realistic number because not all aircraft conflict. To get the a good estimation of conflict the combinations of of aircraft is multiplied with the conflict probability. So in essence, the conflict probability scales the number of combinations of two aircraft to determine conflict rate.

2-3-1 Unstructured Airspace in 2D

In Eq. 2-1 is the basic model for an unstructured airspace where $C_{SS_{UA}}$ is the conflict rate, N_{SS} is the steady state number of aircraft and the p_2 is the instantaneous conflict probability.

$$C_{SS_{UA}} = \binom{N_{SS}}{2} p_2 = \frac{1}{2} N_{SS}(N_{SS} - 1)\ p_2 \tag{2-1}$$

In Jardin's paper (Jardin, 2005), a relationship between the conflict probability p_2 and the ratio between the area that the CD searches, A_c, and the total airspace area A_{total} and was derived. A_c can be expressed in terms of the speed v, time interval t and separation criteria d_{sep}. Figure 2-3 shows a top view visualization of the ratio between A_C and A_{total}.

$$p_2 = \frac{A_c}{A_{total}} \tag{2-2}$$

$$p_2 = \frac{v\ 2d_{sep}\ t}{A_{total}} \tag{2-3}$$

The relations here above say that the conflict rate is proportional to the ratio of the area covered by the aircraft and the airspace area. The conflict probability derived by Jardin does not include the relative velocity. In (Hoekstra et al., 2016) the relative velocity is taken into account. To derive the conflict probability, the speed v in Eq. 2-3 should be substituted for the expected relative velocity.

In Figure 2-4 the relations between the heading difference and relative velocity is demonstrated. With this diagram the relative velocity (v_{rel}) can be derived to Eq. 2-4. However, this equation assumes the speed of all aircraft to be the same. If the scenario that the model is being applied to does not meet the assumptions it stands to reason that the accuracy of the model will be affected.

$$v_{rel}(|\Delta hdg|) = 2\ v \sin\left(\frac{|\Delta hdg|}{2}\right) \tag{2-4}$$

The absolute difference between two uniformly distributed samples like on 2-5a takes the form of triangle distribution like in 2-5b. The probability density function does however only apply when the heading distribution is assumed to be uniform.

$$P(|\Delta hdg| = x) = \frac{2}{\alpha}\left(1 - \frac{x}{\alpha}\right) = \frac{2}{\alpha^2}(\alpha - x) \tag{2-5}$$

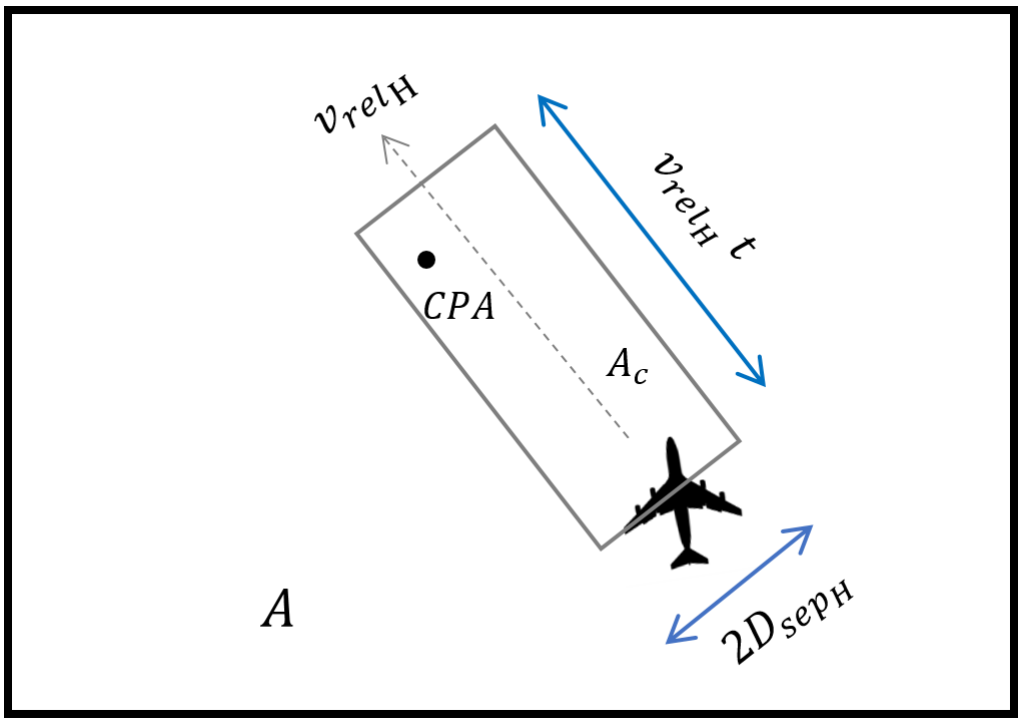

Figure 2-3: A visualization on how the conflict probability (p_2).(Sunil et al., 2017)

Then to derive the expected relative velocity, the probability density function for the absolute heading difference is multiplied with the relative velocity and integrated between 2π and 0 because that is the range of possible heading angles.

$$E_{v_{rel}} = \int_0^{2\pi} P(|\Delta hdg = x|)\ v_{rel}(|\Delta hdg = x|)dx \tag{2-6}$$

$$E_{v_{rel}} = \int_0^{2\pi} \frac{2}{\alpha^2}(\alpha - x)\ 2v \sin\frac{x}{2}dx \tag{2-7a}$$

$$E_{v_{rel}} = \frac{4v}{\pi} \tag{2-7b}$$

Now substituting relative velocity in Eq. 2-7 in the conflict probability results in the final 2D conflict probability:

$$p_2 = \frac{2d_{sep_v}\ t}{A} \cdot \frac{4v}{\pi} \tag{2-8}$$

Then the conflict rate model for the unstructured airspace is:

$$C_{SS_{UA,2D}} = \frac{N_{SS}}{2}\ (N_{SS} - 1) \cdot \frac{2d_{sep_h}\ t}{A} \cdot \frac{4v}{\pi} \tag{2-9}$$

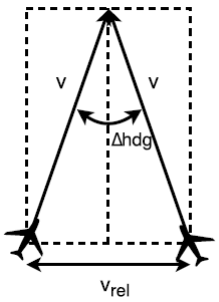

Figure 2-4: The relation between the relative velocity and heading difference.(Tra, 2016)

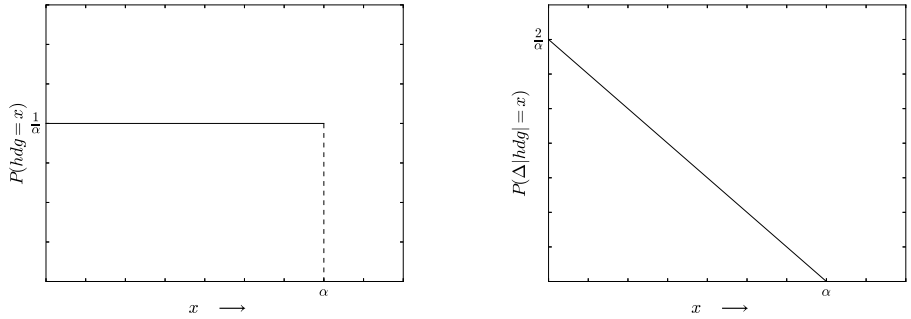

(a) Probability density function for a uniform distribution.

(b) Probability density function for the absolute value of the difference between two uniformly distributed samples.

Figure 2-5

2-3-2 Unstructured Airspace in 3D

The two dimensional model does however not take into consideration climbing and descending aircraft. In unpublished work (Sunil, n.d.), the volume is used instead of the area to compute the conflict probability. The model is inspired by (Endoh, 1982). The ratio between the volume that is searched with conflict detection (V_c) and the total volume of the airspace (V_{total}). In 3D the searched volume is split up to two components for the vertical- and horizontal relative velocity, vertical volume (V_{c_v}) and horizontal volume(V_{c_h}), see Eq. 2-10. V_{c_h} is estimated as a box, extrapolated from the cylindrical volume defined by the separation criteria (see Figure 2-6) and velocity and look ahead time. V_{c_v} is the volume of a cylinder extrapolated with vertical velocity and the look ahead time, described in Eq. 2-12. The conflict probability may be seen in Eq. 2-13, where v_{rel_h} is the horizontal relative velocity, v_{rel_v} is the vertical relative velocity, t is the look ahead time, d_{sep_h} is the horizontal minimum separation typically 5 nm and d_{sep_v} is the vertical separation minimum typically 1000 ft.

$$p_2 = \frac{V_c}{V_{total}} = \frac{V_{c_h}}{V_{total}} + \frac{V_{c_v}}{V_{total}} \tag{2-10}$$

$$V_{c_h} = 4 d_{sep_h} d_{sep_v} \; v_{rel_h} t \tag{2-11}$$

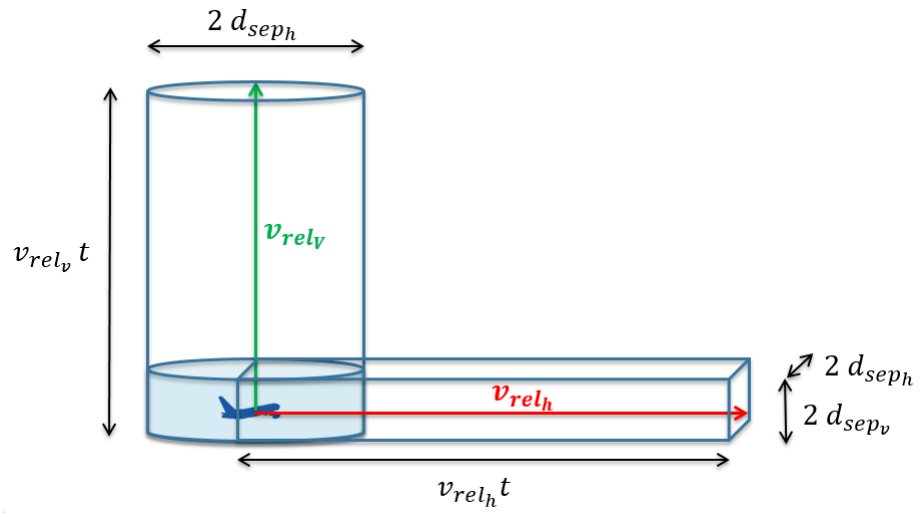

Figure 2-6: A visualization of how the searched volume is calculated.(Sunil, 2017)

$$V_{c_v} = \pi d_{sep_h}^2 \; v_{rel_v} t \tag{2-12}$$

$$p_2 = \frac{4 v_{rel_h} t \; d_{sep_h} d_{sep_v}}{V_{total}} + \frac{v_{rel_v} t \; \pi d_{sep_h}^2}{V_{total}} \tag{2-13}$$

The relative velocity has two parts as well, horizontal and vertical. The horizontal part is described in Eq. 2-7. The vertical relative velocity of an aircraft can be described as:

$$v_v = v \sin \gamma \tag{2-14}$$

Where v is the speed and γ is the climb or descent angle. Then the expected, or weighted average, vertical is derived by multiplying the relative vertical velocity, the probability density function of one interacting aircraft in a possible conflict ($P(|\gamma|_{AC_1} = x)$) and the probability function of the other aircraft interacting in a possible conflict ($P(|\gamma|_{AC_2} = x)$) and then integrating for every possible climbing/descending angle, see Eq. 2-15.

$$E_{v_{rel_v}} = \int_0^{|\gamma|_{max}} \int_0^{|\gamma|_{max}} v_{rel_v}(|\gamma|) \; P(|\gamma|_{AC_1} = x) \; P(|\gamma|_{AC_2} = x) \; d|\gamma|_{AC_1} \; d|\gamma|_{AC_2} \tag{2-15}$$

Aircraft in en-route usually climb and descent at the same angle, and cruising aircraft fly level in en-route with (0 γ). This means that $|\gamma|$ can only take two values. The values being $|\gamma| = 0$ and $|\gamma| = \gamma_{c/d}$, $\gamma_{c/d}$ being the climb and descent angle. Since all the aircraft are assumed to have the same climbing angle and the same descending angle, there are only three types of vertical speed settings, for cruising, climbing and descending aircraft. Eq. 2-15 should be evaluated discretely with respect to all combinations of vertical relative velocities. Permutations can be seen in Table 2-1.

Table 2-1: All possible combinations of vertical relative velocity for the three phases of flight.

AC_1/AC_2	Cruising	Climbing	Descending
Cruising	0	$v \sin \gamma_{c/d}$	$v \sin \gamma_{c/d}$
Climbing	$v \sin \gamma_{c/d}$	0	$2v \sin \gamma_{c/d}$
Descending	$v \sin \gamma_{c/d}$	$2v \sin \gamma_{c/d}$	0

If the aircraft are uniformly distributed both vertically and horizontally then the expected relative velocity can be calculated in phases with the proportion of the cruising aircraft, ϵ being the ratio between cruising aircraft and total number aircraft.

$$\epsilon = \frac{N_{SS_{cruise}}}{N_{SS_{total}}} \tag{2-16}$$

Table 2-2: A discretised version of $P(|\gamma| = x)$ for the three flight phases.

AC_1/AC_2	Cruising	Climbing	Descending
Cruising	ϵ^2	$\frac{\epsilon-\epsilon^2}{2}$	$\frac{\epsilon-\epsilon^2}{2}$
Climbing	$\frac{\epsilon-\epsilon^2}{2}$	$\frac{(1-\epsilon)^2}{4}$	$\frac{(1-\epsilon)^2}{4}$
Descending	$\frac{\epsilon-\epsilon^2}{2}$	$\frac{(1-\epsilon)^2}{4}$	$\frac{(1-\epsilon)^2}{4}$

Now Eq. 2-15 can be rewritten in the discretized form as:

$$E_{v_{rel_v}} = \sum \sum V_{rel_{v_{AC_1 AC_2}}} P(|\gamma|_{AC_1}) \; P(|\gamma|_{AC_2}) \tag{2-17}$$

$$E_{v_{rel_v}} = v \sin(\gamma_{C/D}) \; (1 - \epsilon^2) \tag{2-18}$$

Then adding the expected horizontal relative velocity that contributes to the horizontal volume and expected vertical relative velocity that contributes to the vertical volume to the conflict probability gives:

$$p_{2_{UA,3D}} = \frac{16 \; v \; t \; d_{sep_h} d_{sep_v}}{\pi \; V_{total}} + \frac{v \sin(\gamma_{c/d})(1 - \epsilon^2)\pi \; d_{sep_h}^2}{V_{total}} \tag{2-19}$$

The 3D conflict rate model becomes:

$$C_{SS_{UA,3D}} = \frac{N_{SS}}{2}(N_{SS} - 1) \; \left(\frac{16 \; v \; t \; d_{sep_h} d_{sep_v}}{\pi \; V_{total}} + \frac{v \sin(\gamma_{c/d})(1 - \epsilon^2)\pi \; d_{sep_h}^2}{V_{total}} \right) \tag{2-20}$$

2-3-3 Layers in 3D

The conflict rate model was expanded in (Hoekstra et al., 2016), so that it could be applied to the Layers concept. As the Layers concept has vertical segmentation that separates traffic, the conflict rate for each layer is described in Eq. 2-21, where $C_{SS_{layer_i}}$ is the conflict rate, $N_{SS_{layer}}$ is the number of steady state aircraft in a single layer. The conflict rate for the whole

airspace is then a summation over all the layers, in Eq. 2-22, where $C_{SS_{layers}}$ is the conflict rate for cruising aircraft for all layers. The equation can be simplified, when the number of aircraft is the same for all layers, Eq. 2-23 can be applied in that case. However if the altitude distribution is not uniform the outcome of 2-23 should not be accurate.

$$C_{SS_{layer_i}} = \frac{1}{2} N_{SS_{layer}} (N_{SS_{layer}} - 1)\ p_2 \tag{2-21}$$

$$C_{SS_{layers}} = \sum_{layer=1}^{L} \frac{1}{2} N_{SS_{layer}} (N_{SS_{layer}} - 1)\ p_2 \tag{2-22}$$

$$C_{SS_{layers}} = \frac{1}{2} N_{SS} \left(\tfrac{N_{SS}}{L} - 1\right) p_2 \tag{2-23}$$

The conflict probability for the Layers concept is found the same way as for the unstructured airspace, showcased in Eqs. 2-10 and 2-13. For cruising aircraft, the conflict probability is the same as derived earlier for 2D unstructured airspace. The only difference is that while unstructured airspace allows 2π headings in all altitudes, with layers, the heading range is limited to alpha degrees per cruising flight level. While the unstructured airspace uses 2π as the integral range, the derivation for the Layers concept uses α, the heading range of each layers.

$$E_{v_{rel_h}} = \int_0^{\alpha} P(|\Delta hdg = x|)\ v_{rel_h}(|\Delta hdg = x|) dx \tag{2-24}$$

$$E_{v_{rel_h}} = \int_0^{\alpha} \frac{2}{\alpha^2} (\alpha - x)\ 2v \sin\frac{x}{2} dx \tag{2-25a}$$

$$E_{v_{rel_h}} = \frac{8v}{\alpha} \left(1 - \frac{2}{\alpha} \sin\frac{\alpha}{2}\right) \tag{2-25b}$$

The Layers conflict rate model that includes climbing and descending traffic, is an extension of the model for unstructured airspace. Some steps of the derivation of the relative velocity in Table 2-1 and 2-2. Climbing and descending aircraft do not follow the height rules so the aircraft should be divided into:

- Cruising - Cruising
- Cruising - Climbing/Descending
- Climbing/Descending - Climbing/Descending

The conflict rate model for the Layers concept has to be derived for each of those situations, see Eq. 2-26.

$$C_{SS_{Layers}} = C_{SS_{Cruising}} + C_{SS_{Cruising-C/D}} + C_{SS_{C/D}} \tag{2-26}$$

For the Cruising - Cruising model there is no need to take the vertical relative velocity into consideration, thus the area is used for conflict probability but the volume is not considered.

The number of combinations of aircraft that is used is the one defined Eq. 2-23. To reiterate the model is:

$$C_{SS_{Cruising}} = \frac{N_{SS_{Cruising}}}{2}\left(\frac{N_{SS_{Cruising}}}{L} - 1\right)\ p_{2_{Cruising}} \tag{2-27}$$

Where the conflict probability, $p_{2_{Cruising}}$, is the same as the 2D conflict probability from Eq. 2-3, but the expected relative velocity is from Eq. 2-25b:

$$p_{2_{Cruising}} = \frac{2\ d_{sep_h} t}{A_{total}}\ \frac{8v}{\alpha}\left(1 - \frac{2}{\alpha}\sin\left(\frac{\alpha}{2}\right)\right) \tag{2-28}$$

The model for the Cruising - Climbing/Descending situation is similar to the unstructured airspace model. Because an aircraft cannot be cruising at the same time as they are climbing or descending, there are different sets of aircraft and the number of combinations of cruising and climbing/descending aircraft is $N_{SS_{Cruising}} \times N_{SS_{C/D}}$. For the conflict probability the horizontal relative velocity stays the same but the vertical relative velocity is different. Only aircraft that are cruising on the one hand and climbing or descending on the other are considered when deriving the expected relative velocity, see Tables 2-3 and 2-4. Applying that to Eq. 2-17 results in the expected relative velocity in Eq. 2-29.

Table 2-3: All possible combinations of vertical relative velocity for a combination of cruising and climbing/descending aircraft.

AC_1/AC_2	Cruising	Climbing	Descending
Cruising		$v \sin \gamma_{c/d}$	$v \sin \gamma_{c/d}$
Climbing	$v \sin \gamma_{c/d}$		
Descending	$v \sin \gamma_{c/d}$		

Table 2-4: A discretised version of $P(|\gamma| = x)$ for for a combination of cruising and climbing/descending aircraft.

AC_1/AC_2	Cruising	Climbing	Descending
Cruising		$\frac{\epsilon-\epsilon^2}{2}$	$\frac{\epsilon-\epsilon^2}{2}$
Climbing	$\frac{\epsilon-\epsilon^2}{2}$		
Descending	$\frac{\epsilon-\epsilon^2}{2}$		

$$v_{rel_v} = 2v \sin(\gamma_{C/D})\ (\epsilon - \epsilon^2) \tag{2-29}$$

The Cruising-Climbing/Descending model becomes:

$$C_{SS_{Cruising-C/D}} = N_{SS_{Cruising}}\ N_{SS_{C/D}}\ p_{2_{Cruising-C/D}} \tag{2-30}$$

$$p_{2_{Cruising-C/D}} = \frac{16v\ t\ d_{sep_h}\ d_{sep_v}}{\pi\ V_{total}} + \frac{2v\ \sin(\gamma_{C/D})(\epsilon - \epsilon^2)\ \pi\ d_{sep_h}^2}{V_{total}} \tag{2-31}$$

The model for the Climbing/Descending - Climbing/Descending has the same number of combinations of aircraft as the unstructured airspace model, but uses only the climbing/descending part of Tables 2-1 and 2-2 for the vertical relative velocity.

$$C_{SS_{C/D}} = \frac{N_{SS_{C/D}}}{2}(N_{SS_{C/D}} - 1)\ p_{2_{C/D}} \tag{2-32}$$

$$p_{2_{C/D}} = \frac{16v\ t\ d_{sep_h}\ d_{sep_v}}{\pi\ V_{total}} + \frac{v\ \sin(\gamma_{C/D})(1-\epsilon)^2\ \pi\ d_{sep_h}^2}{V_{total}} \tag{2-33}$$

2-4 Summary of Key Assumptions

- The assumption that the heading angle of aircraft are uniformly distributed between 0° and 360°, is made when deriving the probability density function for the derivation of the relative horizontal velocity in Eq. 2-24. The equation used in the integration assumes uniform heading distribution.
- The aircraft are assumed to be uniformly distributed to flight levels. Eq. 2-23 uses this assumption to simplify the number of combinations of aircraft, which is then used for the cruising conflict in the layers concept. This assumption will probably not affect unstructured airspace as the model takes into account the proportion of aircraft in different flight phases.
- The assumption that the spatial distribution is uniform means that origin points of the aircraft are distributed uniformly over the experiment area. The conflict probability is assumed to be the same everywhere in the airspace, while areas with higher density would logically have higher conflict probability.
- The speed assumption is used in the relative velocity part in Eqs. 2-4 and 2-14, where the speed is assumed to be the same for all aircraft in the simulation. The assumption is used to simplify the relative velocity equations.

Chapter 3

Scenario Design

Different scenarios have been designed to analyze the accuracy of the conflict rate models. The different scenarios will be tested for different airspace concepts, the Unstructured Airspace, and variations of Layers concepts. Different experiments will be made for each assumption that is being tested. This is done to isolate the assumption and see the effect from the singular assumption. The heading range of the Layers concept will be 90°, 180° and 360°. As the conflict rate model is designed to meet specific assumptions, the scenarios are designed to not meet these assumptions, to test the sensitivity of the models to such assumptions. The assumptions are broken by changing the traffic distribution and not having equal speed for all the aircraft. Hypotheses are made about what the scenarios that are designed will result in, in terms of model accuracy. In the main phase of the thesis these scenarios will be simulated and compared with a baseline scenario, which meets all the assumptions made in the derivation of the model.

3-1 Baseline Scenario and Scenario Generation Methods

A traffic scenario defines the heading and routes for all aircraft in the scenario. The route includes origin points, destination points, cruising altitude and speed. One scenario will meet all the assumptions made in the derivation of the model. It will be used for comparison with other scenarios. The baseline has uniform heading distribution, uniform distribution of the origin point where the aircraft starts at, aircraft spread evenly across flight levels and homogeneous speed distribution. As can be seen in Figure 3-2, when all the assumptions are met, the traffic scenario is truly random, with no preferred directions, headings or flight distances. .

The inputs in the scenario generator are the density range which are to be tested, the average True Air Speed (TAS), minimum flight time, duration of the scenario, minimum altitude, height of an individual layer, number of layers and separation criteria. There is a minimum distance which the aircraft can travel, that is the minimum distance possible to travel at the average TAS with respect to the minimum flight time. All aircraft in the simulation have the

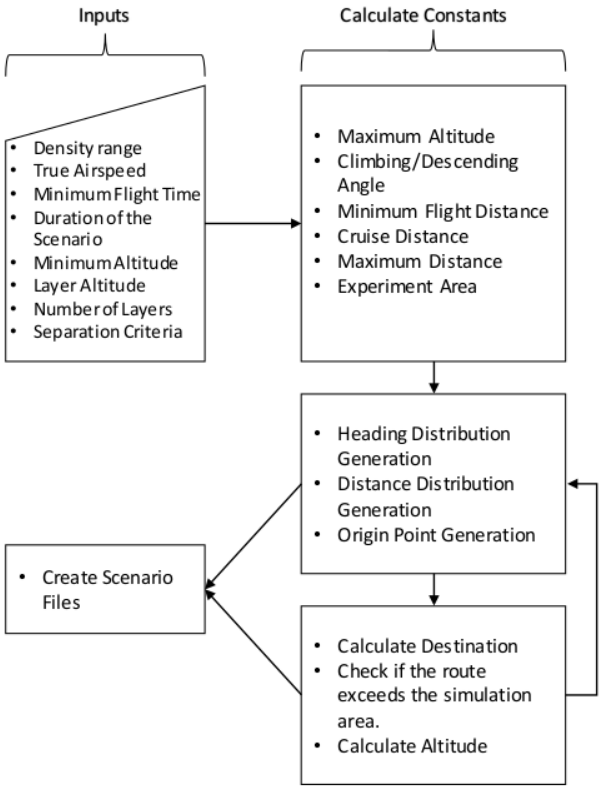

Figure 3-1: A flowchart of how a scenario generator operates.

same cruise distance, and the same climb angle. Consequently, a similar number of aircraft are cruising in each flight level of the layered concepts. The aircraft in the simulation spawn at a certain rate to maintain the constant density in the experiment. The scenario generation process is summarized in Figure 3-1

The first step in generating a scenario is determining the origin points and the destination points. The origin points are chosen with uniform distribution over the simulation area. The distance and the heading are then chosen, in the baseline scenario a uniform distribution is used for both distance and heading. Using the heading and distance, the destination coordinates can be computed given the desired origin of an aircraft. If the destination point is outside the simulation area, a new origin point is chosen to make the trajectory fit. Eq. 3-1 shows the equations used to calculate the destination point, where R is the radius of the earth, hdg is the heading, lat is latitude and lon is longitude, d is the flight distance.

$$lat_{dest} = \arcsin\left(\sin\left(lat_{origin}\right)\cos\left(d/R\right) + \cos\left(lat_{origin}\right)\sin\left(d/R\right)\cos\left(hdg\right)\right) \tag{3-1a}$$

$$lon_{dest} = lon_{origin} + \arctan\left(\frac{\sin\left(hdg\right)\sin\left(d/R\right)\cos\left(lat_{origin}\right)}{\cos\left(d/R\right) - \sin\left(lat_{origin}\right)\sin\left(lat_{dest}\right)}\right) \tag{3-1b}$$

Then the route is computed, where the altitude is determined with the top of climb and descent points. The altitude is determined by the distance, for the unstructured airspace see Equation (3-2) where h is the altitude and d is the distance. See Eq. 3-3 for the Layers concept where γ is the heading angle, α is the heading range, $n_{d_{bins}}$ is the number distance bins, $n_{\gamma_{bins}}$ is the number heading bins (see Eqs. 3-4 and 3-5), and the floor operator rounds the value down to an integer. The heading bins is how many heading ranges there. A flowchart of a scenario generator is in Figure 3-1.

$$h_{UA} = h_{min} + \frac{h_{max} - h_{min}}{d_{max} - d_{min}} \left(d - d_{min}\right) \tag{3-2}$$

$$h_L = h_{min} + \left(h_{layer} \text{ floor} \left(\frac{d - d_{min}}{d_{max} - d_{min}} \; n_{d_{bins}} \right) \; n_{\gamma_{bins}} + \text{floor} \left(\frac{\gamma}{\alpha} \right) \right) \tag{3-3}$$

$$n_{\gamma_{bins}} = \frac{2\pi}{\alpha} \tag{3-4}$$

$$n_{d_{bins}} = \frac{n_{Layers}}{n_{\gamma_{bins}}} \tag{3-5}$$

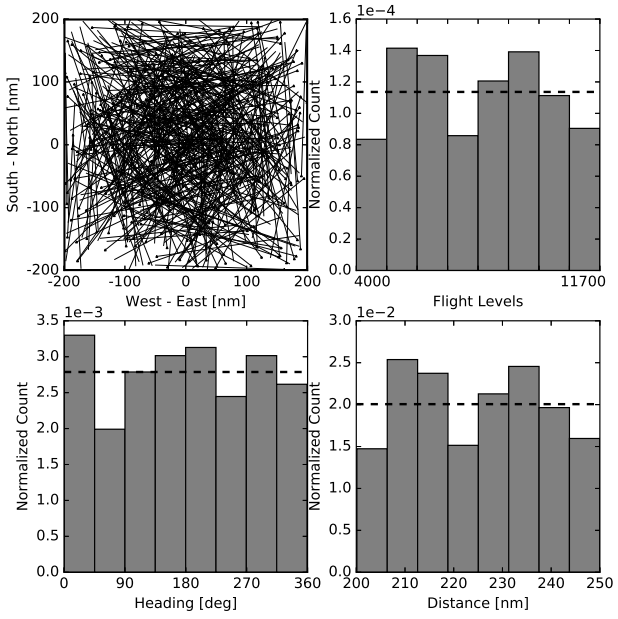

Figure 3-2: The baseline scenario, top view of the trajectories and the distributions of heading, altitude and distance.

3-2 Heading Scenario

In section 2-3 the conflict rate model is explained. As has been mentioned there are assumptions made in deriving the model. One assumption is that the heading distribution is uniform,

which affects the expected horizontal relative velocity (in Eq. 2-24). When the probability density function used for the derivation is uniform, then the probability density function for the absolute heading difference is triangular, see Eq. 2-5 and Figure 2-5b. When using different distributions, it is expected that they affect the accuracy of the model significantly. The first step in checking the change in accuracy is to look at the difference in how the model would be derived for other heading distribution cases.

A normal distribution is selected to represent traffic scenario where aircraft favor a specific heading, for example when it is the time of day where mostly westbound traffic is flying, although a southbound traffic is used in this case. Using bimodal distributions can constitute for a head on traffic. A ranged uniform distribution is used to create traffic that is only southbound, similar with the normal distribution, but with a different distribution.

When using a normal distributions, the probability distribution function for the absolute heading difference is a half normal distribution. Instead of using probability density function in Eq. 2-5 while deriving the relative velocity in Eq. 2-24, a different probability density function is used, in the case of a normal distribution Eq. 3-7 is used. The probability density funciton for the heading difference for a bimodal distribution is a multimodal distribution with 3 curves, when using the absolute heading difference it becomes a bimodal distribution as well, see Eq. 3-8. Eq. 3-9 shows the probability density function for the ranged uniform distribution.

$$P(|\Delta hdg| = x)_{uniform} = \frac{2}{\alpha^2}(\alpha - x) \tag{3-6}$$

$$P(|\Delta hdg| = x)_{normal} = \frac{\sqrt{2}}{\sigma\sqrt{\pi}}\ e^{-\frac{(x)^2}{2\sigma^2}} \tag{3-7}$$

$$P(|\Delta hdg| = x)_{bimodal} = \frac{1}{2\sqrt{2\pi\sigma^2}}\ e^{-\frac{(x-\pi)^2}{2\sigma^2}} + \frac{1}{\sqrt{2\pi\sigma^2}}\ e^{-\frac{x^2}{2\sigma^2}} \tag{3-8}$$

$$P(|\Delta hdg| = x)_{ranged,uniform} = \frac{4}{\alpha^2}(\alpha - 2x) \tag{3-9}$$

Then the probability density function is multiplied with the relative velocity function in 2-4, then integrated as was done in Eq. 2-24. In Eqs. 3-10 to 3-13 $g(\alpha)$ is the value that is multiplied with the speed to get the horizontal relative velocity. Then to investigate how it affects the conflict rate model, values for different distributions are calculated and the error from the uniform distribution is calculated.

$$\bar{v}_{rel_{H_{uniform}}} = \int_0^\alpha \frac{2}{\alpha^2}(\alpha - x)\ 2v \sin\frac{x}{2} dx \tag{3-10}$$

$$\bar{v}_{rel_{H_{normal}}} = \int_0^\alpha \frac{\sqrt{2}}{\sigma\sqrt{\pi}}\ e^{-\frac{(x)^2}{2\sigma^2}}\ 2v \sin\frac{x}{2} dx \tag{3-11}$$

$$\bar{v}_{rel_{H_{bimodal}}} = \int_0^\alpha \left(\frac{1}{2\sqrt{2\pi\sigma^2}}\ e^{-\frac{(x-\pi)^2}{2\sigma^2}} + \frac{1}{\sqrt{2\pi\sigma^2}}\ e^{-\frac{x^2}{2\sigma^2}}\right)\ 2v \sin\frac{x}{2} dx \tag{3-12}$$

$$\bar{v}_{rel_{H_{ranged-uniform}}} = \int_0^\alpha \frac{4}{\alpha^2}(\alpha - 2x)\ 2v \sin\frac{x}{2} dx \tag{3-13}$$

Table 3-1: Values of $\bar{v}_{rel_H}$ and the error from the uniform distribution. This only applies to heading range of 360°. This assumes all aircraft have TAS 400 kts.

Distribution	$\bar{v}_{rel_H}$	Error in %
Uniform	509	0
Normal	226	55.7
Bimodal	485	4.6
Ranged Uniform	370	27.3

Table 3-1 shows the values of $\bar{v}_{rel_H}$ for all distributions that are to be tested. It also shows the error with respect to the uniform distribution. The values for the normal distribution gives the smallest expected relative velocity, which is logical because most aircraft are heading in a similar direction. The bimodal distribution gives the smallest error, but the expected relative velocity is smaller for the bimodal than for the uniform distribution. The ranged uniform distribution has smaller values than for the uniform one, but that makes sense since the heading range is smaller. The values in Table 3-1 are relevant for the Layers 360 and unstructured airspace, as using values for Layers with smaller heading ranges would cause the altitude distribution to be non-uniform, which is not desirable in the heading experiment. Another reason is that, multiple probability density functions are needed to derive expected relative velocity, that is discussed further in Appendix B. Figures 3-3 to 3-5 give examples of 3 heading scenarios. They show histograms of the heading, altitude and distance distribution. They also show a top view of trajectories where the triangles in the figures are the spawning points of the aircraft. The histograms that show the distance and altitude are very similar, this should be expected for the altitude is chosen by distance.

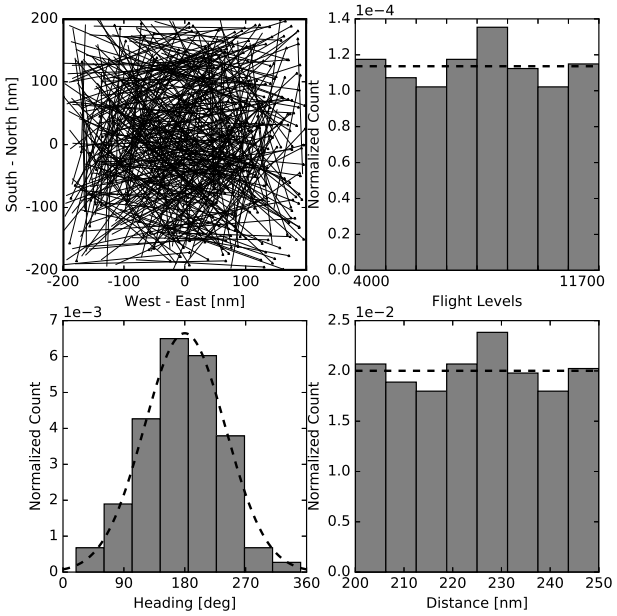

Figure 3-3: An example of a scenario with normal heading distribution. A top view of the trajectories is in the upper left corner. Histograms of the traffic scenario properties are presented as well. The dashed lines mark the reference distribution.

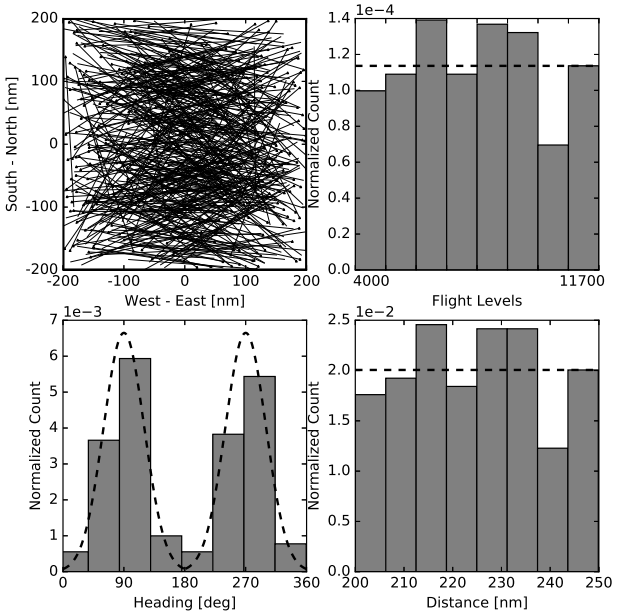

Figure 3-4: An example of a scenario with bimodal heading distribution. A top view of the trajectories is in the upper left corner. Histograms of the traffic scenario properties are presented as well. The dashed lines mark the reference distribution.

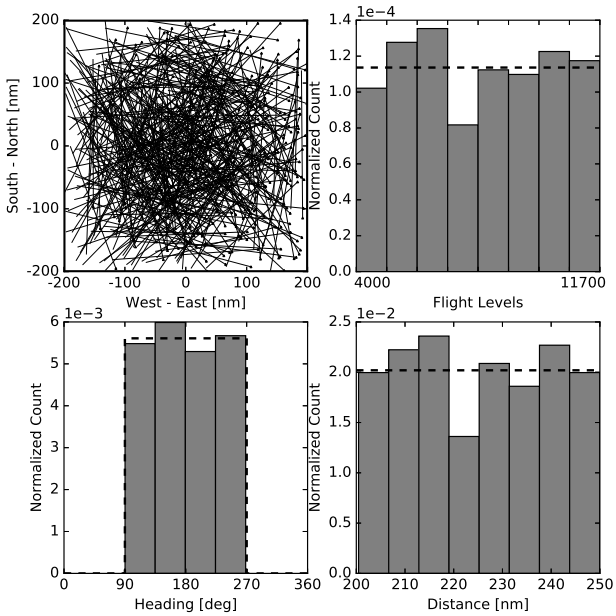

Figure 3-5: An example of a scenario with a uniform heading distribution on the range 90°-270°. A top view of the trajectories is in the upper left corner. Histograms of the traffic scenario properties are presented as well. The dashed lines mark the reference distribution.

3-3 Spatial Distribution Scenario

The spatial distribution refers to the spread of aircraft in the horizontal plane. The model assumes a uniform spatial distribution. Because of uniform spatial distribution the conflict probability is assumed to be equal for the whole experiment area. However, if there are density hot-spots in the airspace, as is usually the case for sectors with crossing routes in current traffic, then the conflict probability in those hot-spots should be higher than in other areas in the airspace with lower densities. To investigate how this affects the conflict probability, simulations will be performed with hot-spots of different sizes.

Eq. 2-2 says, the conflict probability is proportional to the ratio of the separation area of the aircraft extrapolated with the distance it travels and the total area of the experiment. The density is the ratio between the number of instantaneous aircraft and an area. Seeing how the size of a hot-spot will increase the density in a single area, it stands to reason that the conflicts will increase significantly. If the density of the experiment and density of a hot-spot are compared is shows that the density is much higher for the hot-spots.

If the origin points of the aircraft are normally distributed for both latitudes and longitudes, lthough it should be noted that the normal distribution gets disrupted when the program is insuring that the aircraft do not fly out of the simulation area. The center of the area as mean for the normal distribution and standard deviation to determine the size of the hot-spot. Most of the aircraft are generated within a circular are. The size of the area that the origin points are within, are determined by the standard deviation of the latitudes and longitudes. When samples are normally distributed, 99.7 % of the samples are within 3 times the standard deviation. Hot-spot areas are considered to be circular area with a radius of 120 nm, 90 nm and 60 nm for the three hot-spots, which would give 60 nm, 40 nm and 20 nm as the standard deviation. In Table 3-2 three hot-spot areas have been calculated for a scenarios with 5 aircraft per 10000 nm^2 as the experiment density. Hot-Spot 1 has a circular area with a radius of 120 nm and the standard deviation for the normal distribution is 40 nm, see Figure 3-6. Hot-Spot 2 has a radius of 90 nm, with a standard deviation of 30 nm and Hot-Spot 3 has a radius of 60 nm with a standard deviation of 20 nm, see Figures 3-7 and 3-8. The densities of the hot-spots increase as can seen in Table 3-2. The Number of instantaneous aircraft is a parameter in the model, and the area (within the volume) it stands to reason that the conflict count will increase with a decreasing size of hot-spots.

Table 3-2: The densities for various hot-spots compared with an example density for the experiment.

	Hot-Spot 1	Hot-Spot 2	Hot-Spot 3
Hot-spot Radius [nm]	120	90	60
Experiment Density [ac/10000 nm^2]	5	5	5
Hot-Spot Density [ac/10000 nm^2]	11	16	24

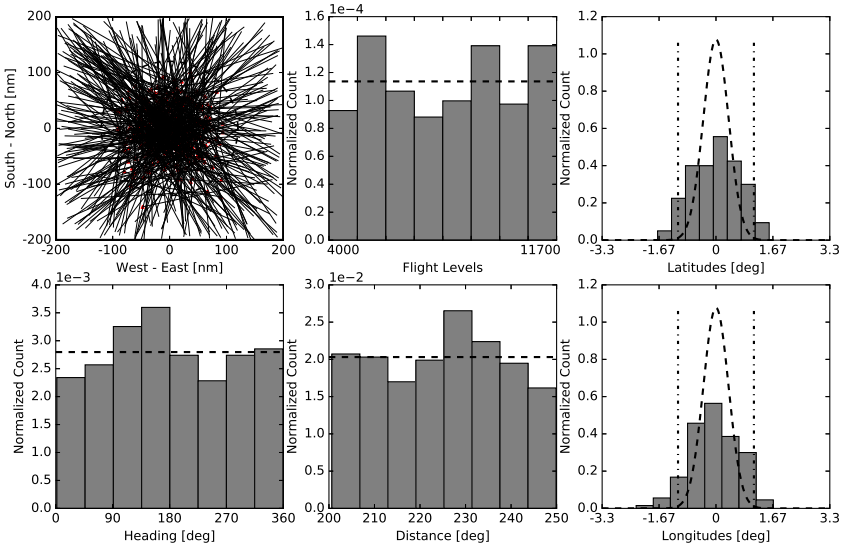

Figure 3-6: An example of a scenario with a hot-spot with a radius of 120 nm. In the far right, the histograms show the distribution of the latitudes and longitudes. A reference normal distribution is shown with a dashed line. The dashed-dotted vertical lines is representing the hot-spot area.

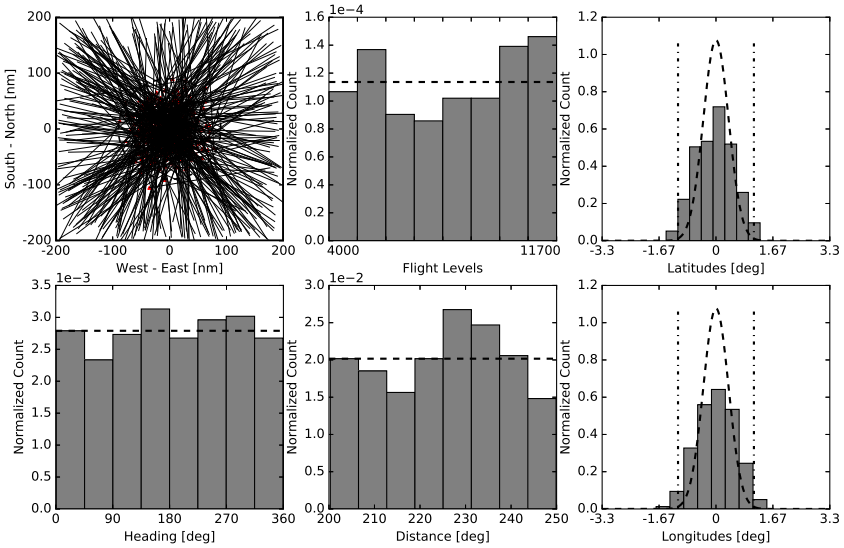

Figure 3-7: An example of a scenario with a hot-spot with a radius of 90 nm. In the far right, the histograms show the distribution of the latitudes and longitudes. A reference normal distribution is shown with a dashed line. The dashed-dotted vertical lines is representing the hot-spot area.

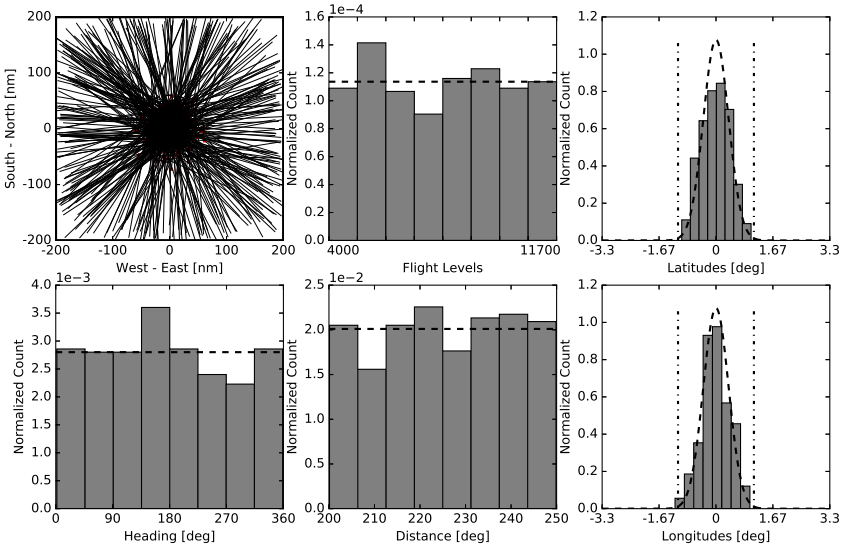

Figure 3-8: An example of a scenario with a hot-spot with a radius of 60 nm. In the far right, the histograms show the distribution of the latitudes and longitudes. A reference normal distribution is shown with a dashed line. The dashed-dotted vertical lines is representing the hot-spot area.

3-4 Altitude Scenario

One of the ways the layers concept reduces conflict rate and improves safety over unstructured airspace is because it reduces the number of combinations of cruising aircraft that can conflict with each other. In the derivation of the model, it was assumed that aircraft are evenly/uniformly distributed in the vertical direction. Consequently, the number of combinations of cruising aircraft for all flight levels is simply a multiple of the number of combinations of cruising aircraft in each layer. However, if this is not the case, then it stand to reason that the accuracy of the model will be negatively affected as the number of combinations will be wrongly computed.

To study the effect of altitude distribution on model accuracy, scenarios with different vertical aircraft distributions are compared. As flight distance affects the altitude selection for all layered and unstructured concepts, different flight distance distributions are used to manipulate the altitude distribution of a traffic scenario. Although altitude is also a function of the heading distribution, the heading distribution also affects the conflict probability via the relative velocity. Therefore, to isolate the effect of vertical aircraft distribution on model accuracy, only the distance is used to determine the altitudes of aircraft (while using uniform distribution).

The different distributions may represent locations with different terrain or destination popularity. A ranged uniform distribution is used where all the aircraft are in the upper half of the airspace, which can be practical for the aircraft for fuel conservation. Traffic with normal altitude distribution represents a traffic that favors the center of the airspace and a bimodal distribution represents a traffic that favors two different flight levels.

In the conflict rate model that applies to the Layers concept, the number of layers is one of the parameters. Eq. 2-23 assumes that the aircraft are spread evenly across all the layers. When the aircraft are not spread evenly it stands to reason that the number of combinations of aircraft is different for every layer. Eq. 2-21 describe how each single layer affects the conflict rate, and Eq. 2-22 is the conflict rate model including all the layers. When the aircraft are uniformly distributed over the altitude Eq. 2-23 applies, because the number of aircraft in each layer is the same. Figure 3-9 shows the number of combinations of 2 aircraft for an increasing number of instantaneous aircraft. The figure shows a clear divergence when normal and ranged-uniform altitude distribution is assumed, but the double normal distribution gives results that are much closer to uniform distribution. This indicates that the model will become less accurate with increased number of aircraft, but the double normal distribution might be more accurate for the altitude scenario than the other two altitude distributions.

The altitude is dependent on the distance as has been mentioned, and for the Layers concept with heading range smaller than 360° it is also dependent on the heading. To control the altitude for the Layers, the heading and the distance need to be synchronized. Different distributions will be tested for the altitude. Uniform distribution is tested in the baseline scenario, the three additional distributions are normally distributed, bimodal distribution and a ranged uniform distribution. For the unstructured airspace and Layers 360, the heading does not need to be taken into account to correctly fix the altitude distribution. So only concepts where altitude is only dependent on distance are considered. Figures 3-10, 3-11 and 3-12 show a visualization of altitude, distance and heading distributions as well as a top view of trajectories.

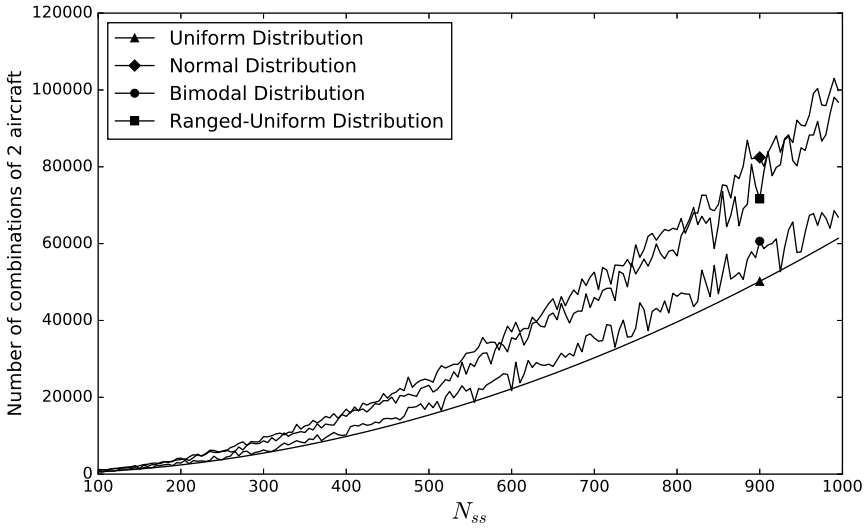

Figure 3-9: The number of combinations of two aircraft with increasing traffic demand.

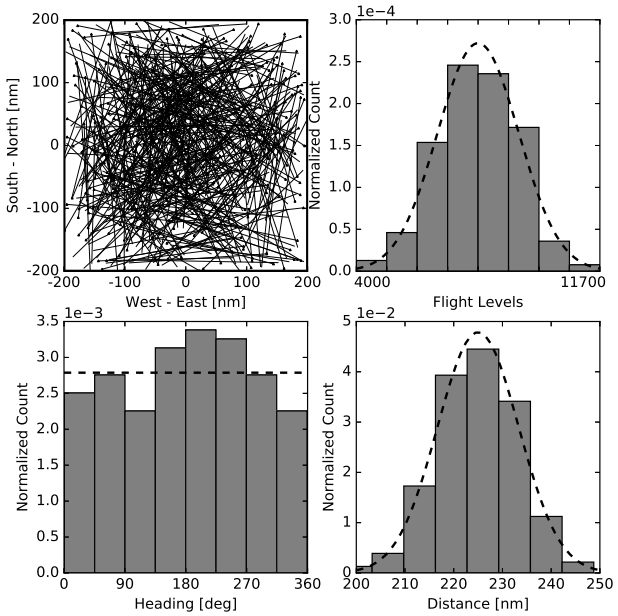

Figure 3-10: An example of a scenario with normal altitude- and distance distribution. A top view of the trajectories is in the upper left corner. Histograms of the traffic scenarios are presented as well.

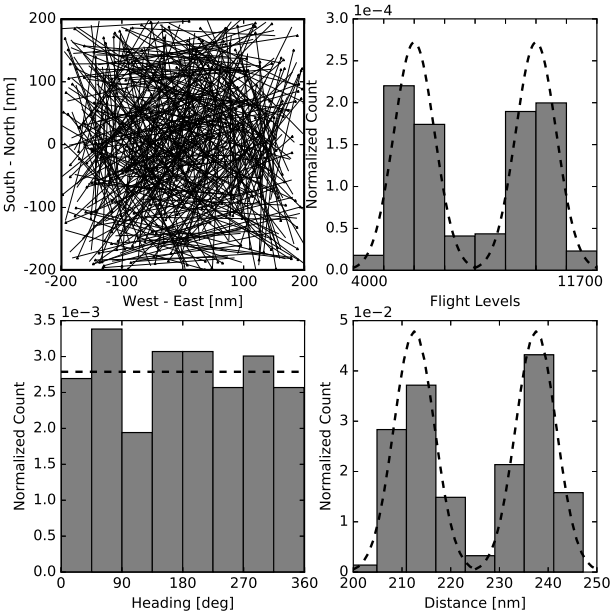

Figure 3-11: An example of a scenario with bimodal altitude- and distance distribution. A top view of the trajectories is in the upper left corner. Histograms of the traffic scenarios are presented as well.

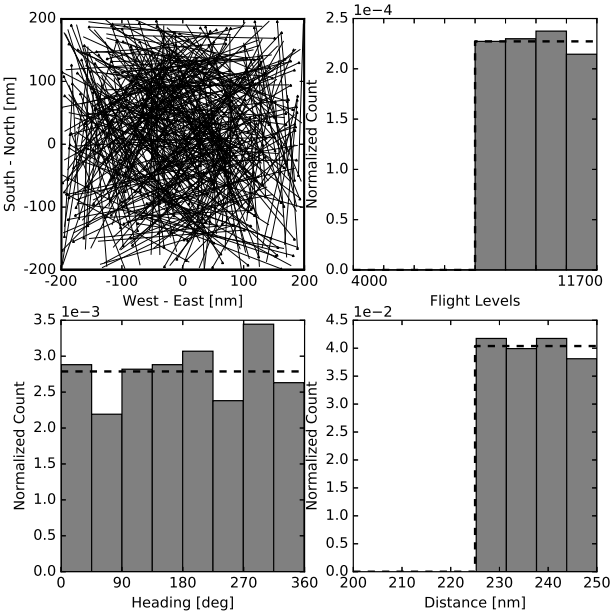

Figure 3-12: An example of a scenario with a uniform altitude- and distance distribution on the range 8400 ft to 11700 ft. A top view of the trajectories is in the upper left corner. Histograms of the traffic scenarios are presented as well.

3-5 Speed Scenario

The derivation of the conflict rate model assumes that the velocity is the same for all aircraft. To test how the the model reacts to the speed being non-homogenous, probability distributions are utilized for the speed. A normal distribution is used for aircraft that favor the speed used in the baseline scenario, but some deviate from it. Bimodal distribution is used for two favored speed settings, but as well some deviating from them. A uniform distribution to get a speed distribution that does not favor any one speed setting. The first step in investigating the effect of the speed being non-homogenous is to determine the expected relative velocities for different distributions of speed.

In literature (Endoh, 1982), the expected relative velocity is presented with two velocity factors for each of the interacting aircraft, see Eq. 3-14. Where v_1 and v_2 are the speeds of the interacting aircraft, α is the heading range, $P(v_1)$ and $P(v_2)$ are the probability density functions for the speeds and $P(|\Delta hdg|)$ is the probability density function for the absolute heading difference. When the velocity magnitudes of the aircraft are constant, this equation becomes the same as Eq. 2-25b. In the conflict rate model, only constant velocity is assumed.

$$E(v_{rel_h}) \int_{v_1} \int_{v_2} \int_{0}^{\alpha} (v_1^2 + v_2^2 - 2v_1 v_2 \cos(|\Delta hdg|))^{\frac{1}{2}} P(v_1)P(v_2)P(|\Delta hdg|)\, d|\Delta hdg|\, dv_2\, dv_1 \tag{3-14}$$

The equation here above was evaluated numerically, for three types of the Layers concept as the L360 and unstructured airspace concepts have the same horizontal relative velocity. In Table 3-3 the results for different speed distribution are shown. It is rather clear by looking at the values that the expected horizontal velocity does not change much when the speed is not constant. So it is not expected that the simulations will result in a different manner.

Table 3-3: The expected horizontal relative velocity factors for different speed distribution types.

Speed Distribution	L360	L180	L90
Constant	509	370	203
Normal	507	370	205
Bimodal	509	373	208
Uniform	512	374	210

3-6 Summary of Hypotheses

To summarize the hypotheses:

- In Table 3-1 the error of the expected relative velocity is the same for normally distributed samples and bimodal distributed sample. It Normally distributed heading and bimodal heading distribution will have similar affect on the accuracy.
- The ranged uniform heading distribution, where all the traffic is between 90° and 270°, will affect the accuracy less than if the traffic is normally distributed as the error of

the expected relative velocity is significantly smaller then for for normal and bimodal distribution, according to Table 3-1.

- When the traffic is not spread evenly through all flight levels for the Layers concept, the accuracy will decrease with increased traffic demand. In Figure 3-9 the number of possible combinations of 2 aircraft is shown with increasing traffic density. The number of combinations diverges from the baseline when using distributions that are not uniform, although when using a bimodal distribution, the profile does not diverge as much as for normal or ranged-uniform distribution.
- It is hypothesized that a decrease in the size of a hot-spot that is formed from non-uniform spatial distribution, increases the conflict rate in the airspace. Table 3-2 shows that when the size of the hot-spot is taken into account, the density is much larger than originally assumed.
- The speed distribution will not have a significant effect on the accuracy of the model. From Table 3-3 we can see that there is very insignificant change in the expected relative velocity changes when different speed distributions are used, when the equations are re-derived for normal-, uniform- and bimodal distributions.

Chapter 4

Fast-Time Simulation Design

Four fast-time simulation experiments will be conducted to determine the accuracy of the conflict rate model. This chapter describes the design of these experiments. The four experiments will be performed for different heading distributions, spatial distribution, altitude distributions and speed distributions, because these correspond to the four main scenario assumptions made during model derivation.

4-1 Simulation Development

4-1-1 Simulation Platform

For the simulations, the open-source ATM simulation platform BlueSky, will be used. It is developed in Python programming language at Delft University of Technology. BlueSky has CD features and is able to to simulate a large number of aircraft at the same time. It was designed to be user friendly and easy to modify. More information on BlueSky is in (Hoekstra & Ellerbroek, 2016).

4-1-2 Conflict Detection

The CD method used is called state-based conflict detection, where an aircraft's future position is predicted as a linear extrapolation of its speed over a predefined look-ahead time. The conflict is detected when an aircraft's trajectory will violate another aircraft's minimum separation. A typical look-ahead time is 5 minutes, and will likely be used as such in these experiments and the separation is 5 nm horizontally and 1000 ft vertically.

4-1-3 Airspace Concepts and Concept Implementation

Four airspace concepts will be tested, an unstructured airspace concept with no procedural restrictions and three types of Layers concepts. The experiments for Layers concepts consist

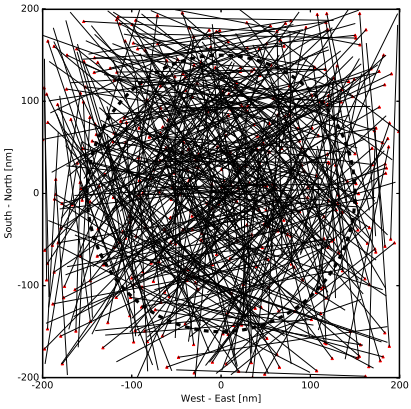

Figure 4-1: A top view of the testing region with trajectories. The simulation region is the outer square and the experiment region is the inner circle.

of 8 layers, the heading ranges that will be used are 360°, 180° and 90°. As the separation criteria used in these experiments is 5 nm and 1000 ft, each layer is separated by 1100 ft, 1000 ft to maintain separation and 100 ft to ensure that that the separation is not violated. The altitude for all concepts, unstructured and layered, will range between 4000 to 12800 ft.

To implement the concepts, scenarios are modified such that they fit the concept's constraints. The scenario generator creates sets of commands which are fed into the BlueSky trajectory functions. Aircraft and trajectories are generated with heading, distance, speed, origin points and destination points. For the unstructured concept, the generator determines the cruising altitude for the flight which is proportional to the flight distance, see Eq. 3-2. For the Layers concept the heading as well as the distance determines the altitude. All layered concepts used 8 cruising flight levels. The number of layer sets, with each layer set providing the complete range of headings from 0-360 degrees, differed for layered concepts: Layers 360 has eight sets, Layers 180 has 4 sets and Layers 90 had 2 sets. The availability of multiple layer sets is taken into account when altitude is selected using Eq 3-3 for Layered concepts.

4-2 Traffic Scenarios

4-2-1 Testing Region and Flight Profiles

The simulation region is 400×400 nm. Origins are randomly chosen, dependent on the spatial distribution type, then the destination point will be chosen according to the heading and distance. The origin and destination points can be located at any point within the simulation area. However as the density will be more towards the center of the simulation area, the results will only be relevant in a circle with a diameter of 300 nm. In Figure 4-1 a top view of the testing region is shown.

Aircraft will spawn at 0 ft and start by climbing up to the cruising altitude. Then travel a fixed cruise distance and then descent, all aircraft will travel the same distance while in the

cruise phase. The aircraft will then descent to the destination point. All aircraft have the same climb and descent angle.

4-2-2 Scenario Generator

The scenario generator will choose semi-random values for heading, spawning points, distance and speed (only for speed experiments) relevant to the distribution type that is being tested. Then derive the correct altitude and which layer is used for the Layers concepts, and choose an appropriate destination point within the simulation area that depends on the heading and distance. The generator must ensure constant density to maintain the correct distribution for the scenario that is being tested at the time.

4-3 Experiment Design

4-3-1 Independent variables

Four experiments will be performed and an additional baseline experiment, all with different independent variables. All experiments have different independent variables, but all of them have the traffic density as an independent variable. In addition to the independent variables, each experiment is repeated 5 times. In Table 4-1, the traffic densities which are tested are presented, in addition the spawn rate and spawn time intervals are presented at which aircraft that are to be spawned to maintain constant density and the number of instantaneous- and total aircraft.

Table 4-1: The values for the different densities, number of instantaneous aircraft, spawn rate, spawn intervals and total number of aircraft in the scenario.

Density [AC/10000 nm^2]	Number of instantaneous AC	Total AC in scenario
5.00	80.00	356
18.93	302.92	1347
36.84	589.45	2620
71.69	1146.99	5098
100.00	1600.00	7112

Baseline Experiment

The baseline scenario has uniform heading and distance distribution, the origin points will be uniformly distributed across the simulation area as well and the speed will stay homogeneous. This experiment should meet all the assumptions of the conflict rate model and will be used as a comparison for the other experiment. The independent variables are:

- Airspace concept: Unstructured Airspace, Layers 360, Layers 180, Layers 90.
- Traffic demand densities: 10 different densities ranging from 5-100 aircraft per 10000 nm^2

- 5 repetitions

Total simulations to run:

- 5 densities × 5 repetitions × 4 concepts = 100 simulations.

Heading Variation Experiment

The heading experiment is to strictly check the effects of heading distributions other than uniform. It is not realistic that all aircraft have uniformly distributed heading. The independent variables for the heading experiments are:

- Airspace concept: Unstructured Airspace, Layers 360, Layers.
- Traffic demand densities: 5 different densities ranging from 5-100 aircraft per 10000 nm^2
- Heading distribution, 3 distributions will be tested. Normal distribution, bimodal distribution and ranged normal distribution.
- 5 repetitions

Total simulations to run:

- 5 densities × 5 repetitions × 2 concepts × 3 densities = 150 simulations.

Spatial Distribution Variation Experiment

This experiment's purpose is to see how the spatial distribution affects the accuracy of the conflict rate model. The spatial distribution is where the origin points are chosen. The origin point is in latitude and longitude degrees.

- Airspace concept: Unstructured Airspace, Layers 360, Layers 180, Layers 90.
- Traffic demand densities: 5 different densities ranging from 5-100 aircraft per 10000 nm^2
- Spatial distribution, 3 distributions will be tested. Latitude and longitudes are both normally distributed for all scenarios, with a standard deviation of 40 nm, 30 nm and 20 nm.
- 5 repetitions

Total simulations to run:

- 5 densities × 5 repetitions × 4 concepts × 3 densities = 300 simulations.

Altitude Variation Experiment

The altitude is modified by modifying the distance. The altitude distribution is more complicated than the other experiments, as for the Layers 180 and Layers 90 need to have heading synchronized with the distance. The heading will only remain uniform for the unstructured airspace and Layers 360.

- Airspace concept: Unstructured Airspace, Layers 360.
- Traffic demand densities: 5 different densities ranging from 5-100 aircraft per 10000 nm^2
- Altitude distribution: 3 distributions will be tested, normal distribution, bimodal distribution and ranged-uniform.
- 5 repetitions

Total simulations to run:

- 5 densities $\times$ 5 repetitions $\times$ 2 concepts $\times$ 3 densities = 150 simulations.

Airspeed Variation Experiment

In the baseline scenario the airspeed is constant, but in this experiment it will vary between aircraft.

- Airspace concept: Unstructured Airspace, Layers 360, Layers 180, Layers 90.
- Traffic demand densities: 5 different densities ranging from 5-100 aircraft per 10000 nm^2
- Speed distribution: 3 distributions will be tested, normal distribution, bimodal distribution and ranged-uniform.
- 5 repetitions

Total simulations to run:

- 5 densities $\times$ 5 repetitions $\times$ 4 concepts $\times$ 3 densities = 300 simulations.

4-3-2 Dependent Variables

As the goal is to compare the conflict rate model with the conflict rate in the simulations, the only variable that is measured is the instantaneous number of conflict that are logged in BlueSky while the simulation is running. To measure the accuracy, an additional parameter is introduced to the models, called the accuracy parameter (k value). See the basic model in Eq. 4-1.

$$C_{SS} = \frac{N_{SS}}{2}(N_{SS} - 1)\ p_2\ k \tag{4-1}$$

Chapter 5

Summary

The focus of this study is to test the accuracy of the conflict rate models which are described in Chapter 2, when introduced to different scenarios. The derivation of the model was analyzed and hypotheses formed. The properties which are tested are heading distribution, spatial distribution, altitude distribution and speed distribution. It is expected that all properties have a significant effect on the result of the conflict rate models, except for the speed scenarios. The models are derived from certain assumptions, which are related to the properties which are being tested. The next phase of the research is to conduct an experiment to measure the effect. Five experiments will be performed, one for each property, and one for the baseline scenario. The total number of simulations is 1000.

The experiments will be performed in BlueSky open source air traffic simulator. Before that the traffic scenarios will be generated in python. The conflict count will be logged in BlueSky and used to derive the conflict count. Then to comparing the conflict rate in the experiment and the output of the conflict rate model gives the accuracy of the model.

Appendix B

Preliminary Appendix

In section 2-3 the conflict rate models are derived for unstructured airspace and the Layers concept. In Eqs. 2-7 and 2-25 the probability density function of the absolute heading difference between two uniformly distributed samples are used. In section 3-2 the probability density functions for ranged-uniform distribution, normal distribution and bimodal distribution are used to calculate the horizontal relative velocity factor. The factor is compared with the factor when uniform distribution is used. The probability density functions are found by creating two samples with the relevant distribution and plotting the absolute heading difference. Figures B-1, B-2, B-3 and B-4.

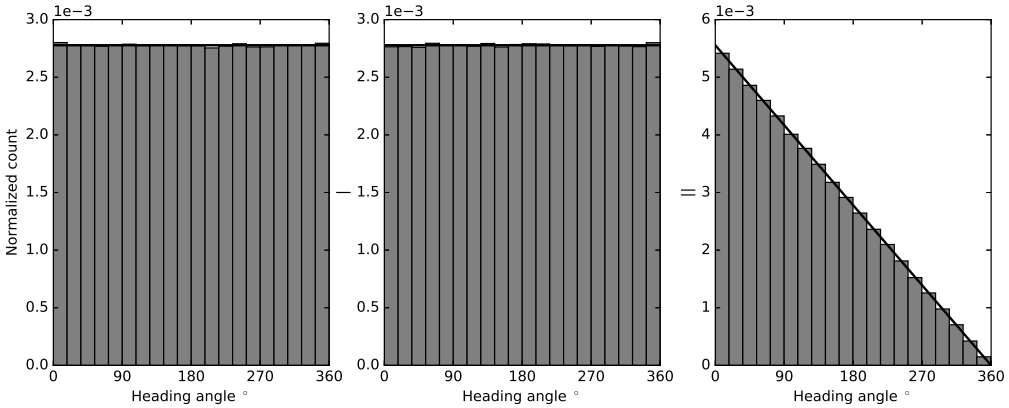

Figure B-1: The absolute heading difference. When a uniformly distributed sample is subtracted from another uniformly distributed sample, the result is a triangularly distributed sample.

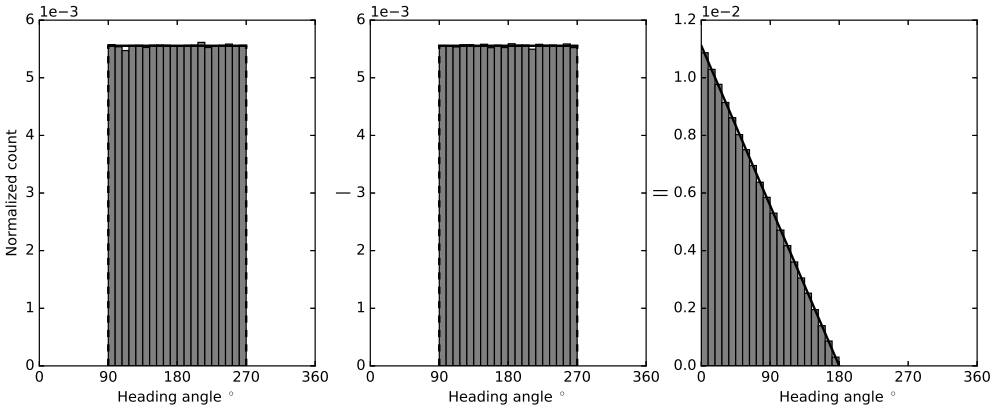

Figure B-2: The absolute heading difference. When a range-uniformly distributed sample is subtracted from another ranged-uniformly distributed sample, the result is a triangularly distributed sample.

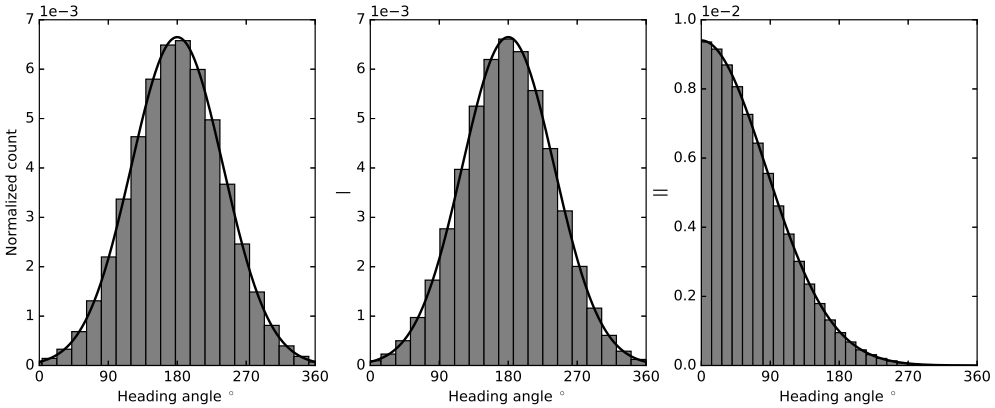

Figure B-3: The absolute heading difference. When a normally distributed sample is subtracted from another normally distributed sample, the result is a normally distributed sample.

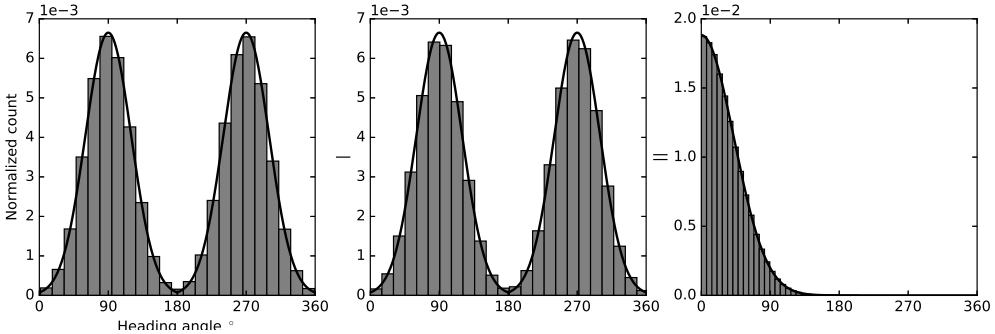

Figure B-4: The absolute heading difference. When a sample that has a bimodal distribution is subtracted from another sample that has a bimodal distribution, the result is a normally distributed sample.

In the heading scenario described in section 3-2 it states that only the Layers 360 concept is considered for a layered concept. The main reason is to maintain uniform altitude distribution, but another reason is that the probability density function is not the same for all layers. To demonstrate see Figures B-6 and B-7, where the probability density functions for the absolute heading difference for the Layers 90 concept are presented. The heading distribution is split up for each layer and the probability density functions are obtained. In the far left of the figures a reference normal distribution is shown, and the absolute heading difference does not fit completely, however a normal distribution could be used as an approximation in this case.

However, see Figure B-5 where normal distribution for the Layers 180 concept is presented. The results from subtracting the heading distributions for each layer results in the same distribution in this case, but it is not completely a normal distribution. In this case, the probability density function can be used, but if the probability density function for a normal distribution were to be used it would only be an approximation. In both cases for Layers 180 and Layers 90 it could be acceptable to use normal distribution as the probability density function as an approximation, but fractions of a normal distribution subtracted from another does not yield a normal distribution. To reiterate, the main reason that only Layers 360 in the heading scenario is that the altitude of the aircraft would not stay uniformly distributed.

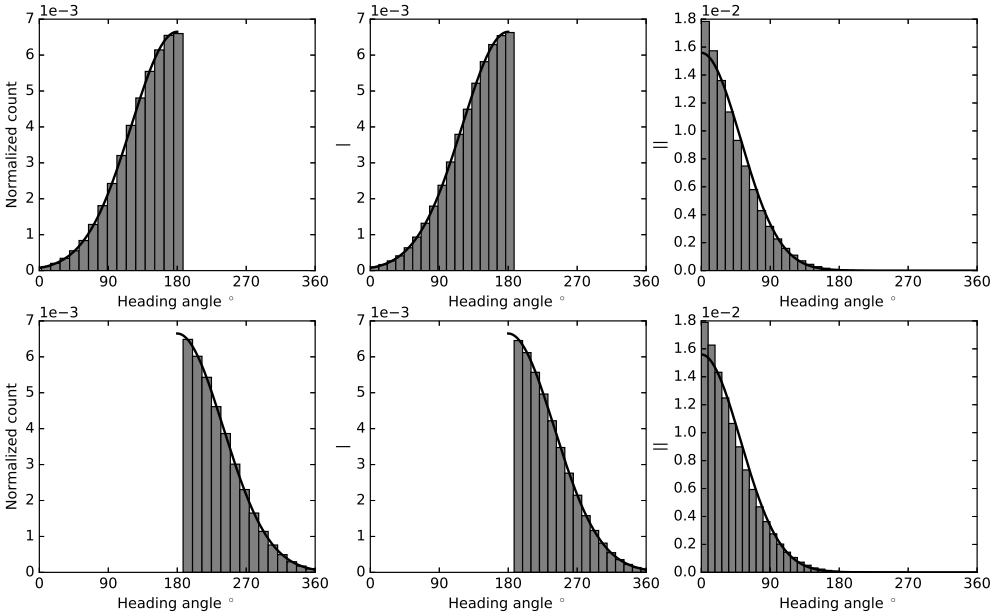

Figure B-5: The absolute heading difference For Layers 180, for both.

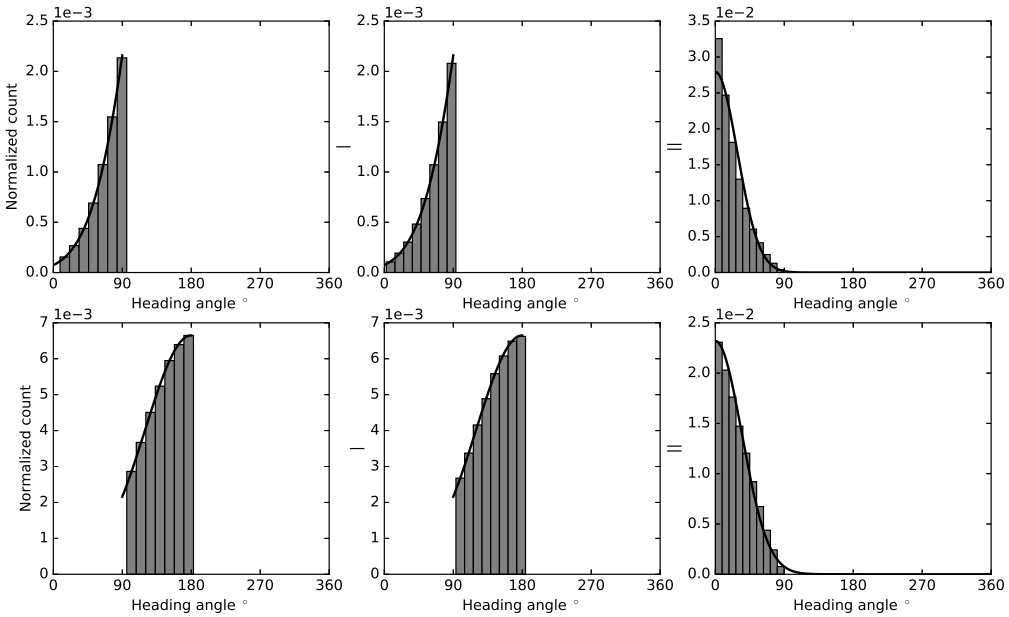

Figure B-6: The absolute heading difference. When a normally distributed sample is subtracted from another normally distributed sample, the result is a normally distributed sample.

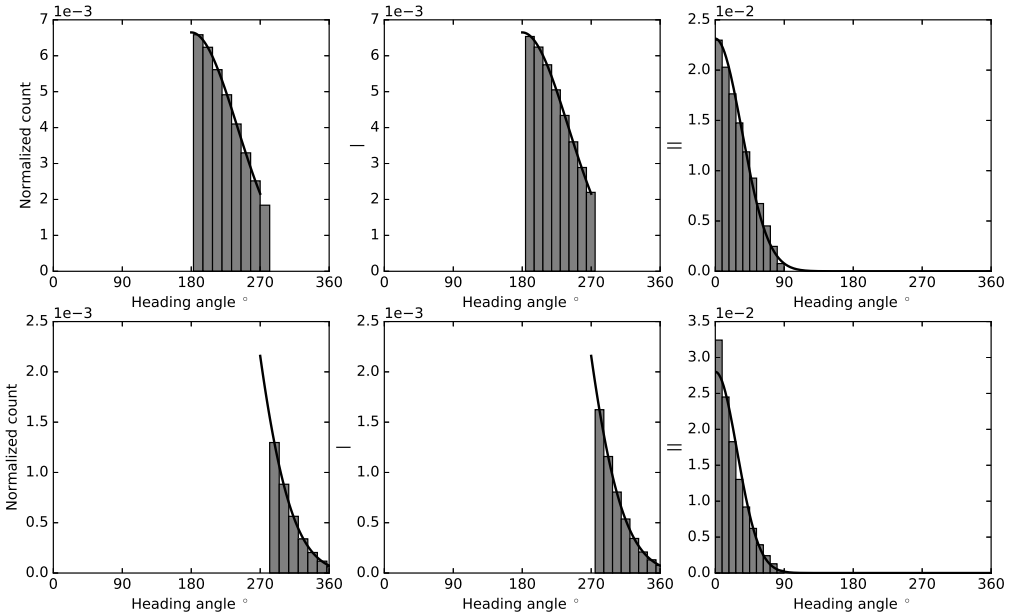

Figure B-7: The absolute heading difference. When a normally distributed sample is subtracted from another normally distributed sample, the result is a normally distributed sample.

Bibliography

Clari, M. S. V. V., Ruigrok, R. C. J., & Hoekstra, J. M. (2000). Cost-benefit study of free flight with airborne separation assurance. *Air Traffic Control Quarterly*, *9*, 287-309.

Endoh, S. (1982). *Aircraft collision models* (Tech. Rep.). MIT Department of Aeronautics and Astraonautics.

Eurocontrol annual report. (2015).

Eurocotrol. (2004, September). *Layers of parallel tracks: A speculative approach to the prevention of crossing conflicts between cruising aircraft.*

Ford, R. L. (1983). On the use of height rules in off-route airspace,. *Journal of Navigation*, *36*, 269-287.

Hicok, D., & Lee, D. (2002). Application of ads-b for airport surface surveillance. In *Digital avionics systems conference, 1998. proceedings., 17th dasc. the aiaa/ieee/sae.*

Hoekstra, J. M., & Ellerbroek, J. (2016). Bluesky atc simulator project: an open data and open source approach. In *Research gate.*

Hoekstra, J. M., Gent, R. N. H. W. van, & Ruigrok, R. C. J. (2002). Designing for safety: the 'free flight' air traffic manangement concept. *Reliability Engineerying and System Safety*, *75*, 215-232.

Hoekstra, J. M., Maas, J., Tra, M., & Sunil, E. (2016). How do layered airspace design parameters affect airspace capacity and safety? In *Safety & human performance.*

Hoekstra, J. M., Ruigrok, R. C. J., & Van Gent, R. (2001). Free flight in a crowded airspace? *Progress in Astronautics and Aeronautics*, *193*, 533-546.

Irvine, R., & Hering, H. (2007). Towards systematic air traffic management in a regular lattice. In *7th aiaa aviation technology, integration and operations confrence (atio).*

Jardin, M. R. (2005). Analytical relationships between conflict counts and air-traffic density. *Journal of Guidance, Control and Dynamics*, *28*, 1150-1156.

Kuchar, J. K., & Yang, L. C. (2000). A review of conflict detection and resolution modeling methods. *IEEE Transactions on Intelligent Transportation Systems*, *1*, 179-189.

Leiden, K., Peters, S., & Quesada, S. (2009). Flight level-based dynamic airspace configuration. In *9th aiaa aviation technology, integration, and operations conference (atio).*

Nacta - a history of air traffic control. (n.d.). Presentation.

RTCA. (1995, October). *Final repost of the rtca task force 3, free flight implementations.*

Sunil, E. (n.d.). *Conflict model in 3d.* (An unpublished derivation of the 3D conflict rate model, (2017))

Sunil, E. (2017). Modeling the intrinsic safety of unstructured and layered airspace design. In *12th usa/europe air traffic management research and development seminar.*

Sunil, E., Ellerbroek, J., & Hoekstra, J. M. (2017). Analysis of airspace structure and capacity for decentralized separation using fast-time simulations. *Journal of Guidance, Control and Dynamics*, *40*, 38-51.

Tra, M. (2016). *The effect of a layered airspace concept on conflict probability and capacity.* (MSc Thesis)